FAA-EE-80-09A

U.S. Department
of Transportation
**Federal Aviation
Administration**

IMPACT OF AIRCRAFT EMISSIONS ON AIR QUALITY IN THE VICINITY OF AIRPORTS

Volume I: Recent Airport Measurement Programs, Data Analyses, and Sub-Model Development

Office of Environment
and Energy
Washington, D.C. 20591

July 1980

R.J. Yamartino
D.G. Smith
S.A. Bremer
D. Heinold
D. Lamich
B. Taylor

Document is available to the public through the National Technical Information Service, Springfield, Virginia 22161

Technical Report Documentation Page

1. Report No.	2. Government Accession No.	3. Recipient's Catalog No.
FAA-EE-80-09A		

4. Title and Subtitle
Impact of Aircraft Emissions on Air Quality in the Vicinity of Airports
Volume I: Recent Airport Measurement Programs, Data and Sub-Model Development

5. Report Date
July 1980

6. Performing Organization Code

7. Author(s) R.J. Yamartino, D.G. Smith*, S.A. Bremer, D. Heinold*, D. Lamich, and B. Taylor*

8. Performing Organization Report No.

9. Performing Organization Name and Address
Argonne National Laboratory
Energy and Environmental Systems Division
9700 S. Cass Avenue
Argonne, Illinois 60439

10. Work Unit No. (TRAIS)

11. Contract or Grant No.
DOT-FA77WAI-736

12. Sponsoring Agency Name and Address
U.S. Department of Transportation
Federal Aviation Administration
Office of Environment and Energy
Washington, D.C. 20591

13. Type of Report and Period Covered
Final Report
January 1978 - July 1980

14. Sponsoring Agency Code

15. Supplementary Notes
*Affiliated with Environmental Research and Technology, Inc.
696 Virginia Road
Concord, Massachusetts 01742

16. Abstract

This report documents the results of the Federal Aviation Administration (FAA)/ Environmental Protection Agency (EPA) air quality study which has been conducted to assess the impact of aircraft emissions of carbon monoxide (CO), hydrocarbons (HC), and oxides of nitrogen (NO_x) in the vicinity of airports. This assessment includes the results of recent modeling and monitoring efforts at Washington National (DCA), Los Angeles International (LAX), Dulles International (IAD), and Lakeland, Florida airports and an updated modeling of aircraft generated pollution at LAX, John F. Kennedy (JFK) and Chicago O'Hare (ORD) airports. The Airport Vicinity Air Pollution (AVAP) model which was designed for use at civil airports was used in this assessment. In addition the results of the application of the military version of the AVAP model the Air Quality Assessment Model (AQAM), are summarized.

Both the results of the pollution monitoring analyses in Volume I and the modeling studies in Volume II suggest that:

- Maximum hourly average CO concentrations from aircraft are unlikely to exceed 5 parts per million (ppm) in areas of public exposure and are thus small in comparison to the National Ambient Air Quality Standard of 35 ppm.
- Maximum hourly HC concentrations from aircraft can exceed 0.25 ppm over an area several times the size of the airport.
- While annual average NO_2 concentrations from aircraft are estimated to contribute only 10 to 20 percent of the NAAQS limit level, these concentrations, when averaged over a one hour time period are estimated to produce concentrations as high as 0.5 ppm if one assumes that all engine produced NO is converted to NO_2 by the time these emissions reach places of public exposure. This value is at the upper end of the concentration range being considered for the short term NO_2 standard presently under review and can not be ignored. However a decision on the influence of aircraft emissions on a short term standard must await the release of this standard and the results of research under way to determine the rate at which engine produced NO converts to NO_2 in the ambient air.

This report, IMPACT OF AIRCRAFT EMISSIONS ON AIR QUALITY IN THE VICINITY OF AIRPORTS, is printed in two volumes with the following subtitles; VOLUME I: Recent Airport Measurement Programs, Data Analyses, and Sub-Model Development; and VOLUME II: An Updated Model Assessment of Aircraft Generated Air Pollution at LAX, JFK, and ORD.

17. Key Words	18. Distribution Statement
Aircraft Emissions Dispersion Modeling Air Quality Impact of Aviation Airport Air Quality Monitoring	This document is available to the public through the National Technical Information Service, Springfield, VA 22161

19. Security Classif. (of this report)	20. Security Classif. (of this page)	21. No. of Pages	22. Price
Unclassified	Unclassified	169	

Technical Report Documentation Page

1. Report No.	2. Government Accession No.	3. Recipient's Catalog No.
FAA-EE-80-09A		

4. Title and Subtitle
Impact of Aircraft Emissions on Air Quality in the Vicinity of Airports
Volume I: Recent Airport Measurement Programs, Data and Sub-Model Development

5. Report Date
July 1980

6. Performing Organization Code

7. Author(s) R.J. Yamartino, D.G. Smith*, S.A. Bremer, D. Heinold*, D. Lamich, and B. Taylor*

8. Performing Organization Report No.

9. Performing Organization Name and Address
Argonne National Laboratory
Energy and Environmental Systems Division
9700 S. Cass Avenue
Argonne, Illinois 60439

10. Work Unit No. (TRAIS)

11. Contract or Grant No.
DOT-FA77WAI-736

12. Sponsoring Agency Name and Address
U.S. Department of Transportation
Federal Aviation Administration
Office of Environment and Energy
Washington, D.C. 20591

13. Type of Report and Period Covered
Final Report
January 1978 - July 1980

14. Sponsoring Agency Code

15. Supplementary Notes
*Affiliated with Environmental Research and Technology, Inc.
696 Virginia Road
Concord, Massachusetts 01742

16. Abstract

This report documents the results of the Federal Aviation Administration (FAA)/ Environmental Protection Agency (EPA) air quality study which has been conducted to assess the impact of aircraft emissions of carbon monoxide (CO), hydrocarbons (HC), and oxides of nitrogen (NO_x) in the vicinity of airports. This assessment includes the results of recent modeling and monitoring efforts at Washington National (DCA), Los Angeles International (LAX), Dulles International (IAD), and Lakeland, Florida airports and an updated modeling of aircraft generated pollution at LAX, John F. Kennedy (JFK) and Chicago O'Hare (ORD) airports. The Airport Vicinity Air Pollution (AVAP) model which was designed for use at civil airports was used in this assessment. In addition the results of the application of the military version of the AVAP model the Air Quality Assessment Model (AQAM), are summarized.

Both the results of the pollution monitoring analyses in Volume I and the modeling studies in Volume II suggest that:

o Maximum hourly average CO concentrations from aircraft are unlikely to exceed 5 parts per million (ppm) in areas of public exposure and are thus small in comparison to the National Ambient Air Quality Standard of 35 ppm.

o Maximum hourly HC concentrations from aircraft can exceed 0.25 ppm over an area several times the size of the airport.

o While annual average NO_2 concentrations from aircraft are estimated to contribute only 10 to 20 percent of the NAAQS limit level, these concentrations, when averaged over a one hour time period are estimated to produce concentrations as high as 0.5 ppm if one assumes that all engine produced NO is converted to NO_2 by the time these emissions reach places of public exposure. This value is at the upper end of the concentration range being considered for the short term NO_2 standard presently under review and can not be ignored. However a decision on the influence of aircraft emissions on a short term standard must await the release of this standard and the results of research under way to determine the rate at which engine produced NO converts to NO_2 in the ambient air.

This report, IMPACT OF AIRCRAFT EMISSIONS ON AIR QUALITY IN THE VICINITY OF AIRPORTS, is printed in two volumes with the following subtitles; VOLUME I: Recent Airport Measurement Programs, Data Analyses, and Sub-Model Development; and VOLUME II: An Updated Model Assessment of Aircraft Generated Air Pollution at LAX, JFK, and ORD.

17. Key Words	18. Distribution Statement
Aircraft Emissions Dispersion Modeling Air Quality Impact of Aviation Airport Air Quality Monitoring	This document is available to the public through the National Technical Information Service, Springfield, VA 22161

19. Security Classif. (of this report)	20. Security Classif. (of this page)	21. No. of Pages	22. Price
Unclassified	Unclassified	169	

PREFACE

This document has been prepared by the Energy and Environmental Systems Division of Argonne National Laboratory at the request of the Federal Aviation Administration. The report attempts to realistically simulate the air quality impact of aircraft in and around the airport property under adverse dispersion conditions. No attempt has been made to include the effect of non-aircraft sources.

PREFACE

This document has been prepared by the Energy and Environmental Systems Division of Argonne National Laboratory at the request of the Federal Aviation Administration. The report attempts to realistically simulate the air quality impact of aircraft in and around the airport property under adverse dispersion conditions. No attempt has been made to include the effect of non-aircraft sources.

TABLE OF CONTENTS

TABLE OF CONTENTS

LIST OF TABLES

LIST OF TABLES

LIST OF FIGURES (Cont'd)

LIST OF FIGURES (Cont'd)

LIST OF FIGURES (Cont'd)

LIST OF FIGURES (Cont'd)

LIST OF FIGURES (Cont'd)

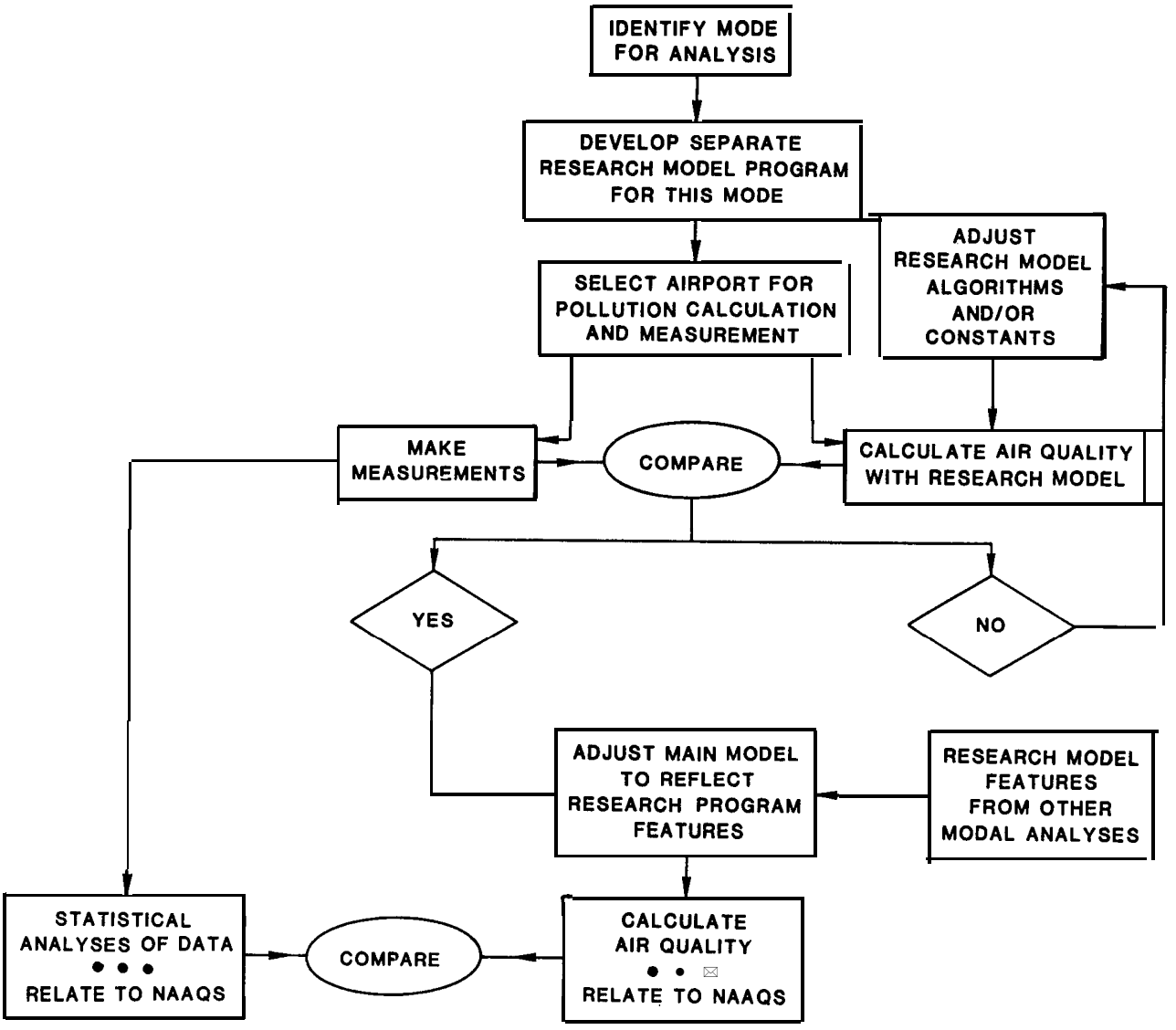

Fig. 1.1. Analysis Procedure

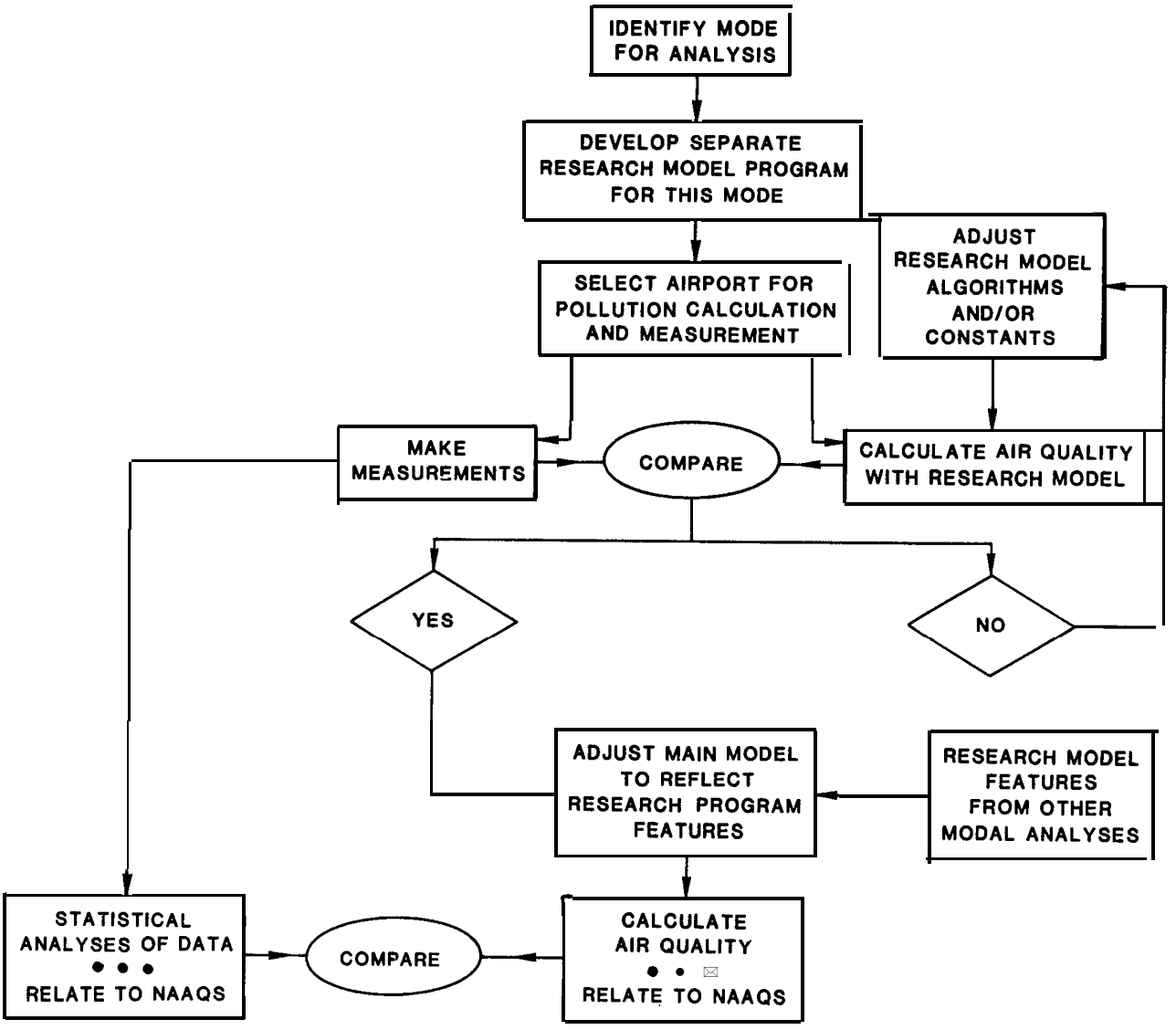

Fig. 1.1. Analysis Procedure

Volume II contains the results of a detailed application of the updated AVAP model to LAX, JFK and ORD airports. The model incorporates the most recent submodels and sub-model parameters obtainable from the airport monitoring programs described herein, as well as the most recent updates to the theory of dispersion of atmospheric pollutants. The principal findings of Volume II have also been incorporated into this Summary.

1.2 OBJECTIVES

During the past several years a number of government agencies, including the EPA, FAA, and USAF have been engaged in a comprehensive program to assess the effects of aircraft emissions upon air quality. While the motivation to evaluate such impacts originated with the 1970 Amendments to the Clean Air Act, the March 24, 1978 Notice of Proposed Rule Making (NPRM), announcing the EPA's intention to modify the 1973 engine emission standards, provided a clear mandate to

- resolve the ambiguities of previous monitoring and modeling efforts,
- update airport dispersion modeling assessments to reflect recent modeling improvements, and
- measure pollutant levels near aircraft in a manner that would clearly determine aircraft emissions impact,

so that realistic engine emissions standards could be established on the basis of the best available information.

While the objective as stated above suggests a program of all-encompassing scope, it is useful at the outset to consider the limitations of this endeavor. The project concerns itself solely with the ground-level, air quality impacts of aircraft exhaust

- on or in the near vicinity of airports,
- in areas of possible public exposure, and
- relative to existing or potential National Ambient Air Quality Standards (NAAQS).

Thus, for example, this report is not concerned with stratospheric impacts, the hydrocarbon odor nuisance problem at airports, the combined effects of pollution from aircraft, access vehicles, and service vehicles, or the level

of pollution inside the passenger terminal, despite the fact that such considerations may have explicit or implicit effects on the determination of adequate aircraft emission standards.

1.3 APPROACH

The principal strategy was to assess the air quality impacts of aircraft exhaust through monitoring of aircraft pollution impacts within 0.5 km of the aircraft. This served the dual purpose of supplying actual measured impacts with which one could infer average and worst case+ pollutant concentrations and of providing a research grade data base with which one could investigate and parameterize the aircraft plume dispersion physics in order to improve the predictive accuracy of sub-models within an airport model, and hence, ultimately improve the predictive power of airport air quality assessment models. With one such improved model, AVAP, it was then possible to simulate worst case pollutant conditions at major U.S. airports: an objective that would have been unacceptably expensive to attain solely through ambient air monitoring programs.

The monitoring programs, that provided the basis for pursuit of the aircraft exhaust impact assessment objective through the above-described strategy, are summarized in Table 1.1. These experiments, described in this report and in other indicated documentation, share two important characteristics that set them apart from previous monitoring programs. First, they were designed to focus in on specific aircraft modes of operation. The orientation of receptors at Washington National (DCA), seen in Figure 1.2, provides an example of such a modal focus. Under winds from the NW-N directions, the pollution cloud from queueing aircraft is transported across the network of monitors while under winds from the NNE-SE directions, the plumes created by the high-thrust takeoff mode are sampled by the same monitors. Second, these experiments achieve a separation of aircraft pollution from other source related pollution via a multi-station receptor array either operating in a low-background environment, such as at Williams AFB, Arizona (Yamartino et al., 1980) or else sampling at a sufficiently high rate to

+"worst case" is generally taken here to indicate the highest hourly average concentration per annum or the meteorological and aircraft operations conditions leading to such concentrations.

of pollution inside the passenger terminal, despite the fact that such considerations may have explicit or implicit effects on the determination of adequate aircraft emission standards.

1.3 APPROACH

The principal strategy was to assess the air quality impacts of aircraft exhaust through monitoring of aircraft pollution impacts within 0.5 km of the aircraft. This served the dual purpose of supplying actual measured impacts with which one could infer average and worst case+ pollutant concentrations and of providing a research grade data base with which one could investigate and parameterize the aircraft plume dispersion physics in order to improve the predictive accuracy of sub-models within an airport model, and hence, ultimately improve the predictive power of airport air quality assessment models. With one such improved model, AVAP, it was then possible to simulate worst case pollutant conditions at major U.S. airports: an objective that would have been unacceptably expensive to attain solely through ambient air monitoring programs.

The monitoring programs, that provided the basis for pursuit of the aircraft exhaust impact assessment objective through the above-described strategy, are summarized in Table 1.1. These experiments, described in this report and in other indicated documentation, share two important characteristics that set them apart from previous monitoring programs. First, they were designed to focus in on specific aircraft modes of operation. The orientation of receptors at Washington National (DCA), seen in Figure 1.2, provides an example of such a modal focus. Under winds from the NW-N directions, the pollution cloud from queueing aircraft is transported across the network of monitors while under winds from the NNE-SE directions, the plumes created by the high-thrust takeoff mode are sampled by the same monitors. Second, these experiments achieve a separation of aircraft pollution from other source related pollution via a multi-station receptor array either operating in a low-background environment, such as at Williams AFB, Arizona (Yamartino et al., 1980) or else sampling at a sufficiently high rate to

+"worst case" is generally taken here to indicate the highest hourly average concentration per annum or the meteorological and aircraft operations conditions leading to such concentrations.

of pollution inside the passenger terminal, despite the fact that such considerations may have explicit or implicit effects on the determination of adequate aircraft emission standards.

1.3 APPROACH

The principal strategy was to assess the air quality impacts of aircraft exhaust through monitoring of aircraft pollution impacts within 0.5 km of the aircraft. This served the dual purpose of supplying actual measured impacts with which one could infer average and worst case+ pollutant concentrations and of providing a research grade data base with which one could investigate and parameterize the aircraft plume dispersion physics in order to improve the predictive accuracy of sub-models within an airport model, and hence, ultimately improve the predictive power of airport air quality assessment models. With one such improved model, AVAP, it was then possible to simulate worst case pollutant conditions at major U.S. airports: an objective that would have been unacceptably expensive to attain solely through ambient air monitoring programs.

The monitoring programs, that provided the basis for pursuit of the aircraft exhaust impact assessment objective through the above-described strategy, are summarized in Table 1.1. These experiments, described in this report and in other indicated documentation, share two important characteristics that set them apart from previous monitoring programs. First, they were designed to focus in on specific aircraft modes of operation. The orientation of receptors at Washington National (DCA), seen in Figure 1.2, provides an example of such a modal focus. Under winds from the NW-N directions, the pollution cloud from queueing aircraft is transported across the network of monitors while under winds from the NNE-SE directions, the plumes created by the high-thrust takeoff mode are sampled by the same monitors. Second, these experiments achieve a separation of aircraft pollution from other source related pollution via a multi-station receptor array either operating in a low-background environment, such as at Williams AFB, Arizona (Yamartino et al., 1980) or else sampling at a sufficiently high rate to

+"worst case" is generally taken here to indicate the highest hourly average concentration per annum or the meteorological and aircraft operations conditions leading to such concentrations.

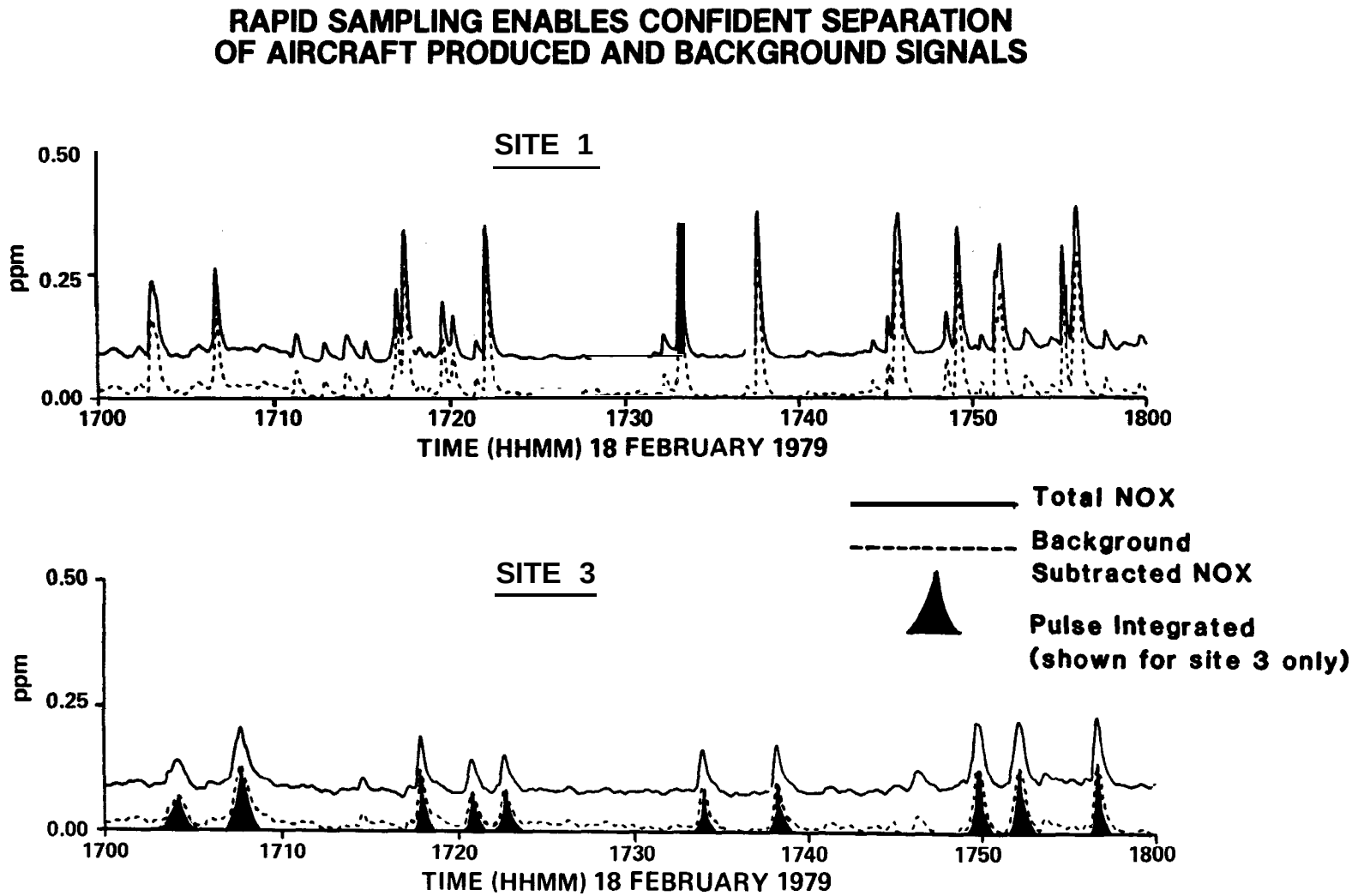

Fig. 1.3. NO_x Concentration Time Histories for Sites 1 and 3 for a Typical One Hour Period as Reconstructed from the High Sampling Rate DAS Tapes. Also shown are the computed background subtracted (dotted lines) and pulse integrated (shaded) time histories.

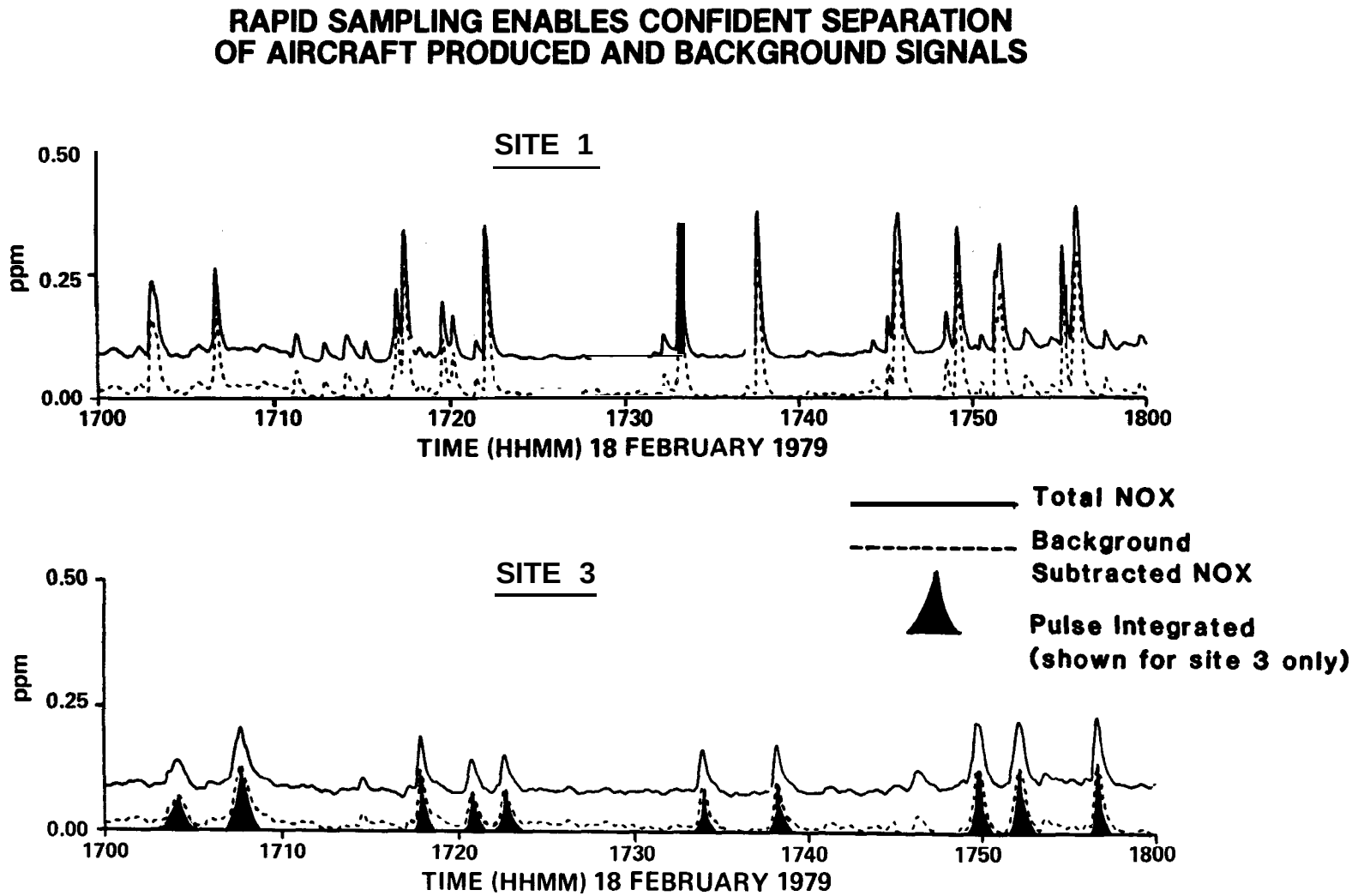

Fig. 1.3. NO_x Concentration Time Histories for Sites 1 and 3 for a Typical One Hour Period as Reconstructed from the High Sampling Rate DAS Tapes. Also shown are the computed background subtracted (dotted lines) and pulse integrated (shaded) time histories.

1.4 RESULTS

Rather than to proceed from experiment to experiment, as is done in the text of the report, let us consider the various engine emitted pollutants and the information regarding those emissions' impacts as determined by these monitoring and modeling exercises.

1.4.1 Carbon Monoxide

Experimental and modeling efforts of the early 70's indicated that violations of the NAAQS one-hour CO standard of 35 ppm were indeed possible at airports. Measured and modeled peak hourly levels of 46 ppm and 24 ppm respectively at LAX (Platt et al., 1971), for example, suggested that aircraft emissions were a serious problem relative to the one-hour standard; however, a number of factors contributed to this misleading implication of aircraft including:

- aircraft source characteristics (i.e., initial plume volume and rise) were not understood and thus not modeled. Modeling of aircraft emissions neglecting initial dispersion can lead to arbitrarily high concentrations depending on source location.
- background concentrations were often not measured, making it difficult to isolate the aircraft or airport contributed concentrations from those of the surrounding region.
- building wake effects can greatly magnify the impact of the multitude of CO sources around the terminal. The modeling of such enhancing effects was (and still generally is because of the complexity) ignored.
- emissions from other sources, particularly service and access vehicles may dominate aircraft sources in the vicinity of the terminal where the highest concentrations were observed.
- peak observed concentrations were underpredicted by a factor of 2-3.

This latter consideration of 2-3-fold model underprediction, coupled with the other uncertainties, particularly the unknown and unmodeled characteristics of the aircraft plume, certainly invited the speculation that aircraft were responsible for the modeling deficit and thus were the principal source.

The CO monitoring experiment along the main taxiway at Dulles International (Smith et al, 1977) was the first to isolate the impact of aircraft emissions alone and indicated that the initial turbulent mixing caused by the

1.4 RESULTS

Rather than to proceed from experiment to experiment, as is done in the text of the report, let us consider the various engine emitted pollutants and the information regarding those emissions' impacts as determined by these monitoring and modeling exercises.

1.4.1 Carbon Monoxide

Experimental and modeling efforts of the early 70's indicated that violations of the NAAQS one-hour CO standard of 35 ppm were indeed possible at airports. Measured and modeled peak hourly levels of 46 ppm and 24 ppm respectively at LAX (Platt et al., 1971), for example, suggested that aircraft emissions were a serious problem relative to the one-hour standard; however, a number of factors contributed to this misleading implication of aircraft including:

- aircraft source characteristics (i.e., initial plume volume and rise) were not understood and thus not modeled. Modeling of aircraft emissions neglecting initial dispersion can lead to arbitrarily high concentrations depending on source location.
- background concentrations were often not measured, making it difficult to isolate the aircraft or airport contributed concentrations from those of the surrounding region.
- building wake effects can greatly magnify the impact of the multitude of CO sources around the terminal. The modeling of such enhancing effects was (and still generally is because of the complexity) ignored.
- emissions from other sources, particularly service and access vehicles may dominate aircraft sources in the vicinity of the terminal where the highest concentrations were observed.
- peak observed concentrations were underpredicted by a factor of 2-3.

This latter consideration of 2-3-fold model underprediction, coupled with the other uncertainties, particularly the unknown and unmodeled characteristics of the aircraft plume, certainly invited the speculation that aircraft were responsible for the modeling deficit and thus were the principal source.

The CO monitoring experiment along the main taxiway at Dulles International (Smith et al, 1977) was the first to isolate the impact of aircraft emissions alone and indicated that the initial turbulent mixing caused by the

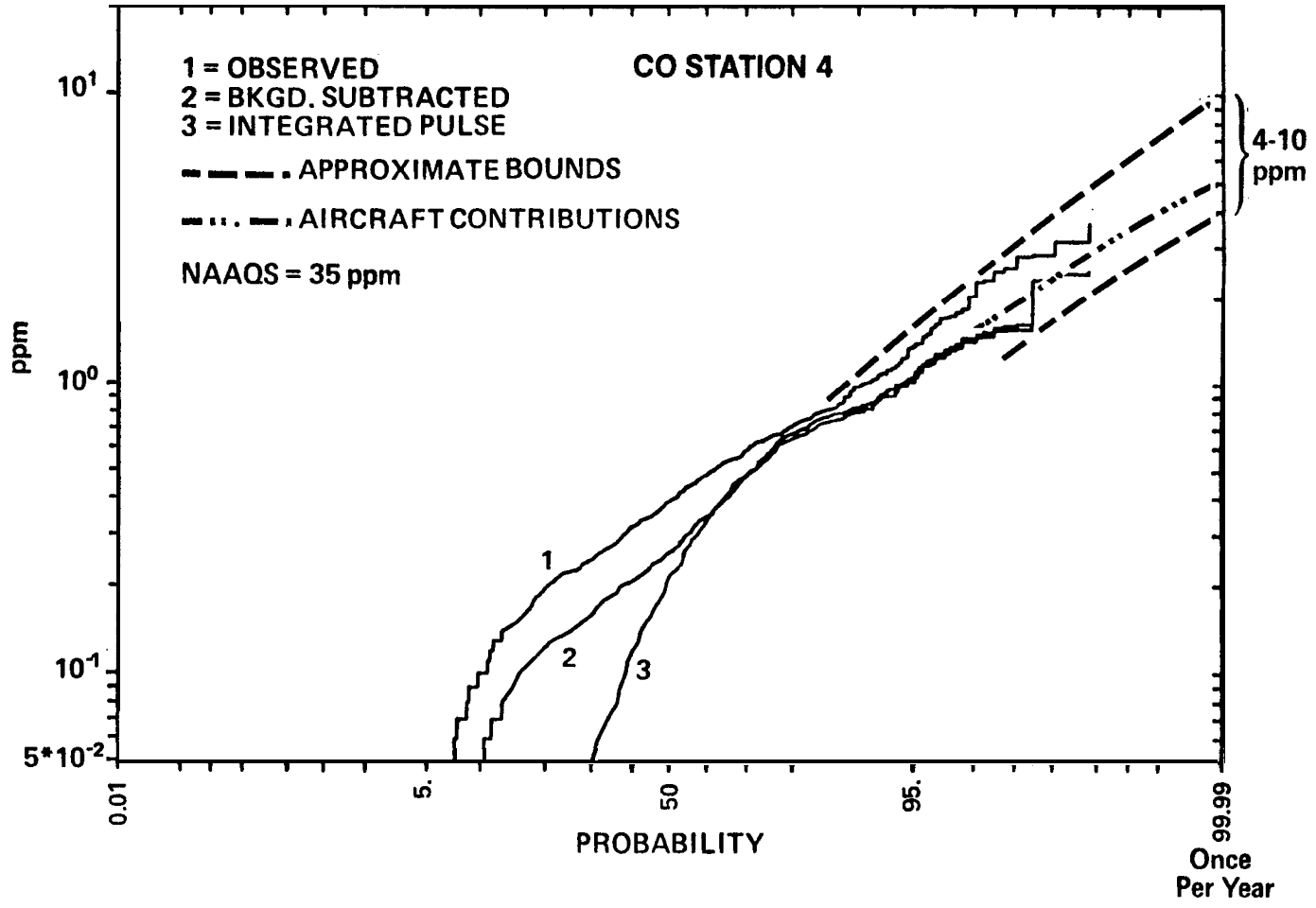

Fig. 1.4. Cumulative Frequency Distributions of Hourly CO Concentrations at DCA Station 4. The three solid curves represent the total (1), background subtracted (2), and pulse integrated (3) CO signal components. The dashed lines are visual guides for estimating the range of expected worst-case, once per year concentrations. The estimated worst-case, aircraft related concentration of ∿5 ppm suggests no violation of the 35 ppm NAAQS.

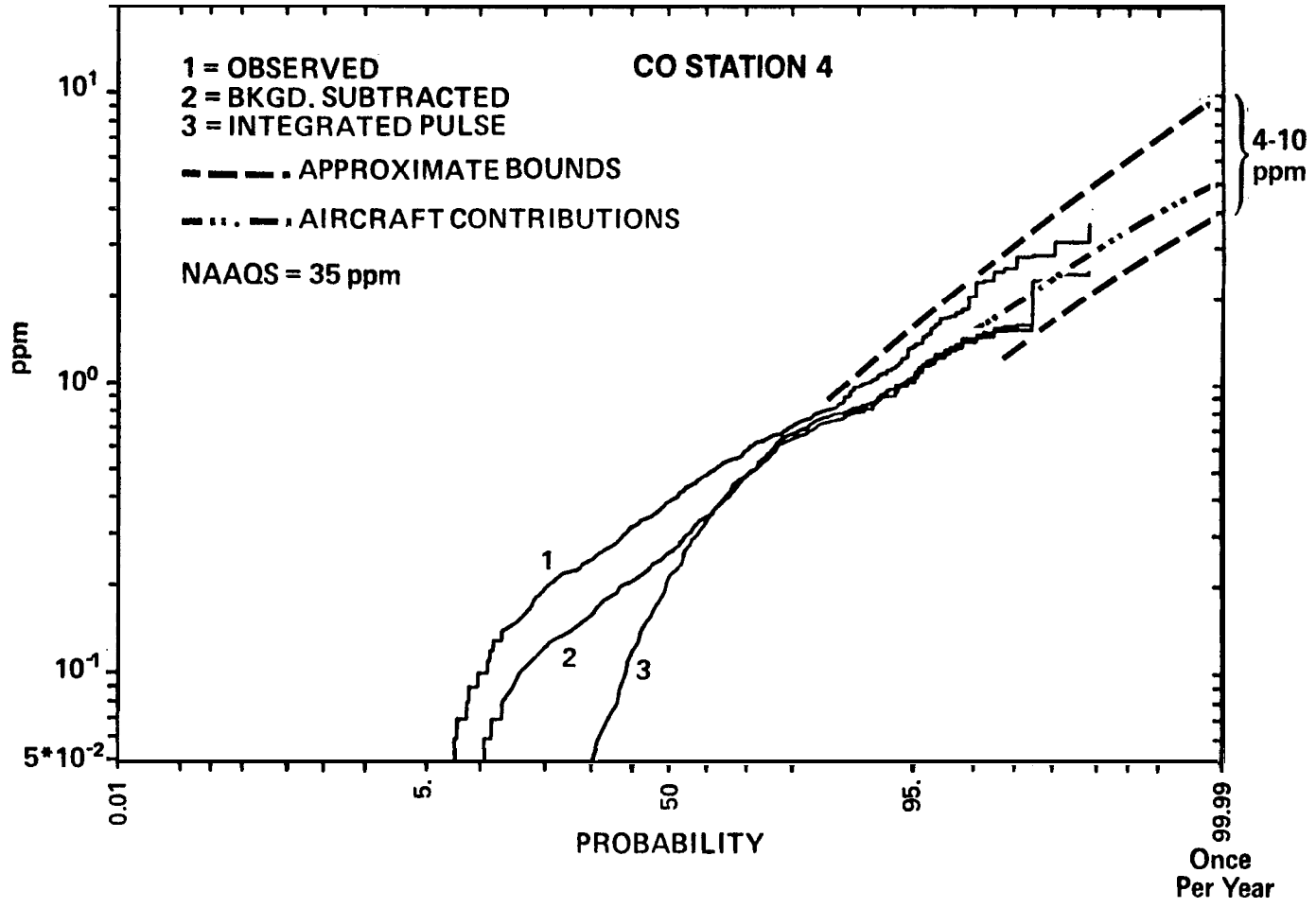

Fig. 1.4. Cumulative Frequency Distributions of Hourly CO Concentrations at DCA Station 4. The three solid curves represent the total (1), background subtracted (2), and pulse integrated (3) CO signal components. The dashed lines are visual guides for estimating the range of expected worst-case, once per year concentrations. The estimated worst-case, aircraft related concentration of ~5 ppm suggests no violation of the 35 ppm NAAQS.

1.4.2 Hydrocarbons

Hydrocarbon emissions are of concern as the presence of reactive hydrocarbon species are conductive to the subsequent formation of ozone. Motivation for control of aircraft emitted HC results partly from estimates that aircraft account for 1-3% of the total HC emitted in an Air Quality Control Region (AQCR) on an annual basis; thus, while aircraft are not a dominant source, they represent a significant source for control as they are comparable with many other source categories.

Measurements at Dulles and AVAP modeling agree that total HC concentrations, expressed as ppm equivalent methane (CH_4), correspond well in space, time, and magnitude with CO levels associated with these commercial aircraft. This is not particularly surprising since hydrocarbons and CO are both emitted during the same, low power setting, aircraft operational modes. Figure 1.6 shows the peak hourly total HC (THC) contour resulting from a "worst case" modeling of LAX during the 8-9AM period. Though restrictive considerations of the reactive (RHC) component and the three-hour average would act to somewhat reduce the area of this contour, it is still anticipated that the 0.25 ppm contour covers an area several times the airport size.

1.4.3 Oxides of Nitrogen

The issue of oxides of nitrogen (NO_x) impacts created by aircraft is, as with CO, a localized "hot-spot" problem related to existing and possible additional NAAQS for nitrogen dioxide (NO_2), and has been addressed primarily through the DCA monitoring program. Unfortunately the issue is further complicated by the fact that

- present and possible future NAAQS standards pertain to NO_2 levels and not NO, levels. ($NO_x \approx NO + NO_2$)
- there is presently only an annual average NAAQS of 0.05 ppm NO_2 though a peak hourly standard in the range 0.2-0.5 ppm is currently being reviewed by the EPA
- plume dispersion, while reducing the concentration of inert species, will entrain more amibient oxidant resulting in further conversion of engine emitted NO to NO_2; thus, NO_2 levels will peak at some distance downwind of the aircraft
- the peak NO_2 attributable to aircraft is a function of existing ambient levels of NO, NO_2, O_3, and sunlight.

1.4.2 Hydrocarbons

Hydrocarbon emissions are of concern as the presence of reactive hydrocarbon species are conductive to the subsequent formation of ozone. Motivation for control of aircraft emitted HC results partly from estimates that aircraft account for 1-3% of the total HC emitted in an Air Quality Control Region (AQCR) on an annual basis; thus, while aircraft are not a dominant source, they represent a significant source for control as they are comparable with many other source categories.

Measurements at Dulles and AVAP modeling agree that total HC concentrations, expressed as ppm equivalent methane (CH_4), correspond well in space, time, and magnitude with CO levels associated with these commercial aircraft. This is not particularly surprising since hydrocarbons and CO are both emitted during the same, low power setting, aircraft operational modes. Figure 1.6 shows the peak hourly total HC (THC) contour resulting from a "worst case" modeling of LAX during the 8-9AM period. Though restrictive considerations of the reactive (RHC) component and the three-hour average would act to somewhat reduce the area of this contour, it is still anticipated that the 0.25 ppm contour covers an area several times the airport size.

1.4.3 Oxides of Nitrogen

The issue of oxides of nitrogen (NO_x) impacts created by aircraft is, as with CO, a localized "hot-spot" problem related to existing and possible additional NAAQS for nitrogen dioxide (NO_2), and has been addressed primarily through the DCA monitoring program. Unfortunately the issue is further complicated by the fact that

- present and possible future NAAQS standards pertain to NO_2 levels and not NO, levels. ($NO_x \approx NO + NO_2$)
- there is presently only an annual average NAAQS of 0.05 ppm NO_2 though a peak hourly standard in the range 0.2-0.5 ppm is currently being reviewed by the EPA
- plume dispersion, while reducing the concentration of inert species, will entrain more amibient oxidant resulting in further conversion of engine emitted NO to NO_2; thus, NO_2 levels will peak at some distance downwind of the aircraft
- the peak NO_2 attributable to aircraft is a function of existing ambient levels of NO, NO_2, O_3, and sunlight.

In order to determine the impact of aircraft emissions on annual average air quality for comparison with the annual NO_2 NAAQS, it was necessary to regress measured NO_2 concentration levels against airplane activity. Figure 1.7 shows this relationship for the pulse integrated NO_2 levels at Station 1. The statistical significance of the slope of the regression coupled with a regression "y" intercept consistent with zero enables one to confidently estimate the annual average aircraft impact. The projected annual average aircraft impact of 0.005 ppm (5 ppb) is small compared with the 0.05 ppm NAAQS.

This paucity of data results in greater uncertainties for estimation of maximum hourly average NO, levels. Figure 1.8 indicates that, assuming log-normality of the hourly NO, cumulative frequency distribution (CFD), maximum hourly per annum NO, levels of 0.2 to 0.5 ppm due to aircraft operations alone may be expected several hundred meters downwind of the location where aircraft begin their takeoff roll. Depending on the oxidation rate of the aircraft emitted NO into NO_2, NO_2 levels is excess of 0.2 ppm may materialize.

AVAP modeling of a typical busy commercial airport under worst case activity and dispersion conditions indicates (Figure 1.9) NO, levels exceeding 0.5 ppm more than one-half mile from the end of the runway complex, but the key question is how these NO, levels translate into NO_2 levels. The NO_2/NO_x ratio is a function of plume dispersion rate and transport time, sunlight intensity, and background levels of NO, NO_2, and O_3 and a reactive plume calculation is required to obtain a more definitive prediction; however, using simple assumptions regarding the amount of NO_2 emitted directly by the aircraft, the rate of NO oxidation, and the ambient O_3 level, it is reasonable to expect several tenths of ppm of NO_2 at distances of possible public exposure. This is within the range of levels under consideration by the EPA as a possible short term NAAQS for NO_2.

1.5 CONCLUSIONS AND RECOMMENDATIONS

Recent airport air quality monitoring studies at four airports suggest maximum hourly average CO concentrations of 5 ppm in areas of expected public exposure. These measurements and estimates based on extrapolation of measured results to probabilities corresponding to one hour per year suggest small liklihood of violating the 35 ppm NAAQS.

In order to determine the impact of aircraft emissions on annual average air quality for comparison with the annual NO_2 NAAQS, it was necessary to regress measured NO_2 concentration levels against airplane activity. Figure 1.7 shows this relationship for the pulse integrated NO_2 levels at Station 1. The statistical significance of the slope of the regression coupled with a regression "y" intercept consistent with zero enables one to confidently estimate the annual average aircraft impact. The projected annual average aircraft impact of 0.005 ppm (5 ppb) is small compared with the 0.05 ppm NAAQS.

This paucity of data results in greater uncertainties for estimation of maximum hourly average NO, levels. Figure 1.8 indicates that, assuming log-normality of the hourly NO, cumulative frequency distribution (CFD), maximum hourly per annum NO, levels of 0.2 to 0.5 ppm due to aircraft operations alone may be expected several hundred meters downwind of the location where aircraft begin their takeoff roll. Depending on the oxidation rate of the aircraft emitted NO into NO_2, NO_2 levels is excess of 0.2 ppm may materialize.

AVAP modeling of a typical busy commercial airport under worst case activity and dispersion conditions indicates (Figure 1.9) NO, levels exceeding 0.5 ppm more than one-half mile from the end of the runway complex, but the key question is how these NO, levels translate into NO_2 levels. The NO_2/NO_x ratio is a function of plume dispersion rate and transport time, sunlight intensity, and background levels of NO, NO_2, and O_3 and a reactive plume calculation is required to obtain a more definitive prediction; however, using simple assumptions regarding the amount of NO_2 emitted directly by the aircraft, the rate of NO oxidation, and the ambient O_3 level, it is reasonable to expect several tenths of ppm of NO_2 at distances of possible public exposure. This is within the range of levels under consideration by the EPA as a possible short term NAAQS for NO_2.

1.5 CONCLUSIONS AND RECOMMENDATIONS

Recent airport air quality monitoring studies at four airports suggest maximum hourly average CO concentrations of 5 ppm in areas of expected public exposure. These measurements and estimates based on extrapolation of measured results to probabilities corresponding to one hour per year suggest small liklihood of violating the 35 ppm NAAQS.

In order to determine the impact of aircraft emissions on annual average air quality for comparison with the annual NO_2 NAAQS, it was necessary to regress measured NO_2 concentration levels against airplane activity. Figure 1.7 shows this relationship for the pulse integrated NO_2 levels at Station 1. The statistical significance of the slope of the regression coupled with a regression "y" intercept consistent with zero enables one to confidently estimate the annual average aircraft impact. The projected annual average aircraft impact of 0.005 ppm (5 ppb) is small compared with the 0.05 ppm NAAQS.

This paucity of data results in greater uncertainties for estimation of maximum hourly average NO, levels. Figure 1.8 indicates that, assuming log-normality of the hourly NO, cumulative frequency distribution (CFD), maximum hourly per annum NO, levels of 0.2 to 0.5 ppm due to aircraft operations alone may be expected several hundred meters downwind of the location where aircraft begin their takeoff roll. Depending on the oxidation rate of the aircraft emitted NO into NO_2, NO_2 levels is excess of 0.2 ppm may materialize.

AVAP modeling of a typical busy commercial airport under worst case activity and dispersion conditions indicates (Figure 1.9) NO, levels exceeding 0.5 ppm more than one-half mile from the end of the runway complex, but the key question is how these NO, levels translate into NO_2 levels. The NO_2/NO_x ratio is a function of plume dispersion rate and transport time, sunlight intensity, and background levels of NO, NO_2, and O_3 and a reactive plume calculation is required to obtain a more definitive prediction; however, using simple assumptions regarding the amount of NO_2 emitted directly by the aircraft, the rate of NO oxidation, and the ambient O_3 level, it is reasonable to expect several tenths of ppm of NO_2 at distances of possible public exposure. This is within the range of levels under consideration by the EPA as a possible short term NAAQS for NO_2.

1.5 CONCLUSIONS AND RECOMMENDATIONS

Recent airport air quality monitoring studies at four airports suggest maximum hourly average CO concentrations of 5 ppm in areas of expected public exposure. These measurements and estimates based on extrapolation of measured results to probabilities corresponding to one hour per year suggest small liklihood of violating the 35 ppm NAAQS.

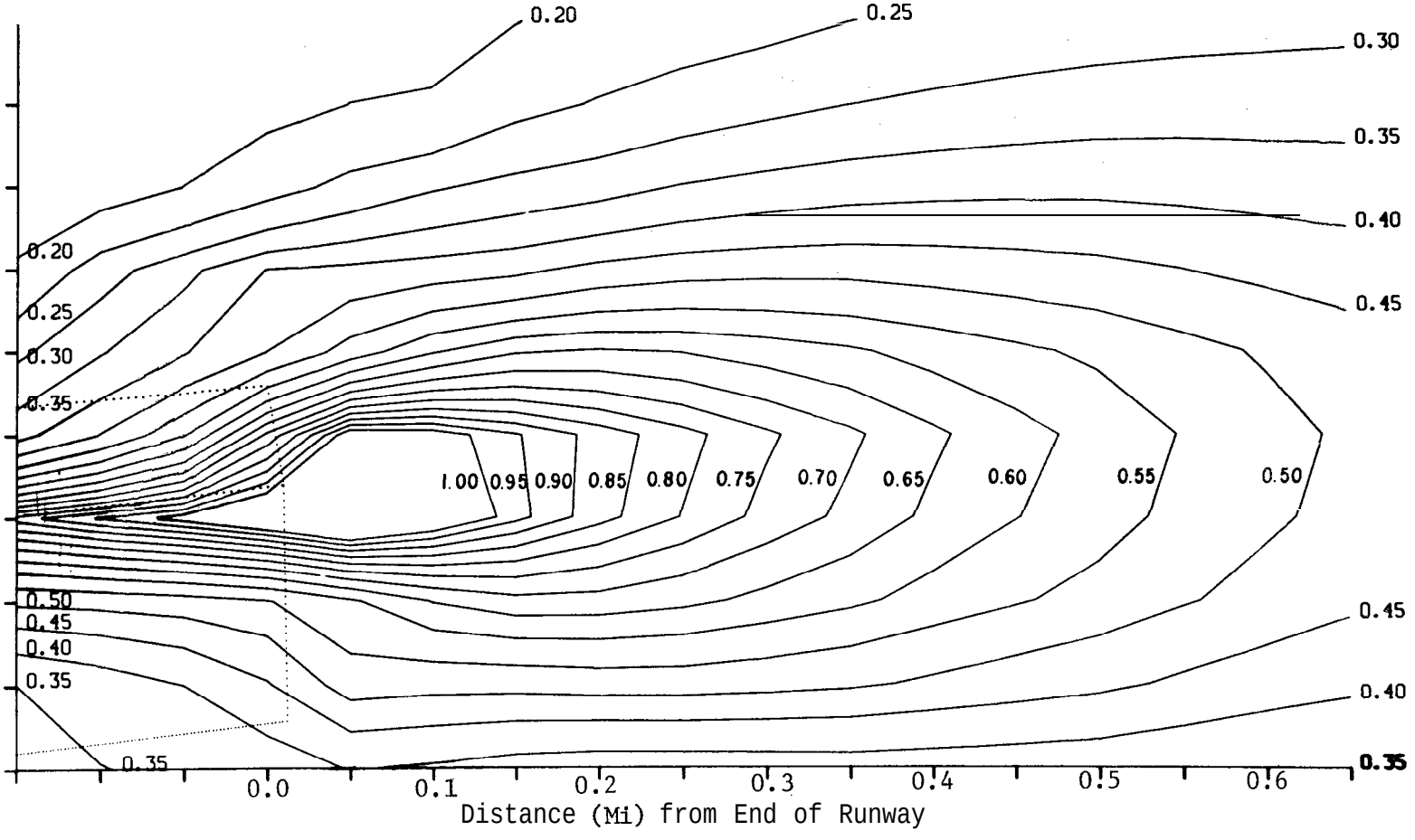

Fig. 1.9. MODIFIED AVAP Simulation of "Worst Case" (E Stability, Westerly 2-Knot Wind, and an Equivalent Departure Rate of Approximately 30 B727 Aircraft) NO, Conditions behind a Typical Busy Runway Complex. Runways and Taxiways are shown as dotted lines. NO, contour levels, given in ppm, suggest possible high NO_2 concentrations but reactive plume calculation needed to confirm this. Computation grid size = 0.05 mile.

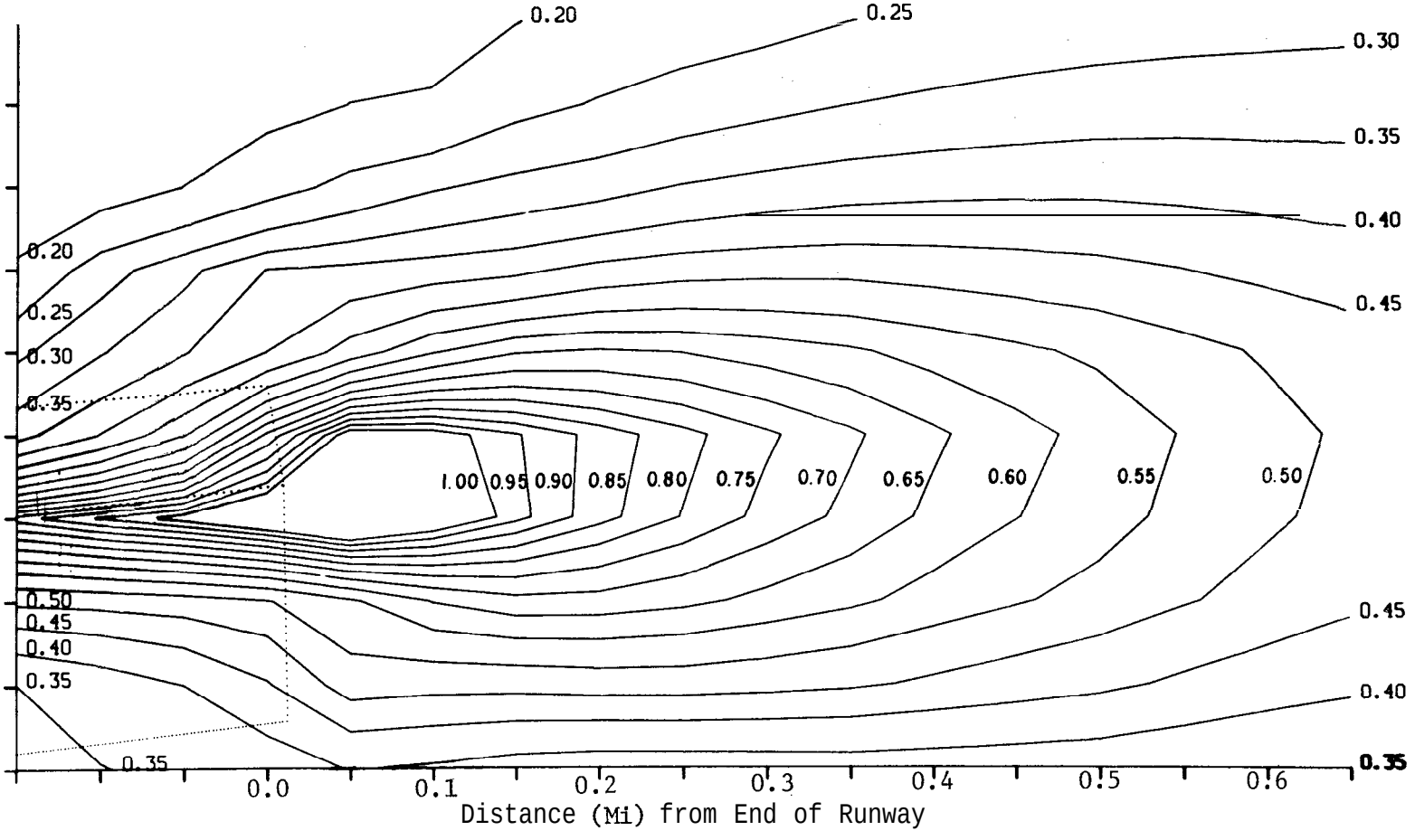

Fig. 1.9. MODIFIED AVAP Simulation of "Worst Case" (E Stability, Westerly 2-Knot Wind, and an Equivalent Departure Rate of Approximately 30 B727 Aircraft) NO, Conditions behind a Typical Busy Runway Complex. Runways and Taxiways are shown as dotted lines. NO, contour levels, given in ppm, suggest possible high NO_2 concentrations but reactive plume calculation needed to confirm this. Computation grid size = 0.05 mile.

Just as the issue of NO_2 impact assessment is more complicated than for CO or HC, so too is the issue of NO, control. Plagued by poor control technology and high control costs, NO,, which originates primarily from the high thrust takeoff mode, cannot be "managed" as effectively through minimization of engine idle time as can be CO and HC.

Just as the issue of NO_2 impact assessment is more complicated than for CO or HC, so too is the issue of NO, control. Plagued by poor control technology and high control costs, NO,, which originates primarily from the high thrust takeoff mode, cannot be "managed" as effectively through minimization of engine idle time as can be CO and HC.

2 HISTORICAL SURVEY OF AIRPORT AIR QUALITY STUDIES

As consequences of the 1967 Air Quality Act (U.S. Congress, 1967) and the 1970 Clean Air Act Amendments (U.S. Congress, 1970) a number of studies have been conducted to determine the contributions of aircraft emissions to the air quality in the vicinity of airports. This chapter summarizes the history of these studies, their purposes, and the conclusions which have been previously drawn from them. Also pointed out is a number of study difficulties which have brought those study conclusions into question, and have led to additional studies aimed at resolving remaining questions. The final section of this chapter discusses the meteorological aspects of "worst case" air quality conditions.

2.1 HISTORICAL OVERVIEW

The contributions of aircraft as sources of air pollution were not seriously considered until the introduction of turbojet aircraft into air carrier service in the late 1950's. Even though the particulate emissions of those earlier engines were highly visible, the first two reviews of their potential contributions by the Los Angeles Air Pollution Control District (George and Burlin, 1960) and the Coordinating Research Council (1960) did not consider the total emissions significant enough to warrant further investigation.

It was not until a second study by the LAAPCD (Lemke et al, 1965) and the Report of the Secretary of HEW on the "Nature and Control of Aircraft Engine Exhaust Emissions" (U.S. DHEW, 1968) that the subject of control was brought into serious discussion as "feasible and desirable." Of principal concern were CO and organic particulates. These findings by the HEW led to further quantification of emissions inventories by Northern Research and Engineering Corporation (NREC) under contract to the Public Health Service of HEW and later to the U.S. EPA (e.g., Bastress et al, 1971). This was followed by the development of an air quality impact assessment technique by the Northern Research and Engineering Corporation (NREC) with assistance from Environmental Research & Technology, Inc. (ERT). The result was the first air quality model specifically designed for airports.

2 HISTORICAL SURVEY OF AIRPORT AIR QUALITY STUDIES

As consequences of the 1967 Air Quality Act (U.S. Congress, 1967) and the 1970 Clean Air Act Amendments (U.S. Congress, 1970) a number of studies have been conducted to determine the contributions of aircraft emissions to the air quality in the vicinity of airports. This chapter summarizes the history of these studies, their purposes, and the conclusions which have been previously drawn from them. Also pointed out is a number of study difficulties which have brought those study conclusions into question, and have led to additional studies aimed at resolving remaining questions. The final section of this chapter discusses the meteorological aspects of "worst case" air quality conditions.

2.1 HISTORICAL OVERVIEW

The contributions of aircraft as sources of air pollution were not seriously considered until the introduction of turbojet aircraft into air carrier service in the late 1950's. Even though the particulate emissions of those earlier engines were highly visible, the first two reviews of their potential contributions by the Los Angeles Air Pollution Control District (George and Burlin, 1960) and the Coordinating Research Council (1960) did not consider the total emissions significant enough to warrant further investigation.

It was not until a second study by the LAAPCD (Lemke et al, 1965) and the Report of the Secretary of HEW on the "Nature and Control of Aircraft Engine Exhaust Emissions" (U.S. DHEW, 1968) that the subject of control was brought into serious discussion as "feasible and desirable." Of principal concern were CO and organic particulates. These findings by the HEW led to further quantification of emissions inventories by Northern Research and Engineering Corporation (NREC) under contract to the Public Health Service of HEW and later to the U.S. EPA (e.g., Bastress et al, 1971). This was followed by the development of an air quality impact assessment technique by the Northern Research and Engineering Corporation (NREC) with assistance from Environmental Research & Technology, Inc. (ERT). The result was the first air quality model specifically designed for airports.

Due to problems resulting from inadequate determination of off-airport sources of CO, the ORD validation effort (Rote et al, 1973) was more successful when NO, measurements were compared with AVAP predictions. A subsequent effort to compare AVAP results with monitoring data from Hartsville International Airport in Atlanta was complicated by troubles with the measurement program (Cirillo, et al, 1975). Though absolute concentrations of CO, NO,, and HC remained in doubt, the Atlanta study results have been useful in exploring the relative sensitivity of concentration patterns to various aircraft operational procedures.

2.2 SUMMARY OF PREVIOUS AIRPORT MODELING AND MONITORING RESULTS

There is continuing concern about impacts of aircraft related emissions upon air quality in public areas both inside and outside of airport boundaries. On a regional basis HC and NO, emissions must be considered because of their role in photochemical oxidant formation, and, not surprisingly, many of the cities with oxidant standard attainment problems have large airports associated with them. An airport's contribution in these major urban areas usually constitutes 1-3% of the emissions burden from all sources of HC and NO,.

An airport at a rural location may represent the largest single contributor on an annual basis to the inventories of CO, HC, and NO, emissions in its area of air quality influence; but, it is local effects of these pollutants in comparison with shorter term standards which are currently of greatest concern.

The continuing questions about the adequacy of airport modeling methods can often be traced to one of the following:

1. There are several airport models which give widely varying results.
2. The modeling assumptions are not always clearly defined; and their applicability to specialized airport source geometries (e.g., jet engine exhausts in terminal areas) has been questioned.
3. The validation experiments for airport models are few, and those validations that do exist have not been particularly successful even for the relatively sophisticated models.
4. The scales of interest to the user may not coincide with those for which the mathematical model was developed. A user may often expect finer resolution of concentration patterns than is reasonable or better agreement between a few short-term measurements and predicted ensemble

Due to problems resulting from inadequate determination of off-airport sources of CO, the ORD validation effort (Rote et al, 1973) was more successful when NO, measurements were compared with AVAP predictions. A subsequent effort to compare AVAP results with monitoring data from Hartsville International Airport in Atlanta was complicated by troubles with the measurement program (Cirillo, et al, 1975). Though absolute concentrations of CO, NO,, and HC remained in doubt, the Atlanta study results have been useful in exploring the relative sensitivity of concentration patterns to various aircraft operational procedures.

2.2 SUMMARY OF PREVIOUS AIRPORT MODELING AND MONITORING RESULTS

There is continuing concern about impacts of aircraft related emissions upon air quality in public areas both inside and outside of airport boundaries. On a regional basis HC and NO, emissions must be considered because of their role in photochemical oxidant formation, and, not surprisingly, many of the cities with oxidant standard attainment problems have large airports associated with them. An airport's contribution in these major urban areas usually constitutes 1-3% of the emissions burden from all sources of HC and NO,.

An airport at a rural location may represent the largest single contributor on an annual basis to the inventories of CO, HC, and NO, emissions in its area of air quality influence; but, it is local effects of these pollutants in comparison with shorter term standards which are currently of greatest concern.

The continuing questions about the adequacy of airport modeling methods can often be traced to one of the following:

1. There are several airport models which give widely varying results.
2. The modeling assumptions are not always clearly defined; and their applicability to specialized airport source geometries (e.g., jet engine exhausts in terminal areas) has been questioned.
3. The validation experiments for airport models are few, and those validations that do exist have not been particularly successful even for the relatively sophisticated models.
4. The scales of interest to the user may not coincide with those for which the mathematical model was developed. A user may often expect finer resolution of concentration patterns than is reasonable or better agreement between a few short-term measurements and predicted ensemble

measurement data quality can often be challenged, the lack of verification for the simpler sub-components of the model calculations has made it difficult to identify with any uncertainty the main reasons for poor overall comparisons.

As just recently pointed out by Turner (1979), it is only through the repeated verification of each of the sub-components of an air quality dispersion model, that the validity of the overall model results will be eventually demonstrated. The last section considers the question of the identification of the meteorological conditions that are associated with the highest ground level concentrations and that are presumably simulated by air quality models.

2.2.1 Carbon Monoxide Studies

The results of the principal investigations of CO concentrations at major airports are given in Table 2.1a. The results of these studies have been reported over the 1971 to 1979 period during which EPA development of aircraft engine control strategies has been continuing. The initial modeling estimates from the 1971 NREC study (Platt et al, 1971) for LAX, ORD, DCA and JFK airports are presented because they represent comparable modeling assumptions applied to a variety of airports. As can be seen in the table the majority of the remaining modeling studies utilized AQAM or AVAP. Careful examination of these results reveals that the majority of maximum measurements observed are within a factor of two of the predicted maximum for the same receptor areas. The model estimates of maxima are also generally higher even though the model may underpredict the majority of the cases which result in moderate concentrations. Interpretation of CO monitoring and modeling data is not complicated by significant chemical reactivity or measurement uncertainty. However, precise modeling of hot spot concentrations adjacent to obstructions requires modeling the flow around obstacles which is beyond the capability of present Gaussian-type airport models. Moreover, the locations where CO violations are often suspected have a large contribution of CO emissions by automobiles and access/service vehicles as well as aircraft.

When violations of the 8-hour standard are encountered, the aircraft may generally be identified as a major source only near the end of runways with heavy queuing activity during worst-case meteorlogical conditions. Since that is not an area in which the public is generally exposed, a modeled violation of ambient standards downwind of a queueing area probably does not

measurement data quality can often be challenged, the lack of verification for the simpler sub-components of the model calculations has made it difficult to identify with any uncertainty the main reasons for poor overall comparisons.

As just recently pointed out by Turner (1979), it is only through the repeated verification of each of the sub-components of an air quality dispersion model, that the validity of the overall model results will be eventually demonstrated. The last section considers the question of the identification of the meteorological conditions that are associated with the highest ground level concentrations and that are presumably simulated by air quality models.

2.2.1 Carbon Monoxide Studies

The results of the principal investigations of CO concentrations at major airports are given in Table 2.1a. The results of these studies have been reported over the 1971 to 1979 period during which EPA development of aircraft engine control strategies has been continuing. The initial modeling estimates from the 1971 NREC study (Platt et al, 1971) for LAX, ORD, DCA and JFK airports are presented because they represent comparable modeling assumptions applied to a variety of airports. As can be seen in the table the majority of the remaining modeling studies utilized AQAM or AVAP. Careful examination of these results reveals that the majority of maximum measurements observed are within a factor of two of the predicted maximum for the same receptor areas. The model estimates of maxima are also generally higher even though the model may underpredict the majority of the cases which result in moderate concentrations. Interpretation of CO monitoring and modeling data is not complicated by significant chemical reactivity or measurement uncertainty. However, precise modeling of hot spot concentrations adjacent to obstructions requires modeling the flow around obstacles which is beyond the capability of present Gaussian-type airport models. Moreover, the locations where CO violations are often suspected have a large contribution of CO emissions by automobiles and access/service vehicles as well as aircraft.

When violations of the 8-hour standard are encountered, the aircraft may generally be identified as a major source only near the end of runways with heavy queuing activity during worst-case meteorlogical conditions. Since that is not an area in which the public is generally exposed, a modeled violation of ambient standards downwind of a queueing area probably does not

present a health hazard. Lorang's review (1978) claims that monitoring has shown that CO violations have occurred in terminal areas and that suggests that aircraft emissions were important contributors at both LAX and DCA. It may also be pointed out, however, that the CO levels due to the airport (as modeled in Atlanta) usually drops off very rapidly with distance. Therefore potential problems are localized within the airport property.

The recent measurement program at Boston's Logan Airport (Smith and Heinold, 1980) illustrated that measured concentrations were much below standards during periods of high airport activity in areas near the ends of runways with long queues of taxiing aircraft. The highest concentrations occurred instead, when winds from nearby urban centers coincided with a strong nocturnal inversion. These CO concentrations tend to be overpredicted by most present airport dispersion models. Therefore, it appears that proper modeling techniques must consider these situations as well as the microscale CO problem in terminal areas. The latter modeling must, however, account for building wake effects and local sources, such as vehicular traffic, if the true relative impacts of aircraft sources are to be realistically portrayed at the terminal.

2.2.2 Hydrocarbon Studies

The results summarized in Table 2.1b are for the same airports as those given in Table 2.1a, except that there were no studies of HC performed at the Seattle or the Van Nuys airports. It is immediately apparent that both nonmethane hydrocarbon (NMHC) and total hydrocarbon (THC) measurements as well as predictions are well above the 160 $\mu g/m^3$ (6 AM-9 AM average) established as an EPA guideline for management of photochemical pollutants. Comparisons of the wide ranging concentrations among receptor points on and near airports reveals that aircraft do indeed contribute to the elevated values in the vicinity of airport boundaries. The maximum on-airport concentrations occur in idling and taxiing areas, and particularly in queues awaiting takeoff. The studies of pollutant control strategies at Atlanta (Cirillo, et al, 1975) and the recent Boston study (Smith and Heinold, 1980) both indicated that regulation of queuing and taxiing times may serve as effective measures for diminishing hydrocarbons and organic particulates (and the odors associated with these) with current aircraft engine designs.

present a health hazard. Lorang's review (1978) claims that monitoring has shown that CO violations have occurred in terminal areas and that suggests that aircraft emissions were important contributors at both LAX and DCA. It may also be pointed out, however, that the CO levels due to the airport (as modeled in Atlanta) usually drops off very rapidly with distance. Therefore potential problems are localized within the airport property.

The recent measurement program at Boston's Logan Airport (Smith and Heinold, 1980) illustrated that measured concentrations were much below standards during periods of high airport activity in areas near the ends of runways with long queues of taxiing aircraft. The highest concentrations occurred instead, when winds from nearby urban centers coincided with a strong nocturnal inversion. These CO concentrations tend to be overpredicted by most present airport dispersion models. Therefore, it appears that proper modeling techniques must consider these situations as well as the microscale CO problem in terminal areas. The latter modeling must, however, account for building wake effects and local sources, such as vehicular traffic, if the true relative impacts of aircraft sources are to be realistically portrayed at the terminal.

2.2.2 Hydrocarbon Studies

The results summarized in Table 2.1b are for the same airports as those given in Table 2.1a, except that there were no studies of HC performed at the Seattle or the Van Nuys airports. It is immediately apparent that both nonmethane hydrocarbon (NMHC) and total hydrocarbon (THC) measurements as well as predictions are well above the 160 $\mu g/m^3$ (6 AM-9 AM average) established as an EPA guideline for management of photochemical pollutants. Comparisons of the wide ranging concentrations among receptor points on and near airports reveals that aircraft do indeed contribute to the elevated values in the vicinity of airport boundaries. The maximum on-airport concentrations occur in idling and taxiing areas, and particularly in queues awaiting takeoff. The studies of pollutant control strategies at Atlanta (Cirillo, et al, 1975) and the recent Boston study (Smith and Heinold, 1980) both indicated that regulation of queuing and taxiing times may serve as effective measures for diminishing hydrocarbons and organic particulates (and the odors associated with these) with current aircraft engine designs.

A report on the air quality associated with Air Force bases (Daley and Naugle, 1978) and (Naugle et al, 1978) suggests that HC and NO, emissions from aircraft at airports present the greatest potential harm according to the EPA's pollution standards index (PSI). Since present and projected jet engine designs are able to effectively decrease hydrocarbon (and CO) emissions by increasing combustion efficiency, control of HC and CO are expected to be less difficult than NO,. Because of its rural location, the study at Williams AFB avoided the problem of high urban background pollution conditions for model-measurement comparisons. Using the AQAM model, THC's displayed the highest PSI levels at distances beyond the airport boundary. However, this PSI approach for HC analysis suffers from the problems inherent in using simple guideline HC levels as measures of O_3 production and oxidant health effects.

Unfortunately, most studies make no distinction between total and reactive hydrocarbons. Even when conservative assumptions are invoked, a distinction should be made between representing NO, (NO, NO_2) and NO_2 and THC and NMHC. In an oxidizing atmosphere, NO is converted to NO_2, whereas CH_4 is nonreactive at ambient temperatures and ozone concentrations. To acknowledge the inconsistency but ignore it in the interpretation of monitoring and modeling studies [as in Lorang (1978)], leads to excessively pessimistic predictions about the role of airports in violations of the Air Quality Guideline.

2.2.3 Oxides of Nitrogen Studies

The results of NO, and NO_2 measurements and NO, model predictions are presented in Table 2.1c for the same airports (and studies) for which HC results were given in Table 2.1b. It should be noted that the values given in the NREC modeling study relate to an annual average standard. For most of the studies involving both measurements and modeling, hourly values are given in both instances. In addition, most measurement studies report both NO_2 and total NO,, even though modeling generally assumes that NO, is the more reliable parameter to predict. (This is especially true for long term average predictions).

Considering an annual standard of 0.05 ppm (100 $\mu g/m^3$) for NO_2, the conservative assumption that NO_2 = NO, concentrations leads to the conclusion that most of the airports modeled by NREC might have a problem meeting the

A report on the air quality associated with Air Force bases (Daley and Naugle, 1978) and (Naugle et al, 1978) suggests that HC and NO, emissions from aircraft at airports present the greatest potential harm according to the EPA's pollution standards index (PSI). Since present and projected jet engine designs are able to effectively decrease hydrocarbon (and CO) emissions by increasing combustion efficiency, control of HC and CO are expected to be less difficult than NO,. Because of its rural location, the study at Williams AFB avoided the problem of high urban background pollution conditions for model-measurement comparisons. Using the AQAM model, THC's displayed the highest PSI levels at distances beyond the airport boundary. However, this PSI approach for HC analysis suffers from the problems inherent in using simple guideline HC levels as measures of O_3 production and oxidant health effects.

Unfortunately, most studies make no distinction between total and reactive hydrocarbons. Even when conservative assumptions are invoked, a distinction should be made between representing NO, (NO, NO_2) and NO_2 and THC and NMHC. In an oxidizing atmosphere, NO is converted to NO_2, whereas CH_4 is nonreactive at ambient temperatures and ozone concentrations. To acknowledge the inconsistency but ignore it in the interpretation of monitoring and modeling studies [as in Lorang (1978)], leads to excessively pessimistic predictions about the role of airports in violations of the Air Quality Guideline.

2.2.3 Oxides of Nitrogen Studies

The results of NO, and NO_2 measurements and NO, model predictions are presented in Table 2.1c for the same airports (and studies) for which HC results were given in Table 2.1b. It should be noted that the values given in the NREC modeling study relate to an annual average standard. For most of the studies involving both measurements and modeling, hourly values are given in both instances. In addition, most measurement studies report both NO_2 and total NO,, even though modeling generally assumes that NO, is the more reliable parameter to predict. (This is especially true for long term average predictions).

Considering an annual standard of 0.05 ppm (100 $\mu g/m^3$) for NO_2, the conservative assumption that NO_2 = NO, concentrations leads to the conclusion that most of the airports modeled by NREC might have a problem meeting the

A report on the air quality associated with Air Force bases (Daley and Naugle, 1978) and (Naugle et al, 1978) suggests that HC and NO, emissions from aircraft at airports present the greatest potential harm according to the EPA's pollution standards index (PSI). Since present and projected jet engine designs are able to effectively decrease hydrocarbon (and CO) emissions by increasing combustion efficiency, control of HC and CO are expected to be less difficult than NO,. Because of its rural location, the study at Williams AFB avoided the problem of high urban background pollution conditions for model-measurement comparisons. Using the AQAM model, THC's displayed the highest PSI levels at distances beyond the airport boundary. However, this PSI approach for HC analysis suffers from the problems inherent in using simple guideline HC levels as measures of O_3 production and oxidant health effects.

Unfortunately, most studies make no distinction between total and reactive hydrocarbons. Even when conservative assumptions are invoked, a distinction should be made between representing NO, (NO, NO_2) and NO_2 and THC and NMHC. In an oxidizing atmosphere, NO is converted to NO_2, whereas CH_4 is nonreactive at ambient temperatures and ozone concentrations. To acknowledge the inconsistency but ignore it in the interpretation of monitoring and modeling studies [as in Lorang (1978)], leads to excessively pessimistic predictions about the role of airports in violations of the Air Quality Guideline.

2.2.3 Oxides of Nitrogen Studies

The results of NO, and NO_2 measurements and NO, model predictions are presented in Table 2.1c for the same airports (and studies) for which HC results were given in Table 2.1b. It should be noted that the values given in the NREC modeling study relate to an annual average standard. For most of the studies involving both measurements and modeling, hourly values are given in both instances. In addition, most measurement studies report both NO_2 and total NO,, even though modeling generally assumes that NO, is the more reliable parameter to predict. (This is especially true for long term average predictions).

Considering an annual standard of 0.05 ppm (100 $\mu g/m^3$) for NO_2, the conservative assumption that NO_2 = NO, concentrations leads to the conclusion that most of the airports modeled by NREC might have a problem meeting the

critical factor in determining the need for further action in controlling aircraft emissions of NO,.

The actual conversion of aircraft NO, emissions to NO_2 is a complex function of meteorology, atmospheric photochemistry, and ambient concentrations of NO,, ozone, and hydrocarbons. NO, emissions from aircraft mainly consist of nitric oxide (NO). For example, emission measurements from Pratt and Whitney JT3D, JT8D, and JT9D jet engines have shown a typical NO_2/NO_x emissions ratio of 4 to 8% by volume (Pratt and Whitney, 1972). This is reflected in ambient air monitoring measurements at airports, where the NO_2/NO_x ambient ratio was found to be lower on the airport grounds than in areas surrounding the airport (Lorang, 1978).

A qualitative assessment has been made of the influence of aircraft NO, and hydrocarbon emissions on ozone formation downwind (Whitten and Hogo, 1976). The conclusion was that the mixing of aircraft jet exhaust with automobile exhaust can cause a more favorable hydrocarbon/NO, ratio for ozone formation than automobile exhaust alone. A simple semi-quantitative treatment of NO to NO_2 conversion at airports considered only one main chemical reaction (Jordan and Broderick, 1978, Jordan and Broderick, 1979); this treatment is valid only over short transport time scales where the presence of hydrocarbons can be neglected.

In order to quantitatively predict the NO_2 conversion of aircraft NO, emissions and the effect of aircraft NO, and hydrocarbon emissions on downwind ozone concentrations, a sophisticated photochemical air quality simulation model may be necessary. A number of photochemical models have been developed which can simulate chemistry, emissions, and atmospheric transport processes with detailed spatial and temporal resolution.* A methodology was developed to integrate an early photochemical model (NEXUS/P) with airport land use development (Norco et al., 1973); however, this photochemical model used a chemical kinetics mechanism that is now obsolete.

Only one study has been conducted that has used a detailed photochemical air quality simulation model to examine the effect of NO, and hydrocarbon

*The discussion here is limited to photochemical models applicable in the urban troposphere. The impact of aircraft emissions aloft on the stratosphere ozone layer requires the use of very different photochemical modeling techniques (Oliver et.al., 1977).

emissions from airport operations on air quality in the vicinity. This study (Duewer and Walton, 1978) was done in the San Francisco Bay area using the LIRAQ-2 grid-based photochemical model. The modeling showed that doubling airport emissions reduced ozone concentrations slightly at San Francisco Airport, but increased ozone downwind by approximately 0.003 ppm.

However, a grid-based photochemical model such as LIRAQ-2 is very expensive to run, both in terms of manpower and computer time, because concentrations must be calculated at a large number of grid cell points covering the entire urban region. A more useful modeling tool for studying the impact of airport emissions would be a trajectory-based photochemical model, such as the new ELSTAR model (Lloyd et al., 1979), which calculates concentrations along a specific path or trajectory of an air parcel. A trajectory-based photochemical model could economically study the effects of various airport emissions control strategies with a detailed consideration of both NO_2 and ozone formation in the vicinity of the airport.

2.3 METEOROLOGICAL ASPECTS OF AIRPORT AIR POLLUTION WORST CASE ANALYSIS

The ambient levels of air pollutants depend not only on the amount of pollutant emitted into the atmosphere but also upon the prevailing meteorological conditions. The dispersive capability of the atmosphere depends upon such meteorological parameters as the wind speed and the vertical temperature profile. Of course, the wind direction also plays an important role when considering any particular source-receptor pair. These parameters vary hourly, diurnally, and seasonally as both small- and large-scale weather patterns change.

The air quality effects of the prevailing meteorological conditions are not the same for all sources. Elevated sources have their greatest impact during unstable or neutral atmospheric conditions. High wind speeds, which may occur during periods of neutral stability will also reduce plume rise and bring plumes to the ground closer to the source than under lighter wind cases, thus diminishing the effect of greater initial dilution. Under stable atmospheric conditions or during a temperature inversion (ambient temperature increasing with height) the plume from an elevated point source may remain aloft and intact for many kilometers downwind. If the inversion layer exists above the elevation of the source, while the layer below is unstable, maximal concentrations may occur at short distances from the base of the source.

emissions from airport operations on air quality in the vicinity. This study (Duewer and Walton, 1978) was done in the San Francisco Bay area using the LIRAQ-2 grid-based photochemical model. The modeling showed that doubling airport emissions reduced ozone concentrations slightly at San Francisco Airport, but increased ozone downwind by approximately 0.003 ppm.

However, a grid-based photochemical model such as LIRAQ-2 is very expensive to run, both in terms of manpower and computer time, because concentrations must be calculated at a large number of grid cell points covering the entire urban region. A more useful modeling tool for studying the impact of airport emissions would be a trajectory-based photochemical model, such as the new ELSTAR model (Lloyd et al., 1979), which calculates concentrations along a specific path or trajectory of an air parcel. A trajectory-based photochemical model could economically study the effects of various airport emissions control strategies with a detailed consideration of both NO_2 and ozone formation in the vicinity of the airport.

2.3 METEOROLOGICAL ASPECTS OF AIRPORT AIR POLLUTION WORST CASE ANALYSIS

The ambient levels of air pollutants depend not only on the amount of pollutant emitted into the atmosphere but also upon the prevailing meteorological conditions. The dispersive capability of the atmosphere depends upon such meteorological parameters as the wind speed and the vertical temperature profile. Of course, the wind direction also plays an important role when considering any particular source-receptor pair. These parameters vary hourly, diurnally, and seasonally as both small- and large-scale weather patterns change.

The air quality effects of the prevailing meteorological conditions are not the same for all sources. Elevated sources have their greatest impact during unstable or neutral atmospheric conditions. High wind speeds, which may occur during periods of neutral stability will also reduce plume rise and bring plumes to the ground closer to the source than under lighter wind cases, thus diminishing the effect of greater initial dilution. Under stable atmospheric conditions or during a temperature inversion (ambient temperature increasing with height) the plume from an elevated point source may remain aloft and intact for many kilometers downwind. If the inversion layer exists above the elevation of the source, while the layer below is unstable, maximal concentrations may occur at short distances from the base of the source.

Table 2.2. Frequency of Poor Atmospheric Dispersion Conditionsa at Five Major Airports

Airport	Time Period Examined	Frequency[b]
DCA	1968-1972	30.7
LAX	1955-1964	35.1
LGA (NY)	1965-1970	19.7
ORD	1960-1964	29.0
Dulles	1966-1970	37.0

[a]Defined here as stable (E of F) stratification with a wind of 1-5 m/sec from any direction.

[b]Frequencies are based on a five year annual average period.

exceeding an hour, and is relatively near an area of high emission density. This definition, in itself, requires some knowledge of the pollutant concentration patterns associated with each wind direction under a range of wind speeds and atmospheric stabilities. Critical receptors are most precisely defined by evaluating a series of dispersion model analyses which cover the range of potentially critical cases. Temporal variation of emission patterns must, of course, also be considered. Preliminary estimates may be made, however, based upon the knowledge of the receptor map, the emissions map, and wind frequency tables. The worst case frequencies identified here are based upon those considerations and model analyses carried out for LAX, JFK, and ORD airports as reported in Volme II of this report. The stability classification scheme used here is the well-known method of Turner, 1964. While this method may be less precise than one which uses actual onsite measurement of turbulence intensity, it is generally the only method available for prospective studies of impacts based on historical meteorological records.

For LAX airport there are two potentially critical receptors: (1) the terminal area and (2) the restaurant and golf course to the East of runway 24L. The worst case wind directions for the terminal as a receptor are N and E to ESE. For the restaurant and golf course receptors W to WNW winds are most important. North winds result in higher concentrations but are

Table 2.2. Frequency of Poor Atmospheric Dispersion Conditionsa at Five Major Airports

Airport	Time Period Examined	Frequency[b]
DCA	1968-1972	30.7
LAX	1955-1964	35.1
LGA (NY)	1965-1970	19.7
ORD	1960-1964	29.0
Dulles	1966-1970	37.0

[a]Defined here as stable (E of F) stratification with a wind of 1-5 m/sec from any direction.

[b]Frequencies are based on a five year annual average period.

exceeding an hour, and is relatively near an area of high emission density. This definition, in itself, requires some knowledge of the pollutant concentration patterns associated with each wind direction under a range of wind speeds and atmospheric stabilities. Critical receptors are most precisely defined by evaluating a series of dispersion model analyses which cover the range of potentially critical cases. Temporal variation of emission patterns must, of course, also be considered. Preliminary estimates may be made, however, based upon the knowledge of the receptor map, the emissions map, and wind frequency tables. The worst case frequencies identified here are based upon those considerations and model analyses carried out for LAX, JFK, and ORD airports as reported in Volme II of this report. The stability classification scheme used here is the well-known method of Turner, 1964. While this method may be less precise than one which uses actual onsite measurement of turbulence intensity, it is generally the only method available for prospective studies of impacts based on historical meteorological records.

For LAX airport there are two potentially critical receptors: (1) the terminal area and (2) the restaurant and golf course to the East of runway 24L. The worst case wind directions for the terminal as a receptor are N and E to ESE. For the restaurant and golf course receptors W to WNW winds are most important. North winds result in higher concentrations but are

Table 2.3. Annual Percentage Frequencies[a] of Stable Stratification at LAX

Wind Direction	All Hours Wind Speed (Knots) 1-3	4-6	7-10	Hours 06-09 Wind Speed (Knots) 1-3	4-6	7-10
N	0.54	0.67	0.34	0.30	0.47	0.25
E	1.61	2.36	0.26	1.10	2.75	0.23
ESE	0.95	1.31	0.13	0.85	1.10	0.10
W	1.03	2.30	1.75	0.17	0.27	0.06
WNW	0.48	0.81	0.28	0.19	0.16	0.06

Table 2.4. Annual Percentage Frequencies[a] of Stable Stratification at DCA. All Hours

Wind Direction	Wind Speed (Knots) 1-3	4-6	7-10
N	0.34	0.96	0.41
NNE	0.15	0.50	0.30
NE	0.24	0.68	0.31
ENE	0.10	0.45	0.12
SSE	0.50	1.30	0.12

[a]Note that 0.02% is approximately two hours per year. Any calculated concentration exceeding a federal ambient air quality standard and associated with a greater frequency could result in a violation.

Table 2.3. Annual Percentage Frequencies[a] of Stable Stratification at LAX

Wind Direction	All Hours Wind Speed (Knots) 1-3	4-6	7-10	Hours 06-09 Wind Speed (Knots) 1-3	4-6	7-10
N	0.54	0.67	0.34	0.30	0.47	0.25
E	1.61	2.36	0.26	1.10	2.75	0.23
ESE	0.95	1.31	0.13	0.85	1.10	0.10
W	1.03	2.30	1.75	0.17	0.27	0.06
WNW	0.48	0.81	0.28	0.19	0.16	0.06

Table 2.4. Annual Percentage Frequencies[a] of Stable Stratification at DCA. All Hours

Wind Direction	Wind Speed (Knots) 1-3	4-6	7-10
N	0.34	0.96	0.41
NNE	0.15	0.50	0.30
NE	0.24	0.68	0.31
ENE	0.10	0.45	0.12
SSE	0.50	1.30	0.12

[a]Note that 0.02% is approximately two hours per year. Any calculated concentration exceeding a federal ambient air quality standard and associated with a greater frequency could result in a violation.

Table 2.3. Annual Percentage Frequencies[a] of Stable Stratification at LAX

Wind Direction	All Hours Wind Speed (Knots) 1-3	4-6	7-10	Hours 06-09 Wind Speed (Knots) 1-3	4-6	7-10
N	0.54	0.67	0.34	0.30	0.47	0.25
E	1.61	2.36	0.26	1.10	2.75	0.23
ESE	0.95	1.31	0.13	0.85	1.10	0.10
W	1.03	2.30	1.75	0.17	0.27	0.06
WNW	0.48	0.81	0.28	0.19	0.16	0.06

Table 2.4. Annual Percentage Frequencies[a] of Stable Stratification at DCA. All Hours

Wind Direction	Wind Speed (Knots) 1-3	4-6	7-10
N	0.34	0.96	0.41
NNE	0.15	0.50	0.30
NE	0.24	0.68	0.31
ENE	0.10	0.45	0.12
SSE	0.50	1.30	0.12

[a]Note that 0.02% is approximately two hours per year. Any calculated concentration exceeding a federal ambient air quality standard and associated with a greater frequency could result in a violation.

d) the proximity of large bodies of water or urban areas adjacent to many airports influences the range of possible stabilities and is generally not considered in worst case air quality assessments; and

e) the large, engine generated turbulence causes engine emitted pollutants to undergo an initial mixing that is somewhat stability class independent.

These considerations together with modeling approximations and limitations discussed in Volume. II suggest that the compromise choice of E stability and a wind speed of ~ 2 mph might best characterize worst case conditions.

d) the proximity of large bodies of water or urban areas adjacent to many airports influences the range of possible stabilities and is generally not considered in worst case air quality assessments; and

e) the large, engine generated turbulence causes engine emitted pollutants to undergo an initial mixing that is somewhat stability class independent.

These considerations together with modeling approximations and limitations discussed in Volume. II suggest that the compromise choice of E stability and a wind speed of ~ 2 mph might best characterize worst case conditions.

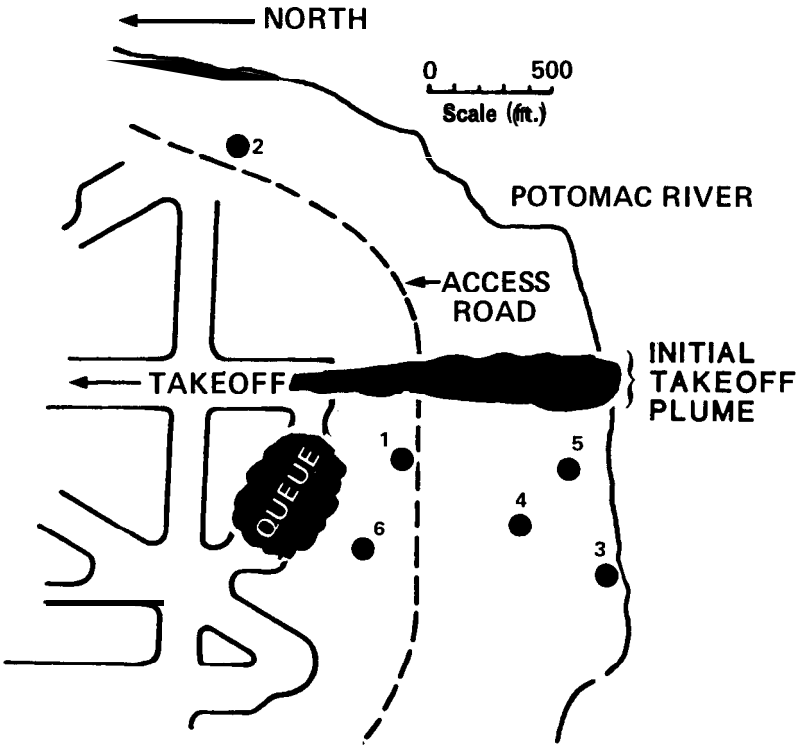

Fig. 3.1. Monitoring Site Locations at DCA. Sites were chosen to focus on the pollution clouds from the takeoff and queueing modes.

during the period January 15-Feburary 27, 1979. With the exception of station 2, which was sited specifically to obtain background pollutant levels under northerly to easterly wind conditions, Table 3.1 indicates the air quality parameters measured at each station. In addition, airport meteorological data were supplemented by measurement of wind speed and direction, wind azimuth and elevation angles, temperature, vertical temperature gradient, and dew point temperature at a site $\simeq 20$ m north of station 5. During the latter half of the program a decibel meter nearby station 4 measured aircraft engine noise and provided a convenient time reference for takeoff and landing operations.

Pollutant concentrations, noise level, and meteorological parameters were recorded on three independent systems: individual strip chart recorders for each instrument, a set of multi-pen strip chart recorders synchronized by an external time reference, and on magnetic tape via a 15-channel data acquisition system (DAS). While hourly average concentrations, as extracted from the strip charts, have been previously analyzed and compared to PAT., predictions

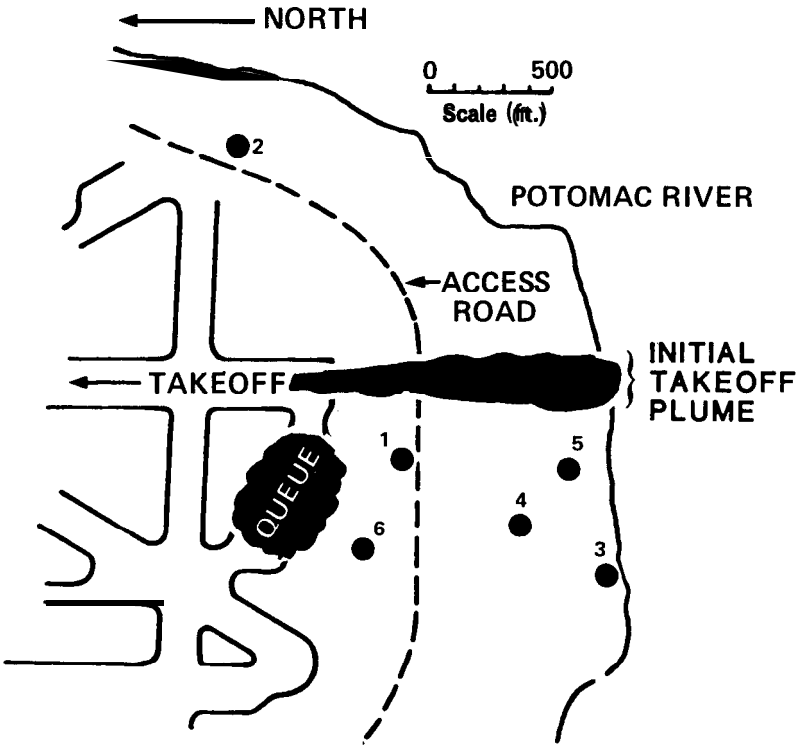

Fig. 3.1. Monitoring Site Locations at DCA. Sites were chosen to focus on the pollution clouds from the takeoff and queueing modes.

during the period January 15-Feburary 27, 1979. With the exception of station 2, which was sited specifically to obtain background pollutant levels under northerly to easterly wind conditions, Table 3.1 indicates the air quality parameters measured at each station. In addition, airport meteorological data were supplemented by measurement of wind speed and direction, wind azimuth and elevation angles, temperature, vertical temperature gradient, and dew point temperature at a site $\simeq 20$ m north of station 5. During the latter half of the program a decibel meter nearby station 4 measured aircraft engine noise and provided a convenient time reference for takeoff and landing operations.

Pollutant concentrations, noise level, and meteorological parameters were recorded on three independent systems: individual strip chart recorders for each instrument, a set of multi-pen strip chart recorders synchronized by an external time reference, and on magnetic tape via a 15-channel data acquisition system (DAS). While hourly average concentrations, as extracted from the strip charts, have been previously analyzed and compared to PAT., predictions

Table 3.1b. List of Monitoring Equipment

Site No.	Shelter No.	Shelter Dimensions	Parameter Measured	Equipment Instrument Manufacturer	Voltage Output
1	Self Propelled EPA #313	27'x8'x 14'*	NO, NO_x	Thermo Electron Company (TECO)	10V
				Bendix	10V 1V
			Single pen strip chart recorders (SCR) for each parameter.		
2 Background	Self Propelled EPA #376	27'x8'x30'**	CO	Bendix	10V
			O_3	Dasibi	
			HC	Bendix	1V
			NO_x	Bendix	1V
			Wind Direction & Velocity	Climatronics	
			Single pen strip chart recorders (SCR) for each parameter which is also input into data processing computer.		
	Trailer EPA #577	8'x14'x14'*	CO	Bendix	10V 1V
			NO_x NO	TECO	10V
			Wind Direction & Velocity	Climet	
			Wind Direction & Velocity (2 Dimensions)	MRI Vector Vane	
			Temperature and Temperature Gradient	Climet	
			Single pen SCR for each paramter.		
	Self Propelled EPA #315	Same as Site 1	NO_x	Bendix	1V
			CO	Bendix	10V 1V
			Single pen SCR for each parameter.		
			4 multi pen SCR coordinated to common time reference to simultaneously record concentrations at Sites 1, 3, 4, 5, 6. Data logger computer to record 15 channels of data from Sites 1, 3, 4, 5, 6.		
	Trailer EPA #575	Same as Site 3	NO_x	Bendix	1V
			Single pen SCR for each parameter		
6	Trailer EPA #576	Same as Site 3	CO	Bendix	10V
			CO	Energetic Sciences Co. (2), mobile	
			HC	Beckman 400	
			Single pen SCR for each parameter		

*Includes Air Intake Probe.

**Includes 22 foot high wind set.

Table 3.1b. List of Monitoring Equipment

Site No.	Shelter No.	Shelter Dimensions	Parameter Measured	Equipment Instrument Manufacturer	Voltage Output
1	Self Propelled EPA #313	27'x8'x 14'*	NO, NO_x	Thermo Electron Company (TECO)	10V
				Bendix	10V 1V
			Single pen strip chart recorders (SCR) for each parameter.		
2 Background	Self Propelled EPA #376	27'x8'x30'**	CO	Bendix	10V
			O_3	Dasibi	
			HC	Bendix	1V
			NO_x	Bendix	1V
			Wind Direction & Velocity	Climatronics	
			Single pen strip chart recorders (SCR) for each parameter which is also input into data processing computer.		
	Trailer EPA #577	8'x14'x14'*	CO	Bendix	10V 1V
			NO_x NO	TECO	10V
			Wind Direction & Velocity	Climet	
			Wind Direction & Velocity (2 Dimensions)	MRI Vector Vane	
			Temperature and Temperature Gradient	Climet	
			Single pen SCR for each paramter.		
	Self Propelled EPA #315	Same as Site 1	NO_x	Bendix	1V
			CO	Bendix	10V 1V
			Single pen SCR for each parameter.		
			4 multi pen SCR coordinated to common time reference to simultaneously record concentrations at Sites 1, 3, 4, 5, 6. Data logger computer to record 15 channels of data from Sites 1, 3, 4, 5, 6.		
	Trailer EPA #575	Same as Site 3	NO_x	Bendix	1V
			Single pen SCR for each parameter		
6	Trailer EPA #576	Same as Site 3	CO	Bendix	10V
			CO	Energetic Sciences Co. (2), mobile	
			HC	Beckman 400	
			Single pen SCR for each parameter		

*Includes Air Intake Probe.

**Includes 22 foot high wind set.

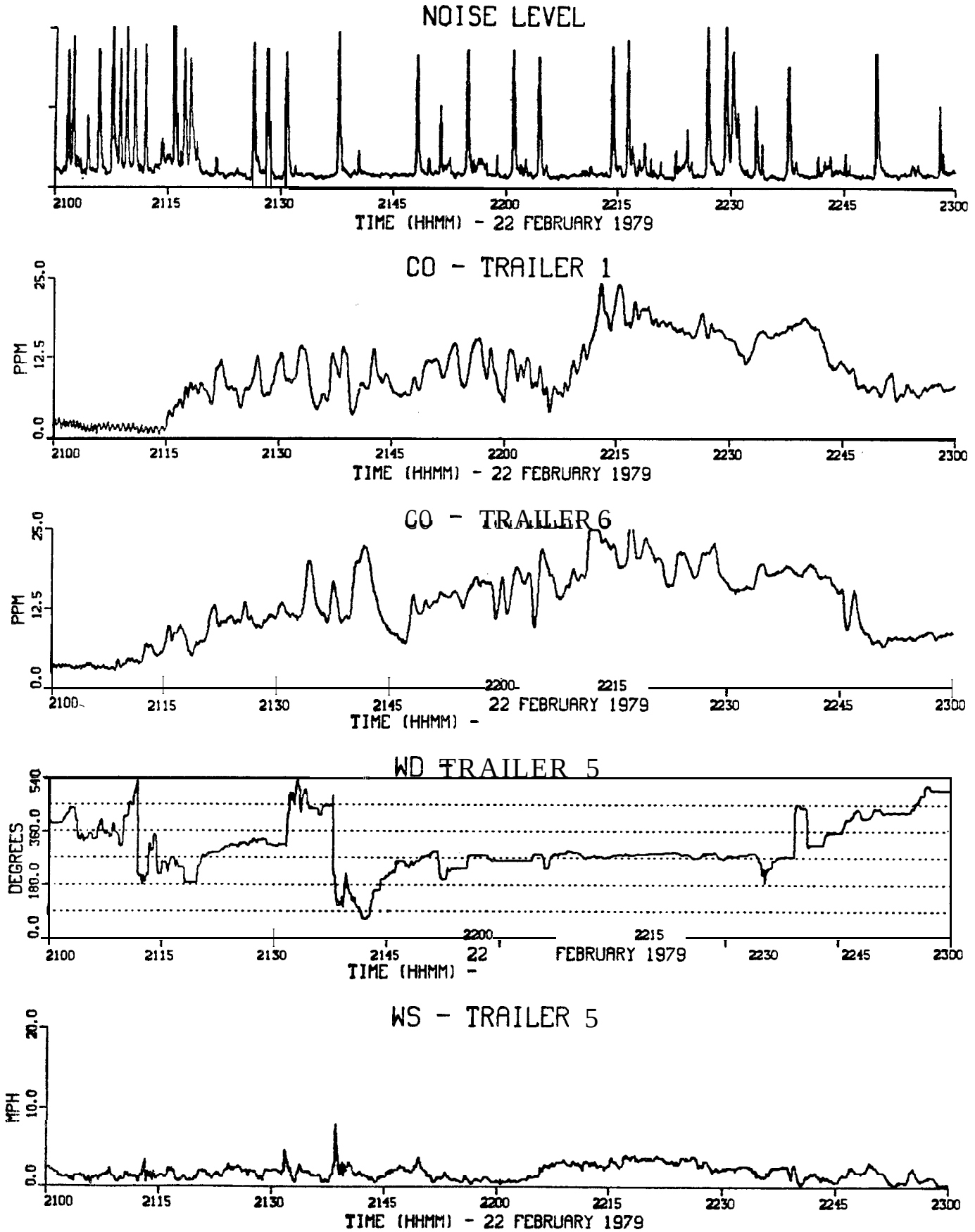

Fig. 3.2b. Synthesized Strip Chart from DAS Tapes for a Typical 2-hr of the CO Episode Beginning 2100 February 22.

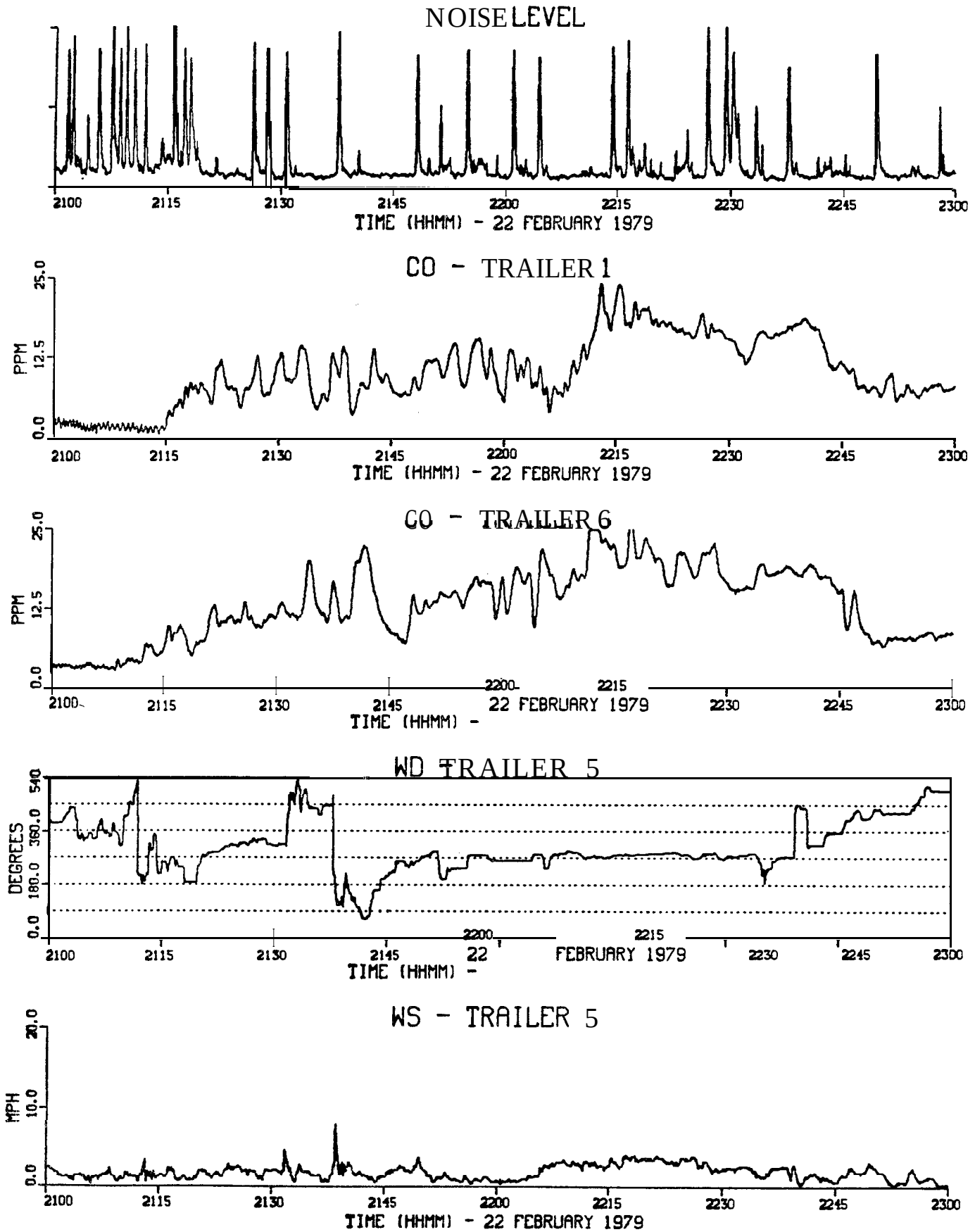

Fig. 3.2b. Synthesized Strip Chart from DAS Tapes for a Typical 2-hr of the CO Episode Beginning 2100 February 22.

seen by the dotted line) or through estimation of the area under the major, aircraft related pulses (i.e. as indicated by the hatched area> via a technique requiring a threshold concentration above background to be reached before integration and thus inclusion of a particular pulse.* Analysis of these individual, aircraft generated NO/NO_x signals, with the aid of an integrated Gaussian-puff type model that simulates the high thrust, high NO_x-emitting takeoff roll and parameterizes the NO_x plume behavior in terms of initial plume dimensions and subsequent plume transport and dilution rates is reported in Section 3.6. These new plume parameterizations permit more realistic prediction of peak, short-term, NO, levels near runways. Analysis of the CO signals, which are more difficult to associate with single aircraft operations due to the complexity of aircraft queueing, will now be discussed.

3.3 HOURLY AVERAGE MONITORING DATA FOR CO

While a number of agencies and groups concerned with the air quality impact of major airports have undertaken monitoring programs as well as theoretical studies based on the use of atmospheric dispersion algorithms, a recent review of these efforts by Lorang (1978) suggests that the issue is particularly confusing with respect to carbon monoxide. Ambient measurements conducted at Los Angeles International by Thayer et. al. (1974) and Washington National Airports by Platt et. al. (1971) were ambiguous as to their attribution of measured levels to either aircraft or non-aircraft sources. Similarly, initial modeling predictions using the NREC model [Platt et. al. (1971)] indicated the likelihood of violations of both the 1-hr ($40\ \mu g/m^3 \simeq 35$ ppm) and 8-hr ($10\ \mu g/m^3 \simeq 9$ ppm) standards for CO, while a more recent modeling exercise [Yamartino and Rote, (1978)] for LAX suggests "worst case" hourly CO concentrations, attributable to aircraft alone, of less than 5 ppm beyond 1000 ft from the aircraft queueing area and 2 ppm or less at the passenger terminals. Given the uncertainties generated by these monitoring and modeling experiences, the EPA and FAA chose to monitor CO near an aircraft queueing area at DCA.

*These techniques will subsequently be referred to as "background subtracted" and "pulse integrated" concentrations.

seen by the dotted line) or through estimation of the area under the major, aircraft related pulses (i.e. as indicated by the hatched area> via a technique requiring a threshold concentration above background to be reached before integration and thus inclusion of a particular pulse.* Analysis of these individual, aircraft generated NO/NO_x signals, with the aid of an integrated Gaussian-puff type model that simulates the high thrust, high NO,-emitting takeoff roll and parameterizes the NO_x plume behavior in terms of initial plume dimensions and subsequent plume transport and dilution rates is reported in Section 3.6. These new plume parameterizations permit more realistic prediction of peak, short-term, NO, levels near runways. Analysis of the CO signals, which are more difficult to associate with single aircraft operations due to the complexity of aircraft queueing, will now be discussed.

3.3 HOURLY AVERAGE MONITORING DATA FOR CO

While a number of agencies and groups concerned with the air quality impact of major airports have undertaken monitoring programs as well as theoretical studies based on the use of atmospheric dispersion algorithms, a recent review of these efforts by Lorang (1978) suggests that the issue is particularly confusing with respect to carbon monoxide. Ambient measurements conducted at Los Angeles International by Thayer et. al. (1974) and Washington National Airports by Platt et. al. (1971) were ambiguous as to their attribution of measured levels to either aircraft or non-aircraft sources. Similarly, initial modeling predictions using the NREC model [Platt et. al. (1971)] indicated the likelihood of violations of both the 1-hr (40 $\mu g/m^3 \simeq$ 35 ppm) and 8-hr (10 $\mu g/m^3 \simeq$ 9 ppm) standards for CO, while a more recent modeling exercise [Yamartino and Rote, (1978)] for LAX suggests 'worst case" hourly CO concentrations, attributable to aircraft alone, of less than 5 ppm beyond 1000 ft from the aircraft queueing area and 2 ppm or less at the passenger terminals. Given the uncertainties generated by these monitoring and modeling experiences, the EPA and FAA chose to monitor CO near an aircraft queueing area at DCA.

*These techniques will subsequently be referred to as "background subtracted" and "pulse integrated" concentrations.

Table 3.2. DCA Monitoring Experiment CO

	Station 1	Station 4	Station 3	Station 6	Ecolyzer 6
Mean (ppm)	0.98	0.46	0.36	1.30	1.68
Standard Deviation (ppm)	1.32	0.41	0.34	1.46	1.57
Minimum (ppm)	0.13	0.13	0.13	0.13	0.29
Maximum (ppm)	13.43	3.14	2.37	16.34	17.81
Number of Hours	562	386	168	679	708
Geometric Mean (ppm)	0.62	0.33	0.26	0.39	1.36
Geometric Standard Deviation (ppm)	2.58	2.55	2.11	2.22	1.81
Number of Values < Threshold*	89	130	74	29	0

*Values < instrument threshold (0.25 ppm) included as 1/2 threshold.

Table 3.2. DCA Monitoring Experiment CO

	Station 1	Station 4	Station 3	Station 6	Ecolyzer 6
Mean (ppm)	0.98	0.46	0.36	1.30	1.68
Standard Deviation (ppm)	1.32	0.41	0.34	1.46	1.57
Minimum (ppm)	0.13	0.13	0.13	0.13	0.29
Maximum (ppm)	13.43	3.14	2.37	16.34	17.81
Number of Hours	562	386	168	679	708
Geometric Mean (ppm)	0.62	0.33	0.26	0.39	1.36
Geometric Standard Deviation (ppm)	2.58	2.55	2.11	2.22	1.81
Number of Values < Threshold*	89	130	74	29	0

*Values < instrument threshold (0.25 ppm) included as 1/2 threshold.

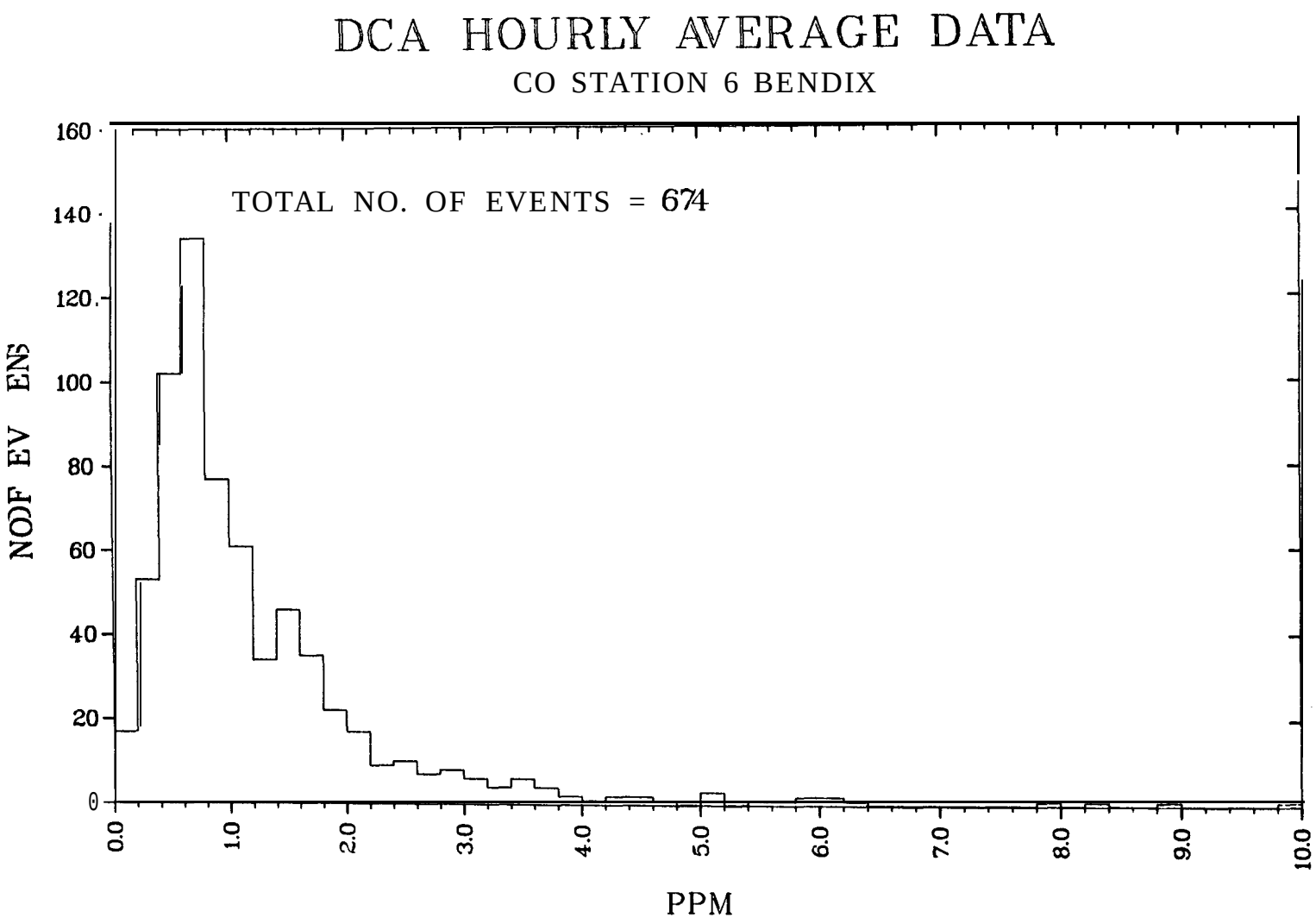

Fig. 3.5. Histogram of Hourly Average CO Concentrations at Station 6. Not Shown are Four Values Between 10 and 16.3 ppm.

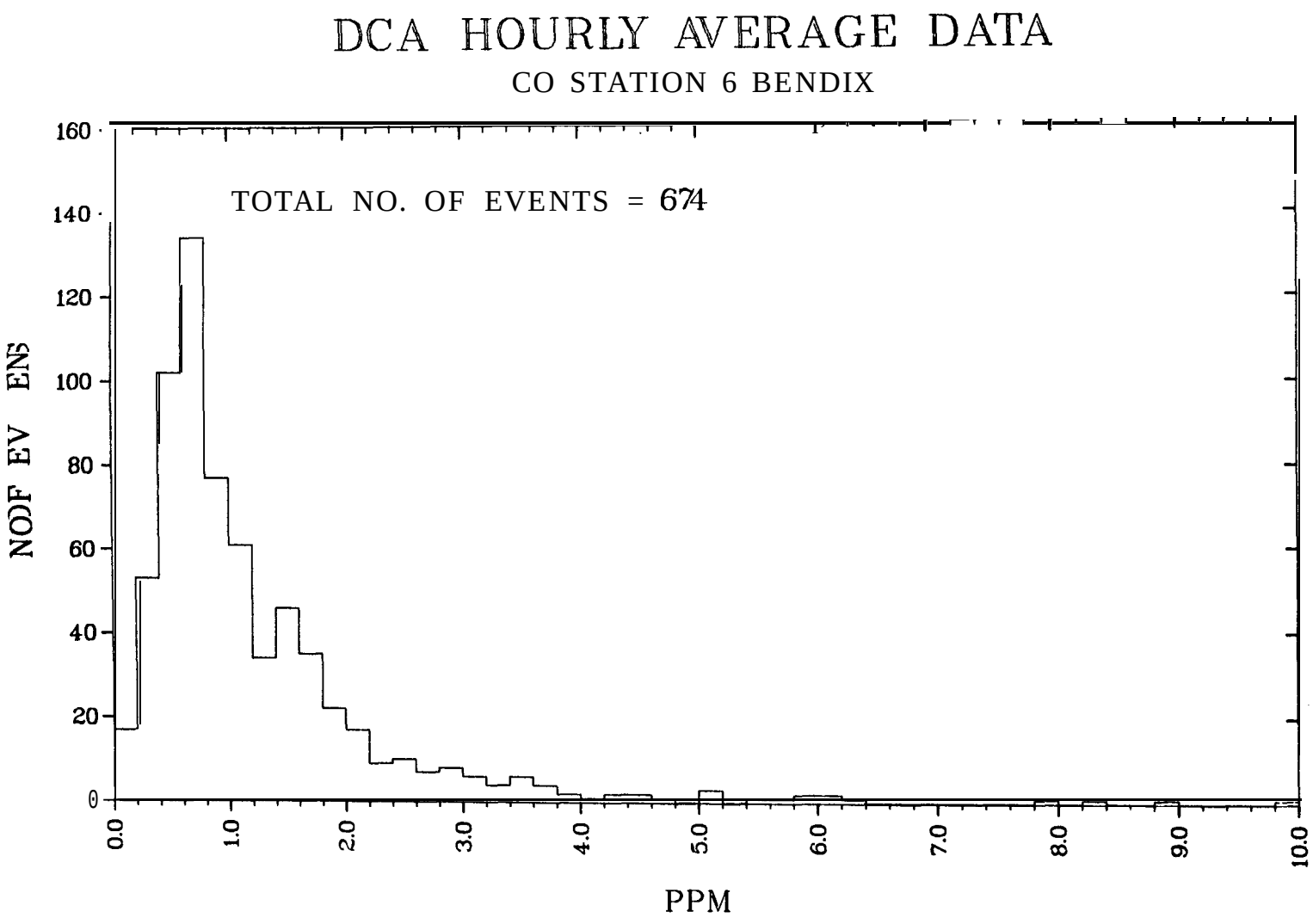

Fig. 3.5. Histogram of Hourly Average CO Concentrations at Station 6. Not Shown are Four Values Between 10 and 16.3 ppm.

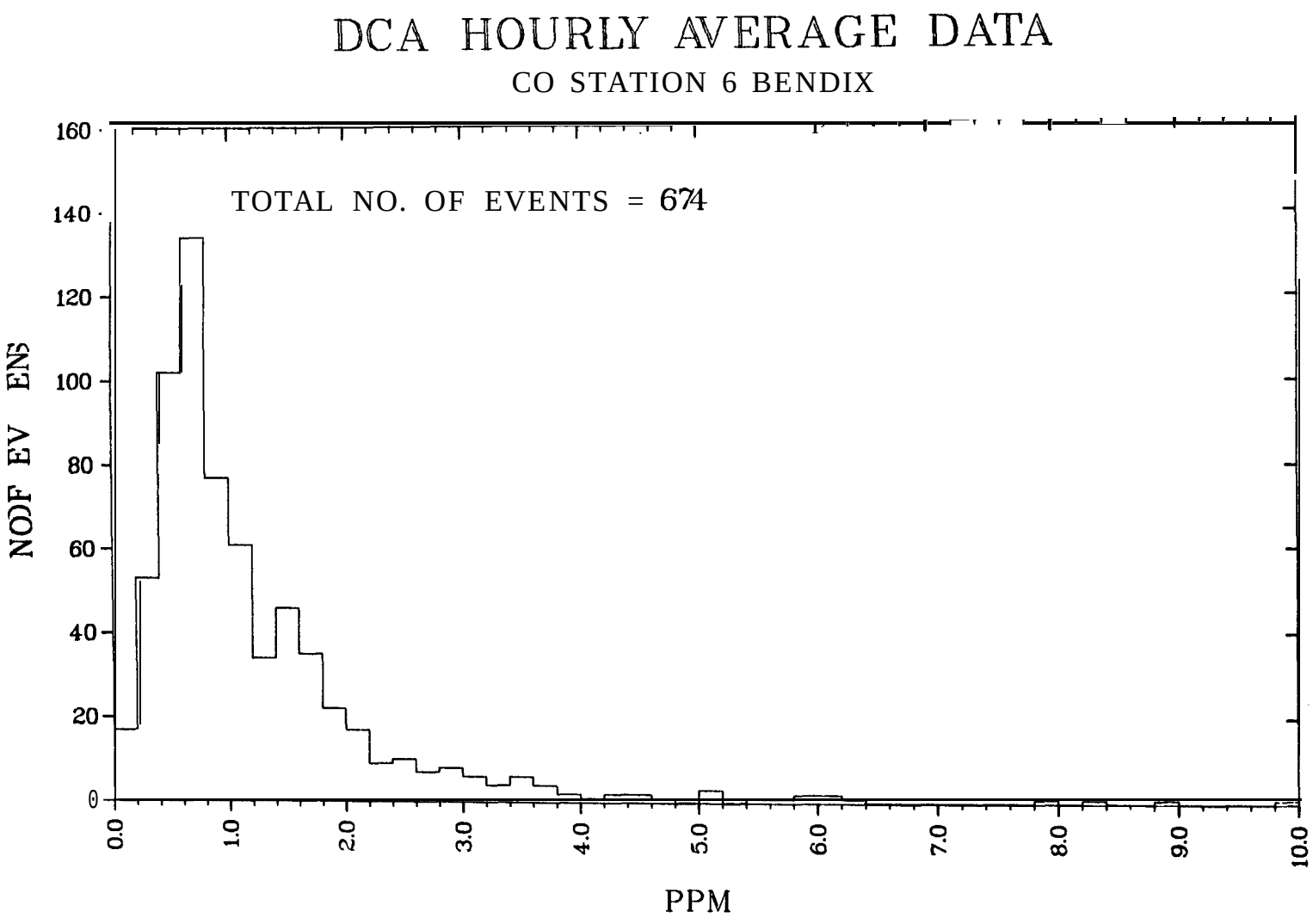

Fig. 3.5. Histogram of Hourly Average CO Concentrations at Station 6. Not Shown are Four Values Between 10 and 16.3 ppm.

lognormal concentration distributions) of the cumulative frequency distribution upward from below 10 ppm suggests that these greater-than-10 ppm values could occur. However, there is some question whether the observation of high concentrations at locations in such close proximity to the aircraft is relevant to the question of NAAQS violations. Lastly, we note that similarly high CO values were observed during this period by the local pollution control agency monitors throughout the entire Washington area.

Extrapolation of the curves in Fig. 3.6 out to the 99.99% probability level (i.e., 1 hr in 10,000 or approximately once per year), while informative, should be viewed with caution, as not only is such extrapolation based on only 1/12 of a year's data, but all these data come from a single contiguous set of hours rather than from a random selection of hours throughout the year.

Figures 3.8-3.10 represent an attempt at setting bounds on the aircraft contribution to the three curves in Fig. 3.6. In each of these figures the uppermost curve represents the distribution of total hourly average CO concentrations (same as Fig. 3.6), and thus represents the maximum possible impact of aircraft. The next lower lying curves (labeled 2) represent the "background" subtracted concentrations, where, in lieu of station 2 observations, "background" is defined as the average of the 12 minimum concentrations observed during the consecutive 5-min periods making up the hour. Coincidence of curves 1 and 2 at the lower concentrations arises when actual background is below instrument threshold and thus yields a "zero background" upon subtraction. The lowest lying curves (labeled 3) represent the average concentrations contributed by pollution pulses rising at least 0.35 ppm* above a 15-min average "background" and subsequently corrected upward by the factor $1/\mathrm{erf}\left[\sqrt{\ln (C_p/C_T)}\right]$, where C_p is the peak pulse concentration above background, to compensate for this 0.35 ppm "barrier" CT. Curve 3 thus isolates the contribution of nearby transient pollution sources. The fixed size of the "barrier" accounts for convergence of curves 2 and 3 at high concentrations. Thus, the actual aircraft (or more properly, local source) contribution to observed concentrations probably lies somewhere within the band defined by curves 1 and 3.

*This threshold barrier and the 0.035 ppm barrier for the NO, analysis were chosen by searching for the plateau region which is observed when the pulse integrated concentration is plotted as a function of threshold barrier level.

lognormal concentration distributions) of the cumulative frequency distribution upward from below 10 ppm suggests that these greater-than-10 ppm values could occur. However, there is some question whether the observation of high concentrations at locations in such close proximity to the aircraft is relevant to the question of NAAQS violations. Lastly, we note that similarly high CO values were observed during this period by the local pollution control agency monitors throughout the entire Washington area.

Extrapolation of the curves in Fig. 3.6 out to the 99.99% probability level (i.e., 1 hr in 10,000 or approximately once per year), while informative, should be viewed with caution, as not only is such extrapolation based on only 1/12 of a year's data, but all these data come from a single contiguous set of hours rather than from a random selection of hours throughout the year.

Figures 3.8-3.10 represent an attempt at setting bounds on the aircraft contribution to the three curves in Fig. 3.6. In each of these figures the uppermost curve represents the distribution of total hourly average CO concentrations (same as Fig. 3.6), and thus represents the maximum possible impact of aircraft. The next lower lying curves (labeled 2) represent the "background" subtracted concentrations, where, in lieu of station 2 observations, "background" is defined as the average of the 12 minimum concentrations observed during the consecutive 5-min periods making up the hour. Coincidence of curves 1 and 2 at the lower concentrations arises when actual background is below instrument threshold and thus yields a "zero background" upon subtraction. The lowest lying curves (labeled 3) represent the average concentrations contributed by pollution pulses rising at least 0.35 ppm* above a 15-min average "background" and subsequently corrected upward by the factor $1/\mathrm{erf}\left[\sqrt{\ln (C_p/C_T)}\right]$, where C_p is the peak pulse concentration above background, to compensate for this 0.35 ppm "barrier" CT. Curve 3 thus isolates the contribution of nearby transient pollution sources. The fixed size of the "barrier" accounts for convergence of curves 2 and 3 at high concentrations. Thus, the actual aircraft (or more properly, local source) contribution to observed concentrations probably lies somewhere within the band defined by curves 1 and 3.

*This threshold barrier and the 0.035 ppm barrier for the NO, analysis were chosen by searching for the plateau region which is observed when the pulse integrated concentration is plotted as a function of threshold barrier level.

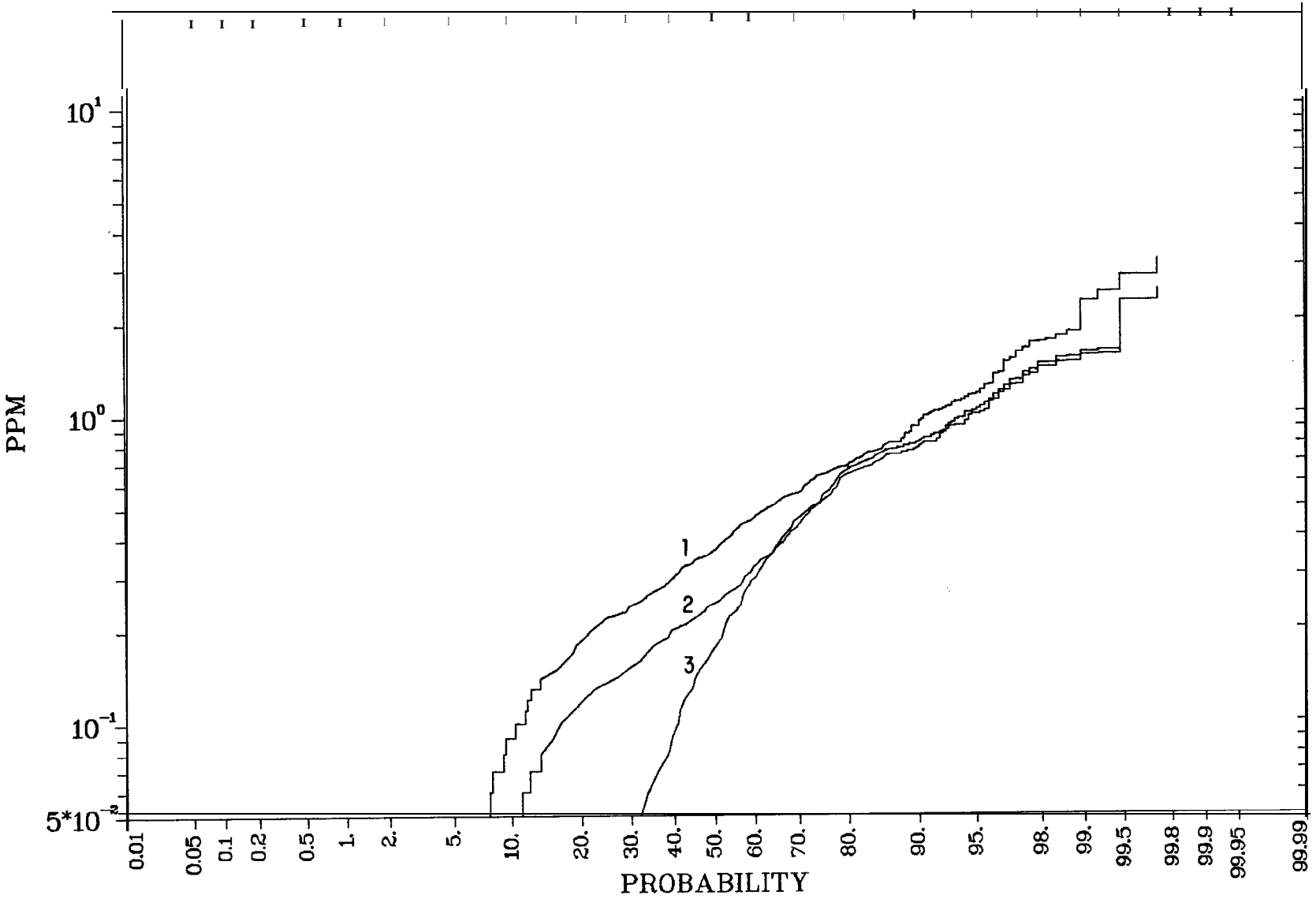

Fig. 3.9. Cumulative Frequency Distributions of Hourly CO Concentrations at Station 4. The three curves are explained in the text.

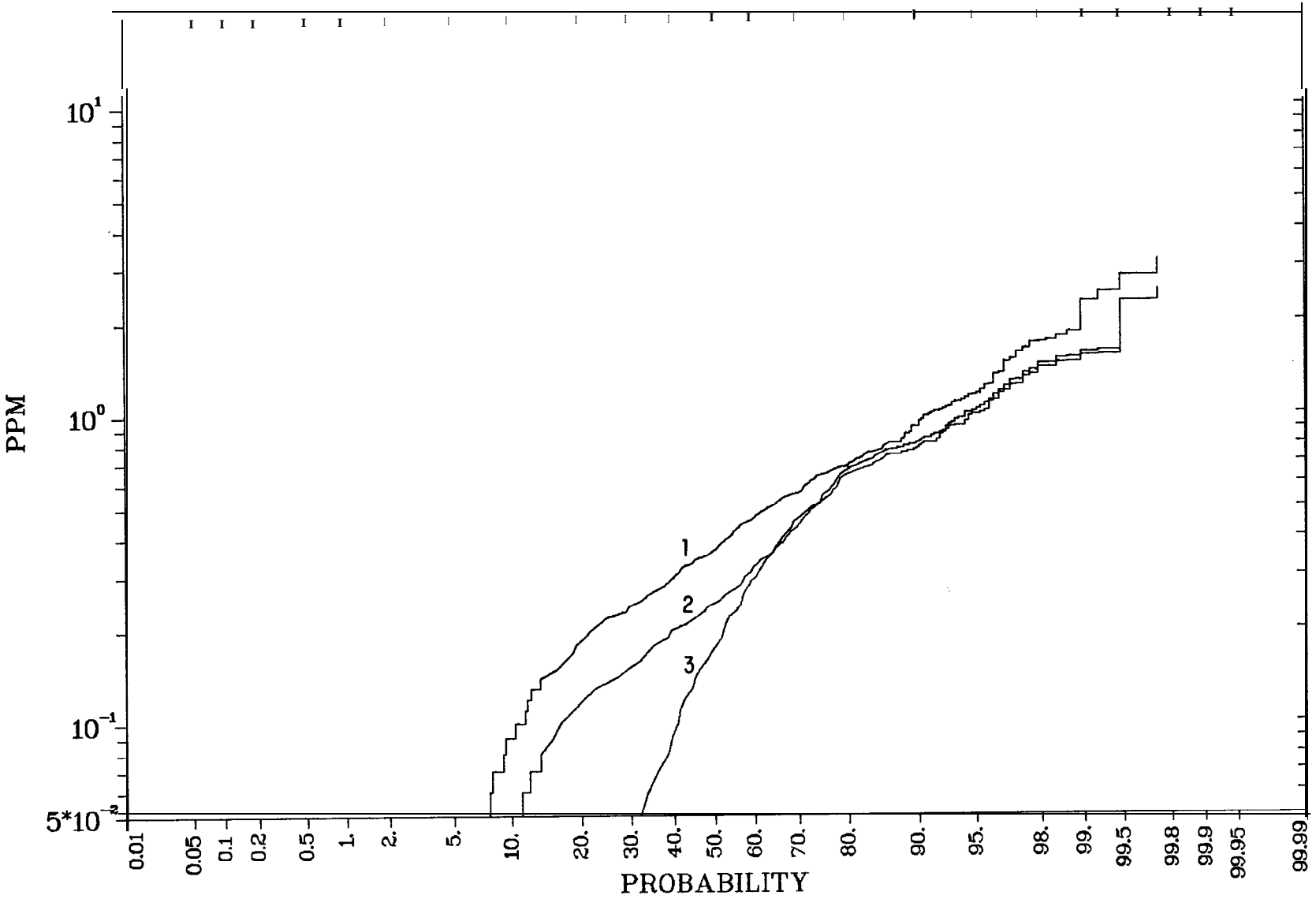

Fig. 3.9. Cumulative Frequency Distributions of Hourly CO Concentrations at Station 4. The three curves are explained in the text.

Keeping in mind previous cautions about extrapolation of these curves, one notes that at station 4, located ≃ 1000 ft from the queueing area, a maximum hourly CO concentration of ≃ 5 ppm may be expected about once per year. This result is consistent with "worst case" predictions for LAX, seen in Fig. 3.11, where a fleet mix and queueing emissions comparable to DCA are assumed. Further extrapolations or generalizations from the DCA results to other airports should be tempered by the following considerations:

- DCA is closed between 10:00 p.m. and 6:00 a.m. These nighttime hours are associated with stable atmospheric conditions and thus potentially poor pollutant dispersion conditions.
- Runway 36 at DCA is shared between arrivals and departures. Though not an unusual situation, airports having dedicated departure runways should, for the same departure rate, have shorter queueing times and correspondingly reduced CO emissions and concentrations.
- Nearly all operations at DCA are by medium range jets (e.g., 727, 737, DC9) primarily using the JT8D-17 engine. This engine has a relatively low CO emission rate at idle (≃40 lbs/hr)[8] compared to some other engines (e.g., 88 lbs/hr for the CF6-50C and ≃ 140 lbs/hr for the JT9D-7 and RB-211-22B).[8]

3.4 HOURLY AVERAGE MONITORING DATA FOR OXIDES OF NIRTOGEN

The issue of oxides of nitrogen (NO_x) impacts created by aircraft is, as with CO, a localized "hot-spot" problem related to existing and potential NAAQS. Unfortunately the issue is further complicated by the fact that

- present and possible future NAAQS standards pertain to NO_2 levels and not NO, levels. ($NO_x \approx NO + NO_2$)
- there is presently only an annual average NAAQS of 0.05 ppm NO_2 through a one hour average standard in the range 0.2-0.5 ppm is presently being considered by the EPA
- plume dispersion, while reducing the concentration of inert species, will entrain more amibient oxidant resulting in further conversion of engine emitted NO to NO_2; thus, NO_2 levels will peak at some distance downwind of the aircraft
- the peak NO_2 attributable to aircraft is a function of existing ambient levels of NO, NO_2, O_3, and sunlight.

Keeping in mind previous cautions about extrapolation of these curves, one notes that at station 4, located ≃ 1000 ft from the queueing area, a maximum hourly CO concentration of ≃ 5 ppm may be expected about once per year. This result is consistent with "worst case" predictions for LAX, seen in Fig. 3.11, where a fleet mix and queueing emissions comparable to DCA are assumed. Further extrapolations or generalizations from the DCA results to other airports should be tempered by the following considerations:

- DCA is closed between 10:00 p.m. and 6:00 a.m. These nighttime hours are associated with stable atmospheric conditions and thus potentially poor pollutant dispersion conditions.
- Runway 36 at DCA is shared between arrivals and departures. Though not an unusual situation, airports having dedicated departure runways should, for the same departure rate, have shorter queueing times and correspondingly reduced CO emissions and concentrations.
- Nearly all operations at DCA are by medium range jets (e.g., 727, 737, DC9) primarily using the JT8D-17 engine. This engine has a relatively low CO emission rate at idle (≃40 lbs/hr)[8] compared to some other engines (e.g., 88 lbs/hr for the CF6-50C and ≃ 140 lbs/hr for the JT9D-7 and RB-211-22B).[8]

3.4 HOURLY AVERAGE MONITORING DATA FOR OXIDES OF NIRTOGEN

The issue of oxides of nitrogen (NO_x) impacts created by aircraft is, as with CO, a localized "hot-spot" problem related to existing and potential NAAQS. Unfortunately the issue is further complicated by the fact that

- present and possible future NAAQS standards pertain to NO_2 levels and not NO, levels. ($NO_x \approx NO + NO_2$)
- there is presently only an annual average NAAQS of 0.05 ppm NO_2 through a one hour average standard in the range 0.2-0.5 ppm is presently being considered by the EPA
- plume dispersion, while reducing the concentration of inert species, will entrain more amibient oxidant resulting in further conversion of engine emitted NO to NO_2; thus, NO_2 levels will peak at some distance downwind of the aircraft
- the peak NO_2 attributable to aircraft is a function of existing ambient levels of NO, NO_2, O_3, and sunlight.

The potential for violation of possible NO_2 peak hourly standards at airports has recently been reveiwed by Jordan and Broderick (1978). Finding that both worst case modeling predictions and previous monitoring results were in the same 0.25-0.5 ppm range as the potential NO_2 standards, was one of the principal motivating factors for the DCA experiment. Rather than simply accumulating more NO/NO_x data, the placement of monitors and data recording rate at DCA were chosen so as to enable separation of the aircraft contribution (i.e. in the form of short pulses associated with takeoff/landing) from continuous source and background contributions. Such a resolution of aircraft from non-aircraft sources was considered vital to the assessment of the aircraft impact on the NO_2 standard since previous monitoring [Lorang, (1978)] identified NO_2 levels of 0.3 ppm without such a separation while AVAP modeling, unable to separately predict NO_2 levels, indicates that under worst case conditions, aircraft contribute NO, concentrations of the order of 1 ppm.

Statistical summaries of the hourly average concentrations, as computed from the high sampling rate data, are given in Tables 3.3-3.5 for $NO_,$, NO, and NO_2 (= $NO_,$-NO) respectively. The fact that the highest observed values of NO and $NO_,$ saturate the recording equipment and are outside the calibrated range of the NO/NO_x instruments is indeed unfortunate and casts some doubt upon the validity of the NO_2 data computed by subtraction of the NO from the $NO_,$ concentrations.

Figures 3.12-3.14 show the cumulative frequency distributions of concentrations for $NO_,$, NO, and NO_2 respectively. Aside from slightly lower NO and $NO_,$ values at station 1, one notes a striking similarity between the distributions from the different stations. Examination of these plots indicates that 95% of the time concentrations of $NO_,$, NO, and NO_2 are less than 0.2 ppm, 0.1, and 0.07 ppm respectively.

Interestingly, the hours corresponding to saturations of the recorders for NO and $NO_,$ are the same hours of the CO episode. The fact that NO and $NO_,$ from station 1 were not recorded during this episode period (due to the severing of the signal lines by a snowplow) accounts for the lowered distribution in these highest percentile ranges. Further, the fact that this pollution episode affected stations 3 and 5, in addition to 1 and 6, tends to further confirm that the episode covered a wider area than could be inferred from the CO data.

The potential for violation of possible NO_2 peak hourly standards at airports has recently been reveiwed by Jordan and Broderick (1978). Finding that both worst case modeling predictions and previous monitoring results were in the same 0.25-0.5 ppm range as the potential NO_2 standards, was one of the principal motivating factors for the DCA experiment. Rather than simply accumulating more NO/NO_x data, the placement of monitors and data recording rate at DCA were chosen so as to enable separation of the aircraft contribution (i.e. in the form of short pulses associated with takeoff/landing) from continuous source and background contributions. Such a resolution of aircraft from non-aircraft sources was considered vital to the assessment of the aircraft impact on the NO_2 standard since previous monitoring [Lorang, (1978)] identified NO_2 levels of 0.3 ppm without such a separation while AVAP modeling, unable to separately predict NO_2 levels, indicates that under worst case conditions, aircraft contribute NO, concentrations of the order of 1 ppm.

Statistical summaries of the hourly average concentrations, as computed from the high sampling rate data, are given in Tables 3.3-3.5 for $NO_,$, NO, and NO_2 (= $NO_,$-NO) respectively. The fact that the highest observed values of NO and $NO_,$ saturate the recording equipment and are outside the calibrated range of the NO/NO_x instruments is indeed unfortunate and casts some doubt upon the validity of the NO_2 data computed by subtraction of the NO from the $NO_,$ concentrations.

Figures 3.12-3.14 show the cumulative frequency distributions of concentrations for $NO_,$, NO, and NO_2 respectively. Aside from slightly lower NO and $NO_,$ values at station 1, one notes a striking similarity between the distributions from the different stations. Examination of these plots indicates that 95% of the time concentrations of $NO_,$, NO, and NO_2 are less than 0.2 ppm, 0.1, and 0.07 ppm respectively.

Interestingly, the hours corresponding to saturations of the recorders for NO and $NO_,$ are the same hours of the CO episode. The fact that NO and $NO_,$ from station 1 were not recorded during this episode period (due to the severing of the signal lines by a snowplow) accounts for the lowered distribution in these highest percentile ranges. Further, the fact that this pollution episode affected stations 3 and 5, in addition to 1 and 6, tends to further confirm that the episode covered a wider area than could be inferred from the CO data.

Table 3.4. DCA Monitoring Experiment NO

	Station 1	Station 3
Mean (ppb)	25.06	29.26
Standard Deviation (ppb)	38.92	62.70
Minimum (ppb)	2.50	2.50
Maximum (ppb)	360.50	549.20[s]
Number of Hours	683	683
Geometric Mean (ppb)	10.85	11.32
Geometric Standard Deviation	3.66	3.62
Number of Values < Threshold*	227	196

*Values < instrument threshold (5 ppb) included as 1/2 threshold
[s]indicates instrument saturation

Table 3.5. DCA Monitoring Experiment NO_2

	Station 1	Station 3
Mean (ppb)	30.22	29.38
Standard Deviation (ppb)	17.39	15.04
Minimum (ppb)	2.5	2.7
Maximum (ppb)	91.90	86.70
Number of Hours	679	683
Geometric Mean (ppb)	24.84	25.49
Geometric Standard Deviation	1.97	1.74
Number of Values < Threshold*		

*Values < instrument threshold (5 ppb) included as 1/2 threshold

Table 3.4. DCA Monitoring Experiment NO

	Station 1	Station 3
Mean (ppb)	25.06	29.26
Standard Deviation (ppb)	38.92	62.70
Minimum (ppb)	2.50	2.50
Maximum (ppb)	360.50	549.20[s]
Number of Hours	683	683
Geometric Mean (ppb)	10.85	11.32
Geometric Standard Deviation	3.66	3.62
Number of Values < Threshold*	227	196

*Values < instrument threshold (5 ppb) included as 1/2 threshold
[s]indicates instrument saturation

Table 3.5. DCA Monitoring Experiment NO_2

	Station 1	Station 3
Mean (ppb)	30.22	29.38
Standard Deviation (ppb)	17.39	15.04
Minimum (ppb)	2.5	2.7
Maximum (ppb)	91.90	86.70
Number of Hours	679	683
Geometric Mean (ppb)	24.84	25.49
Geometric Standard Deviation	1.97	1.74
Number of Values < Threshold*		

*Values < instrument threshold (5 ppb) included as 1/2 threshold

Table 3.4. DCA Monitoring Experiment NO

	Station 1	Station 3
Mean (ppb)	25.06	29.26
Standard Deviation (ppb)	38.92	62.70
Minimum (ppb)	2.50	2.50
Maximum (ppb)	360.50	549.20[s]
Number of Hours	683	683
Geometric Mean (ppb)	10.85	11.32
Geometric Standard Deviation	3.66	3.62
Number of Values < Threshold*	227	196

*Values < instrument threshold (5 ppb) included as 1/2 threshold
[s]indicates instrument saturation

Table 3.5. DCA Monitoring Experiment NO_2

	Station 1	Station 3
Mean (ppb)	30.22	29.38
Standard Deviation (ppb)	17.39	15.04
Minimum (ppb)	2.5	2.7
Maximum (ppb)	91.90	86.70
Number of Hours	679	683
Geometric Mean (ppb)	24.84	25.49
Geometric Standard Deviation	1.97	1.74
Number of Values < Threshold*		

*Values < instrument threshold (5 ppb) included as 1/2 threshold

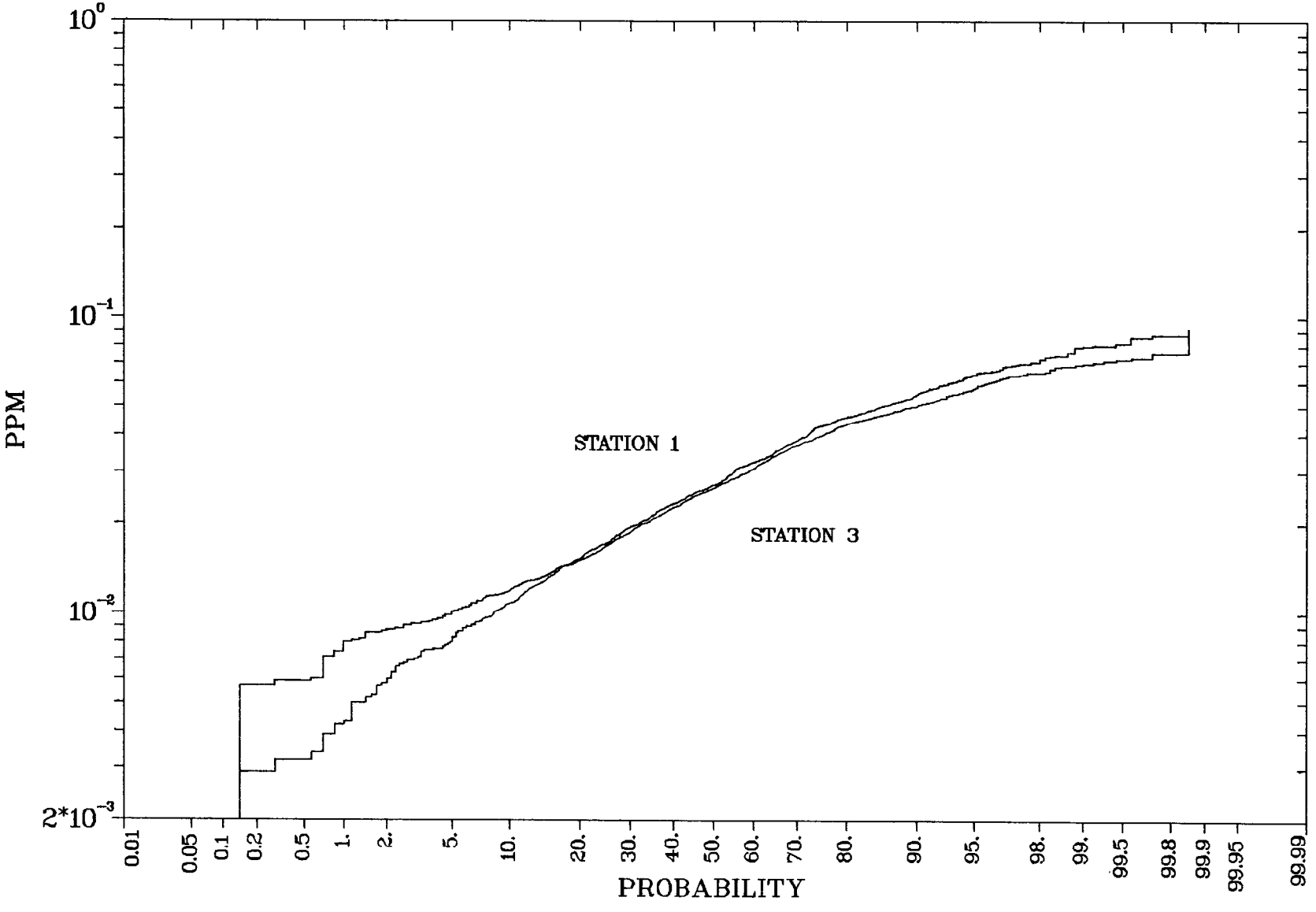

Fig. 3.14. Cumulative Frequency Distributions of Hourly NO_2 ($\equiv NO_2 - NO$) Concentrations at Stations 1 and 3.

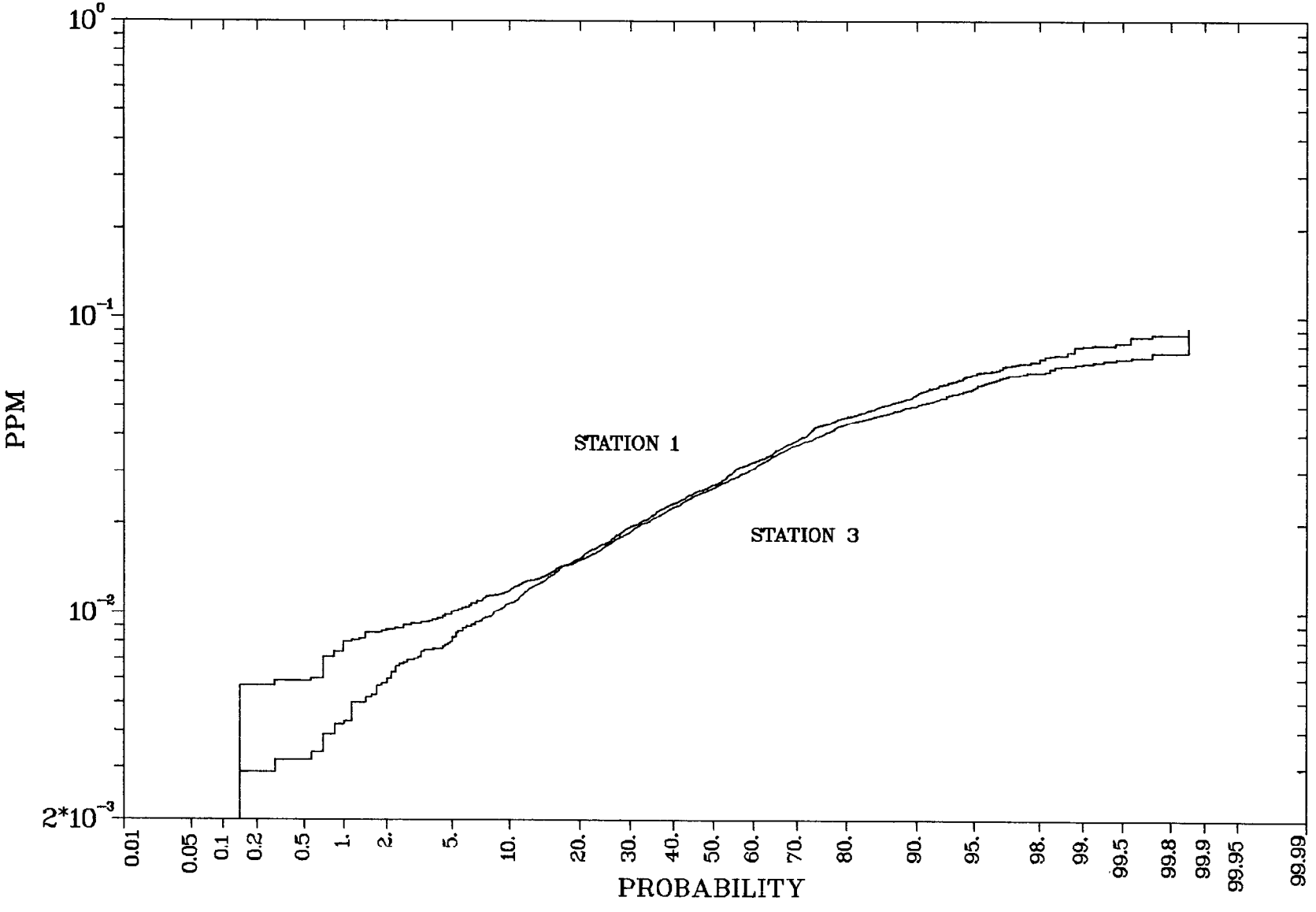

Fig. 3.14. Cumulative Frequency Distributions of Hourly NO_2 ($\equiv NO_2 - NO$) Concentrations at Stations 1 and 3.

Table 3.6. Estimated Highest Hourly per Annum* Concentrations for Oxides of Nitrogen (in ppm)

	NO_x	NO	NO_2
Total Concentration	1.0-4.0	0.8-4.0	0.1-0.3
Background Subtracted	0.2-0.4	0.1-0.3	0.05^3-0.1^1
Pulse Integrated	0.2-0.5	0.2-0.3	0.1^3-0.3^1

*Based on visual linear extrapolation of cumulative frequency distributions to 99.99% probability. Care has been taken to avoid underestimates caused by NO/NO, saturation at 0.5 ppm. A range is given where linear extrapolation is not unambiguous.

[1]Station 1

[3]Station 3

transport time, sunlight intensity, and background levels of NO, NO_2, and O_3 and a reactive plume calculation is required to obtain a more definitive prediction; however, using simple assumptions regarding the amount of NO_2 emitted directly by the aircraft, the rate of NO oxidation, and the ambient O_3 level, it is reasonable to expect several tenths of ppm of NO_2 at distances of possible public exposure. Further extrapolations or generalizations to other airports should be tempered by the following considerations:

- DCA is closed between 10:00 p.m. and 6:00 a.m. These nighttime hours are associated with stable atmospheric conditions and thus potentially poor pollutant dispersion conditions.
- Nearly all operations at DCA are by medium range jets (e.g., 727, 737, DC9) primarily using the JT8D-17 engine. This engine has a relatively low NO, emission rate at takeoff (≃200 lbs/hr)[8] compared to some other engines (e.g., 670 lbs/hr for the CF6-50C and ≃ 475-500 lbs/hr for the JT9D-7 and RB-211-22B).[8]
- This experiment was conducted during winter months. A similar experiment during summer months could be accompanied by higher oxidant levels with resulting higher NO_2 levels.

Table 3.6. Estimated Highest Hourly per Annum* Concentrations for Oxides of Nitrogen (in ppm)

	NO_x	NO	NO_2
Total Concentration	1.0-4.0	0.8-4.0	0.1-0.3
Background Subtracted	0.2-0.4	0.1-0.3	0.05^3-0.1^1
Pulse Integrated	0.2-0.5	0.2-0.3	0.1^3-0.3^1

*Based on visual linear extrapolation of cumulative frequency distributions to 99.99% probability. Care has been taken to avoid underestimates caused by NO/NO, saturation at 0.5 ppm. A range is given where linear extrapolation is not unambiguous.

[1]Station 1

[3]Station 3

transport time, sunlight intensity, and background levels of NO, NO_2, and O_3 and a reactive plume calculation is required to obtain a more definitive prediction; however, using simple assumptions regarding the amount of NO_2 emitted directly by the aircraft, the rate of NO oxidation, and the ambient O_3 level, it is reasonable to expect several tenths of ppm of NO_2 at distances of possible public exposure. Further extrapolations or generalizations to other airports should be tempered by the following considerations:

- DCA is closed between 10:00 p.m. and 6:00 a.m. These nighttime hours are associated with stable atmospheric conditions and thus potentially poor pollutant dispersion conditions.
- Nearly all operations at DCA are by medium range jets (e.g., 727, 737, DC9) primarily using the JT8D-17 engine. This engine has a relatively low NO, emission rate at takeoff (≃200 lbs/hr)[8] compared to some other engines (e.g., 670 lbs/hr for the CF6-50C and ≃ 475-500 lbs/hr for the JT9D-7 and RB-211-22B).[8]
- This experiment was conducted during winter months. A similar experiment during summer months could be accompanied by higher oxidant levels with resulting higher NO_2 levels.

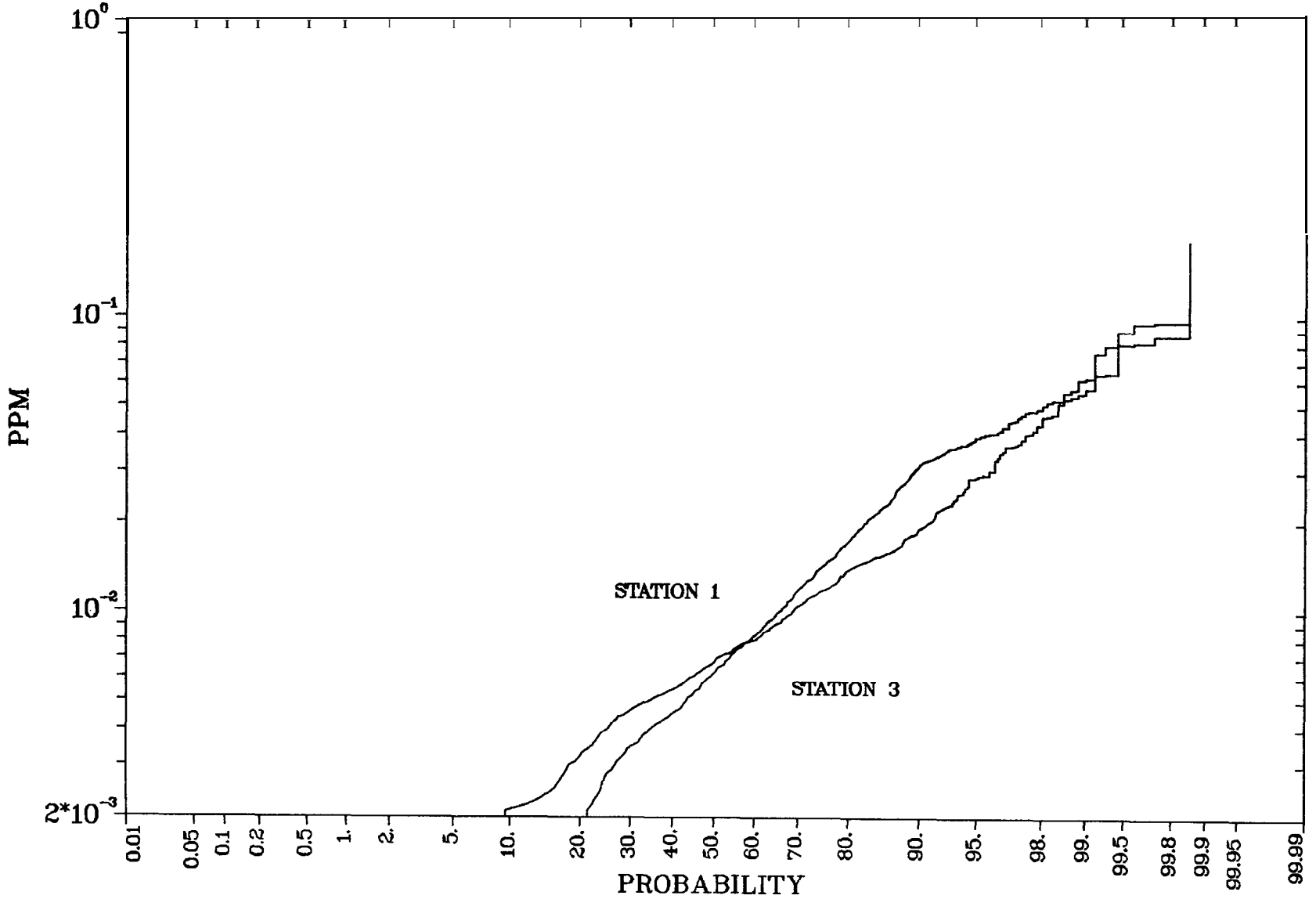

Fig. 3.16. Cumulative Frequency Distributions of Hourly Background Subtracted NO Concentrations at Stations 1, and 3.

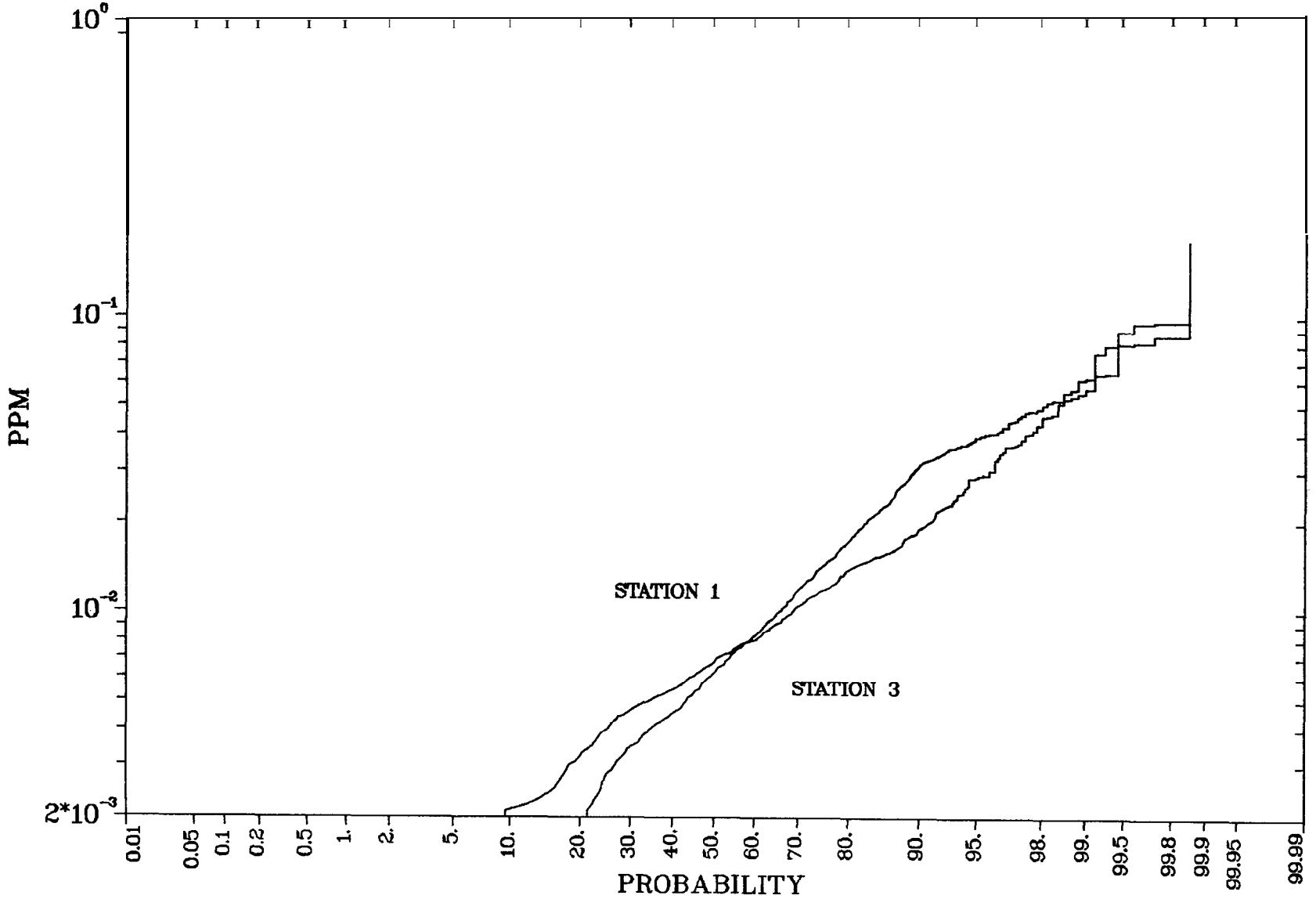

Fig. 3.16. Cumulative Frequency Distributions of Hourly Background Subtracted NO Concentrations at Stations 1, and 3.

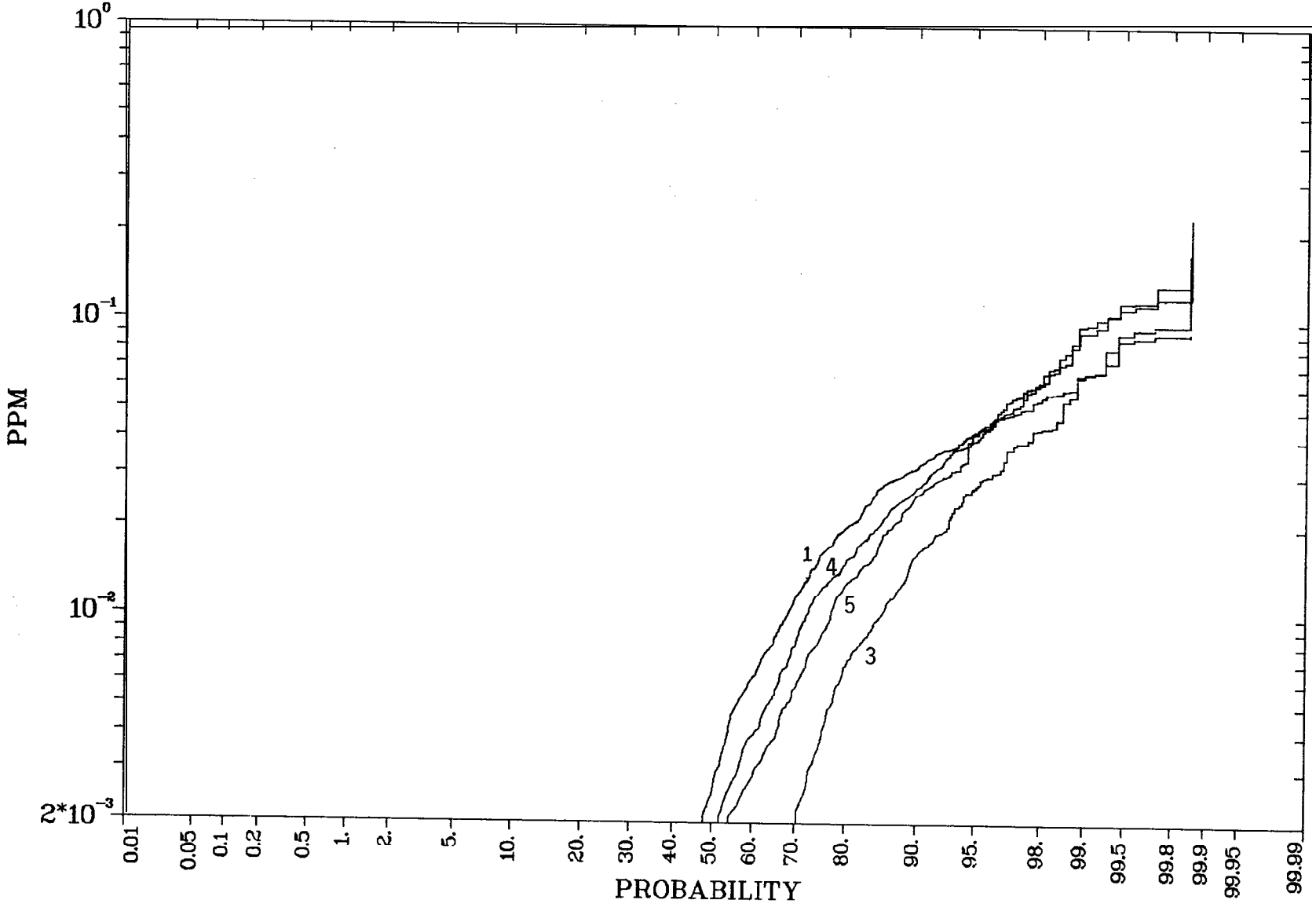

Fig. 3.18. Cumulative Frequency Distributions of Hourly Integrated Pulse NO, Concentrations at Stations 1, 3, 4, and 5.

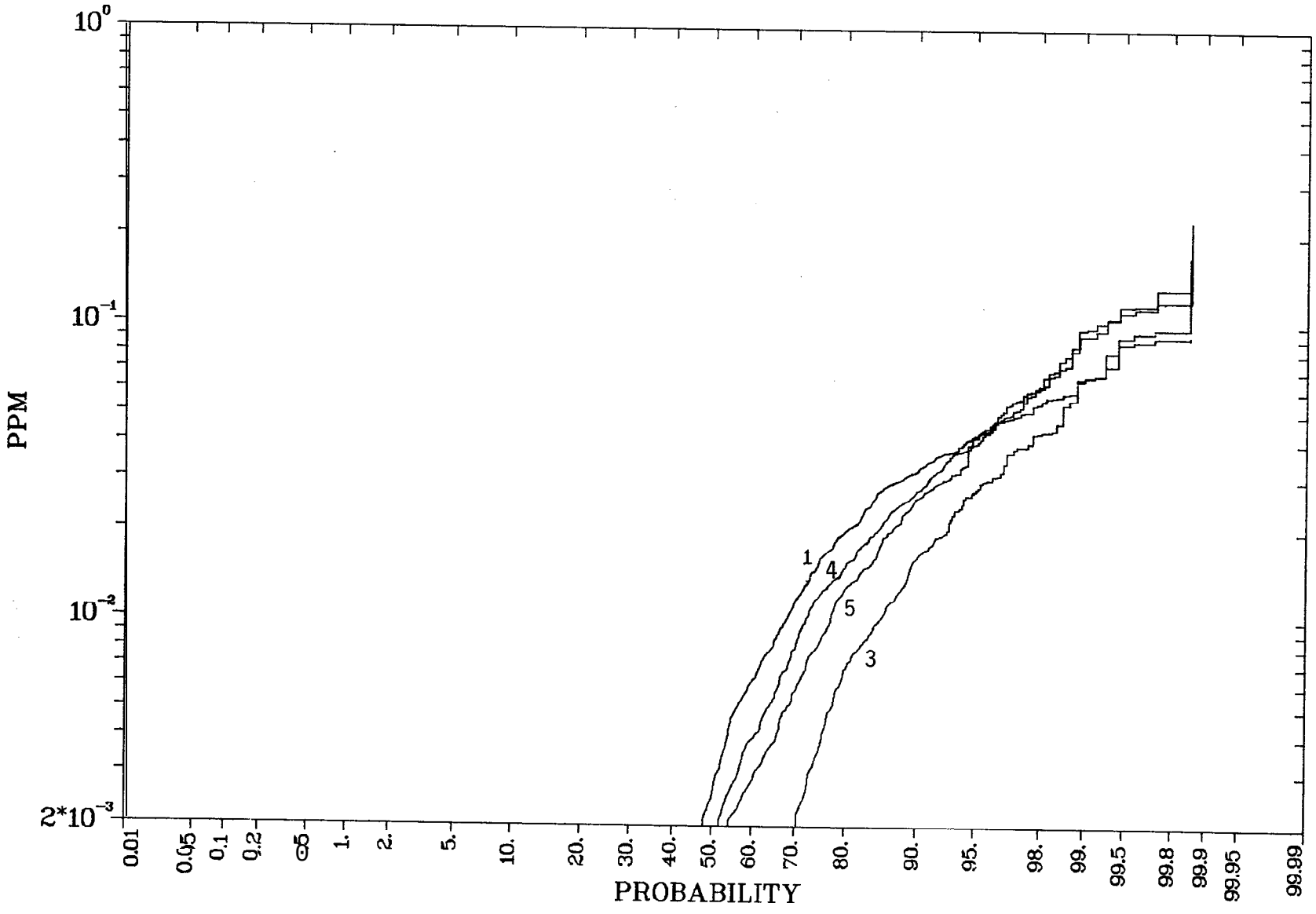

Fig. 3.18. Cumulative Frequency Distributions of Hourly Integrated Pulse NO, Concentrations at Stations 1, 3, 4, and 5.

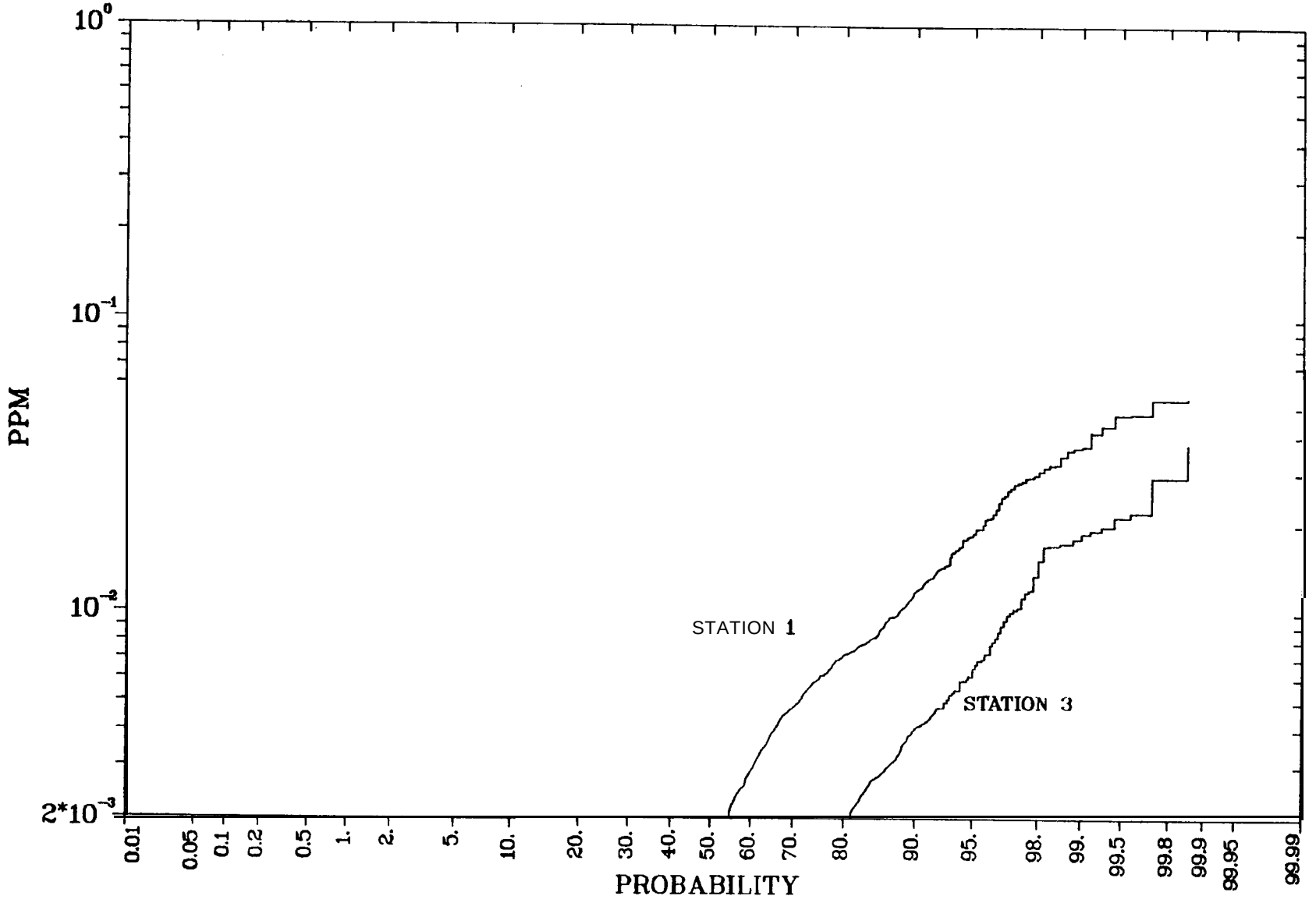

Fig. 3.20. Cumulative Frequency Distributions of Hourly Integrated Pulse NO_2 ($\equiv$ NO, - NO) Concentrations at Stations 1 and 3.

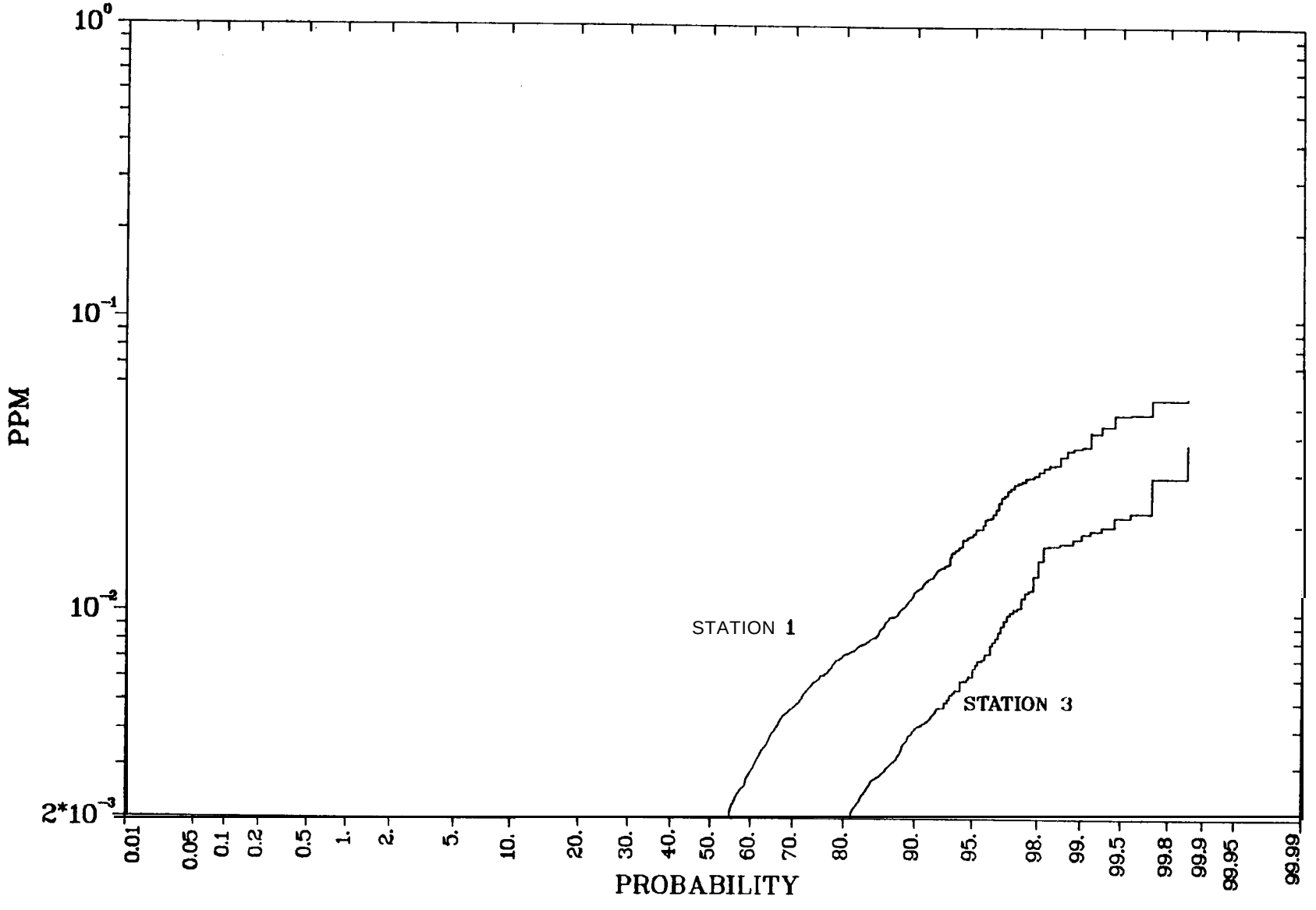

Fig. 3.20. Cumulative Frequency Distributions of Hourly Integrated Pulse NO_2 ($\equiv$ NO, - NO) Concentrations at Stations 1 and 3.

In order to relate observed NO_2 and NO, levels with modeled NO_x concentrations it is essential to note the difference in behavior of the $[NO]/[NO_x]$ ratios for ambient air and for aircraft plumes, before such plumes have completely mixed with the ambient air. During periods of good ventilation (sufficient mixing depth and moderate windspeed), the value of $[NO]/[NO_x]$ is generally near 0.4 during the morning decreasing to 0.10 or less during the afternoon, remaining low throughout the night. This temporal decrease in the ratio is due to photochemical processes during daylight hours. It has been observed that at takeoff thrust more than 95% of the NO, emitted by jet aircraft engines is in the form of NO. The concentrations above background for aircraft induced peaks measured at the sites generally have a $[NO]/[NO_x]$ ratio exceeding 0.8, indicating that some transformation of NO to NO_2 is taking place in the near field under the winter conditions observed.

The actual NO to NO_2 plume oxidation rate is a complex function of plume dispersion rate and transport time, sunlight intensity, and background levels of NO, NO_2, and O_3, and a reactive plume calculation is required to predict the $[NO]/[NO_x]$ ratio. Clear evidence for this oxidation process, on the short transport time scales of the DCA experiment, is seen in Figure 3.22 Plotted is the ratio of the hourly integrated-pulse concentrations of NO to NO, as a function of estimated plume travel time from the departing aircraft to the receptor. The linear regression line is indicated for comparison purposes only and has no theoretical basis.

During periods of light, variable winds, the hourly NO, concentrations surpassed 0.1 ppm on more than ten (10) separate occasions. For such periods hourly background accounts for greater than 70% of the mean total NO, implying that most of the important sources are nonlocal. The $[NO]/[NO_x]$ ratio of this background component generally is between 0.5 and 0.8. Several of these high concentration episodes are coincident with low airport activity and/or non-airport wind directions.

Considering now the issue of aircraft impact on the annual NO_2 standard of 0.05 ppm, one notes that the regression of observed pollutant levels against departure rate should provide some insight. Figure 3.23 shows the distributions and regression lines for the hourly total, background subtracted, and pulse integrated NO_2 concentrations at stations 1 and 3 versus aircraft departure rate. The regression parameters are then summarized in Table 3.7 along with

In order to relate observed NO_2 and NO, levels with modeled NO, concentrations it is essential to note the difference in behavior of the $[NO]/[NO_x]$ ratios for ambient air and for aircraft plumes, before such plumes have completely mixed with the ambient air. During periods of good ventilation (sufficient mixing depth and moderate windspeed), the value of $[NO]/[NO_x]$ is generally near 0.4 during the morning decreasing to 0.10 or less during the afternoon, remaining low throughout the night. This temporal decrease in the ratio is due to photochemical processes during daylight hours. It has been observed that at takeoff thrust more than 95% of the NO, emitted by jet aircraft engines is in the form of NO. The concentrations above background for aircraft induced peaks measured at the sites generally have a $[NO]/[NO_x]$ ratio exceeding 0.8, indicating that some transformation of NO to NO_2 is taking place in the near field under the winter conditions observed.

The actual NO to NO_2 plume oxidation rate is a complex function of plume dispersion rate and transport time, sunlight intensity, and background levels of NO, NO_2, and O_3, and a reactive plume calculation is required to predict the $[NO]/[NO_x]$ ratio. Clear evidence for this oxidation process, on the short transport time scales of the DCA experiment, is seen in Figure 3.22 Plotted is the ratio of the hourly integrated-pulse concentrations of NO to NO, as a function of estimated plume travel time from the departing aircraft to the receptor. The linear regression line is indicated for comparison purposes only and has no theoretical basis.

During periods of light, variable winds, the hourly NO, concentrations surpassed 0.1 ppm on more than ten (10) separate occasions. For such periods hourly background accounts for greater than 70% of the mean total NO, implying that most of the important sources are nonlocal. The $[NO]/[NO_x]$ ratio of this background component generally is between 0.5 and 0.8. Several of these high concentration episodes are coincident with low airport activity and/or non-airport wind directions.

Considering now the issue of aircraft impact on the annual NO_2 standard of 0.05 ppm, one notes that the regression of observed pollutant levels against departure rate should provide some insight. Figure 3.23 shows the distributions and regression lines for the hourly total, background subtracted, and pulse integrated NO_2 concentrations at stations 1 and 3 versus aircraft departure rate. The regression parameters are then summarized in Table 3.7 along with

In order to relate observed NO_2 and NO, levels with modeled NO, concentrations it is essential to note the difference in behavior of the $[NO]/[NO_x]$ ratios for ambient air and for aircraft plumes, before such plumes have completely mixed with the ambient air. During periods of good ventilation (sufficient mixing depth and moderate windspeed), the value of $[NO]/[NO_x]$ is generally near 0.4 during the morning decreasing to 0.10 or less during the afternoon, remaining low throughout the night. This temporal decrease in the ratio is due to photochemical processes during daylight hours. It has been observed that at takeoff thrust more than 95% of the NO, emitted by jet aircraft engines is in the form of NO. The concentrations above background for aircraft induced peaks measured at the sites generally have a $[NO]/[NO_x]$ ratio exceeding 0.8, indicating that some transformation of NO to NO_2 is taking place in the near field under the winter conditions observed.

The actual NO to NO_2 plume oxidation rate is a complex function of plume dispersion rate and transport time, sunlight intensity, and background levels of NO, NO_2, and O_3, and a reactive plume calculation is required to predict the $[NO]/[NO_x]$ ratio. Clear evidence for this oxidation process, on the short transport time scales of the DCA experiment, is seen in Figure 3.22 Plotted is the ratio of the hourly integrated-pulse concentrations of NO to NO, as a function of estimated plume travel time from the departing aircraft to the receptor. The linear regression line is indicated for comparison purposes only and has no theoretical basis.

During periods of light, variable winds, the hourly NO, concentrations surpassed 0.1 ppm on more than ten (10) separate occasions. For such periods hourly background accounts for greater than 70% of the mean total NO, implying that most of the important sources are nonlocal. The $[NO]/[NO_x]$ ratio of this background component generally is between 0.5 and 0.8. Several of these high concentration episodes are coincident with low airport activity and/or non-airport wind directions.

Considering now the issue of aircraft impact on the annual NO_2 standard of 0.05 ppm, one notes that the regression of observed pollutant levels against departure rate should provide some insight. Figure 3.23 shows the distributions and regression lines for the hourly total, background subtracted, and pulse integrated NO_2 concentrations at stations 1 and 3 versus aircraft departure rate. The regression parameters are then summarized in Table 3.7 along with

Table 3.7. Regressions of Hourly Average Concentrations Vs. Aircraft Departure Rate

	Station 1			Station 3		
	Ave.(ppb)	Intercept(ppb)	Slope (ppb/Departure)	Ave.(ppb)	Intercept(ppb)	Slope (ppb/Departure)
			NO_x			
Total	82.7	66.5 ± 5.2	1.60 ± 0.39	90.7	93.8 ± 8.4	-0.35 ± 0.64
Background Subtracted	23.8	11.2 ± 1.3	1.24 ± 0.10	17.5	12.3 ± 1.3	0.52 ± 0.10
Pulse Integrated	16.3	3.4 ± 1.4	1.27 ± 0.11	9.1	4.0 ± 1.5	0.50 ± 0.11
			NO			
Total	42.2	30.7 ± 4.4	1.13 ± 0.33	52.0	56.8 ± 7.9	-0.48 ± 0.60
Background Subtracted	17.8	8.2 ± 1.5	0.95 ± 0.11	14.4	10.5 ± 1.4	0.39 ± 0.11
Pulse Integrated	11.6	3.1 ± 1.6	0.84 ± 0.12	7.3	4.2 ± 1.6	0.31 ± 0.12
			NO_2			
Total	40.5	35.7 ± 1.5	0.47 ± 0.11	38.3	37.0 ± 1.4	0.13 ± 0.11
Background Subtracted	6.5	3.2 ± 0.5	0.34 ± 0.04	4.3	3.8 ± 0.4	0.05 ± 0.03
Pulse Integrated	5.2	0.6 ± 0.6	0.46 ± 0.05	2.6	1.2 ± 0.4	0.14 ± 0.03

Based on 295 hours obtained during February 1979

Average Departure Rate of 10.1 Aircraft/hr (primarily B727, B737, DC-9)

Pulse integrated data for Station 3 is somewhat questionable

Table 3.7. Regressions of Hourly Average Concentrations Vs. Aircraft Departure Rate

	Station 1			Station 3		
	Ave.(ppb)	Intercept(ppb)	Slope (ppb/Departure)	Ave.(ppb)	Intercept(ppb)	Slope (ppb/Departure)
			NO_x			
Total	82.7	66.5 ± 5.2	1.60 ± 0.39	90.7	93.8 ± 8.4	-0.35 ± 0.64
Background Subtracted	23.8	11.2 ± 1.3	1.24 ± 0.10	17.5	12.3 ± 1.3	0.52 ± 0.10
Pulse Integrated	16.3	3.4 ± 1.4	1.27 ± 0.11	9.1	4.0 ± 1.5	0.50 ± 0.11
			NO			
Total	42.2	30.7 ± 4.4	1.13 ± 0.33	52.0	56.8 ± 7.9	-0.48 ± 0.60
Background Subtracted	17.8	8.2 ± 1.5	0.95 ± 0.11	14.4	10.5 ± 1.4	0.39 ± 0.11
Pulse Integrated	11.6	3.1 ± 1.6	0.84 ± 0.12	7.3	4.2 ± 1.6	0.31 ± 0.12
			NO_2			
Total	40.5	35.7 ± 1.5	0.47 ± 0.11	38.3	37.0 ± 1.4	0.13 ± 0.11
Background Subtracted	6.5	3.2 ± 0.5	0.34 ± 0.04	4.3	3.8 ± 0.4	0.05 ± 0.03
Pulse Integrated	5.2	0.6 ± 0.6	0.46 ± 0.05	2.6	1.2 ± 0.4	0.14 ± 0.03

Based on 295 hours obtained during February 1979

Average Departure Rate of 10.1 Aircraft/hr (primarily B727, B737, DC-9)

Pulse integrated data for Station 3 is somewhat questionable

3.5 SUMMARY AND CONCLUSIONS BASED ON THE HOURLY AVERAGE CONCENTRATIONS

Results of CO monitoring near an aircraft queueing area at DCA suggest that observed worst-case, aircraft contributions to hourly CO concentrations on the order of 10 ppm are not unexpected at distances of 500 ft from the aircraft. These highest observed concentrations decrease to about 5 ppm at a distance of 1000 ft., a minimum distance where public exposure might normally be anticipated and in good agreement with worst-case modeling results for LAX. No violations of the 35 ppm hourly standard were observed even as close as 500 ft from the aircraft and the single observed violation of the 8 hr standard is thought to be primarily related to high observed CO values throughout the D.C. area and augmented by intensive operations of airport snowplows very near the monitoring stations.

Preliminary results of CO monitoring at DCA suggest that violation of the hourly NAAQS CO standard, in areas accessible to the general public and by 'aircraft alone, is highly improbable.

Results of NO, NO, monitoring indicate that NO, NO,, and NO_2 concentration distrubutions are nearly independent of station location (i.e., within the limited spatial regime of monitoring). Worst case NO, concentrations of $\sim$ 1 ppm are consistent with modeling predictions for LAX.

No NO_2 concentrations in excess of 0.1 ppm were observed though a conservative extrapolation to once a year probability yields a concentration (i.e., $\sim$0.3 ppm) in the same range as possible short-term standards. Regressions of the NO_2 hourly average data against aircraft departure rate suggests that aircraft are responsible for only about 0.005 ppm of the estimated annual average NO_2 of 0.03 ppm seen near the runway at DCA. This projected annual average aircraft impact of 0.005 ppm is small compared to the 0.05 ppm NAAQS and is in agreement with the concentration differential observed between DCA and other Washington area monitors.

3.6 ANALYSIS OF SINGLE EVENT DATA

The locations of the monitors with respect to takoffs and landings on Runway 36 and the terminal area at DCA allow the impact of airport operations to be measured in several different ways. In addition to the hourly average analysis, pollution from take-off events may be evaluated by subjective analysis of single events or by use of an objective single event evaluation

3.5 SUMMARY AND CONCLUSIONS BASED ON THE HOURLY AVERAGE CONCENTRATIONS

Results of CO monitoring near an aircraft queueing area at DCA suggest that observed worst-case, aircraft contributions to hourly CO concentrations on the order of 10 ppm are not unexpected at distances of 500 ft from the aircraft. These highest observed concentrations decrease to about 5 ppm at a distance of 1000 ft., a minimum distance where public exposure might normally be anticipated and in good agreement with worst-case modeling results for LAX. No violations of the 35 ppm hourly standard were observed even as close as 500 ft from the aircraft and the single observed violation of the 8 hr standard is thought to be primarily related to high observed CO values throughout the D.C. area and augmented by intensive operations of airport snowplows very near the monitoring stations.

Preliminary results of CO monitoring at DCA suggest that violation of the hourly NAAQS CO standard, in areas accessible to the general public and by 'aircraft alone, is highly improbable.

Results of NO, NO, monitoring indicate that NO, NO,, and NO_2 concentration distrubutions are nearly independent of station location (i.e., within the limited spatial regime of monitoring). Worst case NO, concentrations of $\sim$ 1 ppm are consistent with modeling predictions for LAX.

No NO_2 concentrations in excess of 0.1 ppm were observed though a conservative extrapolation to once a year probability yields a concentration (i.e., $\sim$0.3 ppm) in the same range as possible short-term standards. Regressions of the NO_2 hourly average data against aircraft departure rate suggests that aircraft are responsible for only about 0.005 ppm of the estimated annual average NO_2 of 0.03 ppm seen near the runway at DCA. This projected annual average aircraft impact of 0.005 ppm is small compared to the 0.05 ppm NAAQS and is in agreement with the concentration differential observed between DCA and other Washington area monitors.

3.6 ANALYSIS OF SINGLE EVENT DATA

The locations of the monitors with respect to takoffs and landings on Runway 36 and the terminal area at DCA allow the impact of airport operations to be measured in several different ways. In addition to the hourly average analysis, pollution from take-off events may be evaluated by subjective analysis of single events or by use of an objective single event evaluation

With this objective in mind, approximately 120 individual aircraft departure events were measured through digitization of the concentration time histories. Peak concentration, time from peak noise to peak concentration, full width at half maximum above background, and background concentration were extracted for subsequent input into the ensemble research model for the takeoff mode, described in Section 3.6.3. The data extraction technique is referred to as the "subjective" approach primarily because of the element of judgment involved in the estimation of background levels.

3.6.2 DCA Single Event Finding Program

An attempt has been made to develop an objective algorithm to extract peak concentrations and dosages from the month of high sampling rate data gathered at DCA. After the measurements had been transferred to a master archive tape, calibrated in a preliminary fashion, and edited to minimize inclusion of periods of uncertain data, the following procedure was adopted to isolate and quantify events associated with individual aircraft departures.

1. Period of interest is specified such that periods of missing data, zero airport activity, non-optimal wind direction, etc. may be avoided. Only wind directions between 10 and 80° were selected since, for other directions, the plume is transported away from the monitoring sites.
2. The search for a usable event occurs as follows: a noise pulse is searched for that is sufficiently separated from other pulses to allow transport to the furthest receptor before the next aircraft's plume impacts the closest receptor. An event pulse is defined by an 80 dB noise threshold. When runway 18 is in use the noise spikes are similar but the wind is from the south! The screening in step 1 then becomes important to avoid the possibility of erroneous results. The transport time is defined as D/u where D is the along wind distance from station 3 to the runway. Five minute average wind speed (u) and direction values are utilized. If the transport time exceeds the noise event separation the event is skipped.
3. Once a noise event is identified as giving rise to an analyzable "dose event", 3-minute averages, background values, σ_θ, and σ_ϕ are evaluated (1 min prior to noise pulse, 2 min after noise pulse). Missing data or data exceeding 0.5 ppm will cause the event to abort.

4. The peak concentrations, triangular doses, and numerically integrated doses are now found by subtracting out the background values of the 3 minute period.

   a. For each receptor the search for the event begins after a delay time equal to the time of transport from the runway. A window the size of the minimum pulse separation used in step 2 is searched for a maximum.

   b. The times of half-maximum (above background) are determined, to calculate the triangular dose.

   c. The endpoints of the numerical dose integration are defined as follows:
   The starting point is the time where the search for the maximum begins. The end point the time at which the concentration becomes smaller than (1.1 x background) or (background + 10 ppb), whichever is greater, or the end of the window in (a), whichever comes first. For a weak pulse above a high background at station 3 the size of the integration interval may be underestimated. Early versions use Simpson's rule but later attempts employ a Gaussian quadrature technique.

Application and limitations of the above described technique include:

1. Care must be taken to specify periods with the proper wind direction or for each 5 minute period the average wind direction must be screened to insure acceptable events (i.e., $10° \leq \theta \leq 80°$ only).

2. Priority should be given to the subset of hours when onsite observations are available because noise network printouts of runway activity are not entirely reliable.

3. The dose of NO sometimes exceeds that of NO_x: this is most likely due to a calibration problem and not inherent in the method. The same problem is evident in the subjectively analyzed single events.

4. The specification of the "window" to search for an event is subject to further experimentation and refinement. A better way to find the endpoints for the integration may be required.

5. The temporal spacing requirements will cause many legitimate events to be skipped. However, with the data base provided, the present program should provide an adequate cross-section of "well defined" single events.

4. The peak concentrations, triangular doses, and numerically integrated doses are now found by subtracting out the background values of the 3 minute period.

   a. For each receptor the search for the event begins after a delay time equal to the time of transport from the runway. A window the size of the minimum pulse separation used in step 2 is searched for a maximum.

   b. The times of half-maximum (above background) are determined, to calculate the triangular dose.

   c. The endpoints of the numerical dose integration are defined as follows:
   The starting point is the time where the search for the maximum begins. The end point the time at which the concentration becomes smaller than (1.1 x background) or (background + 10 ppb), whichever is greater, or the end of the window in (a), whichever comes first. For a weak pulse above a high background at station 3 the size of the integration interval may be underestimated. Early versions use Simpson's rule but later attempts employ a Gaussian quadrature technique.

Application and limitations of the above described technique include:

1. Care must be taken to specify periods with the proper wind direction or for each 5 minute period the average wind direction must be screened to insure acceptable events (i.e., $10° \leq \theta \leq 80°$ only).

2. Priority should be given to the subset of hours when onsite observations are available because noise network printouts of runway activity are not entirely reliable.

3. The dose of NO sometimes exceeds that of NO_x: this is most likely due to a calibration problem and not inherent in the method. The same problem is evident in the subjectively analyzed single events.

4. The specification of the "window" to search for an event is subject to further experimentation and refinement. A better way to find the endpoints for the integration may be required.

5. The temporal spacing requirements will cause many legitimate events to be skipped. However, with the data base provided, the present program should provide an adequate cross-section of "well defined" single events.

4. The peak concentrations, triangular doses, and numerically integrated doses are now found by subtracting out the background values of the 3 minute period.

   a. For each receptor the search for the event begins after a delay time equal to the time of transport from the runway. A window the size of the minimum pulse separation used in step 2 is searched for a maximum.

   b. The times of half-maximum (above background) are determined, to calculate the triangular dose.

   c. The endpoints of the numerical dose integration are defined as follows:
   The starting point is the time where the search for the maximum begins. The end point the time at which the concentration becomes smaller than (1.1 x background) or (background + 10 ppb), whichever is greater, or the end of the window in (a), whichever comes first. For a weak pulse above a high background at station 3 the size of the integration interval may be underestimated. Early versions use Simpson's rule but later attempts employ a Gaussian quadrature technique.

Application and limitations of the above described technique include:

1. Care must be taken to specify periods with the proper wind direction or for each 5 minute period the average wind direction must be screened to insure acceptable events (i.e., $10° \leq \theta \leq 80°$ only).

2. Priority should be given to the subset of hours when onsite observations are available because noise network printouts of runway activity are not entirely reliable.

3. The dose of NO sometimes exceeds that of NO_x: this is most likely due to a calibration problem and not inherent in the method. The same problem is evident in the subjectively analyzed single events.

4. The specification of the "window" to search for an event is subject to further experimentation and refinement. A better way to find the endpoints for the integration may be required.

5. The temporal spacing requirements will cause many legitimate events to be skipped. However, with the data base provided, the present program should provide an adequate cross-section of "well defined" single events.

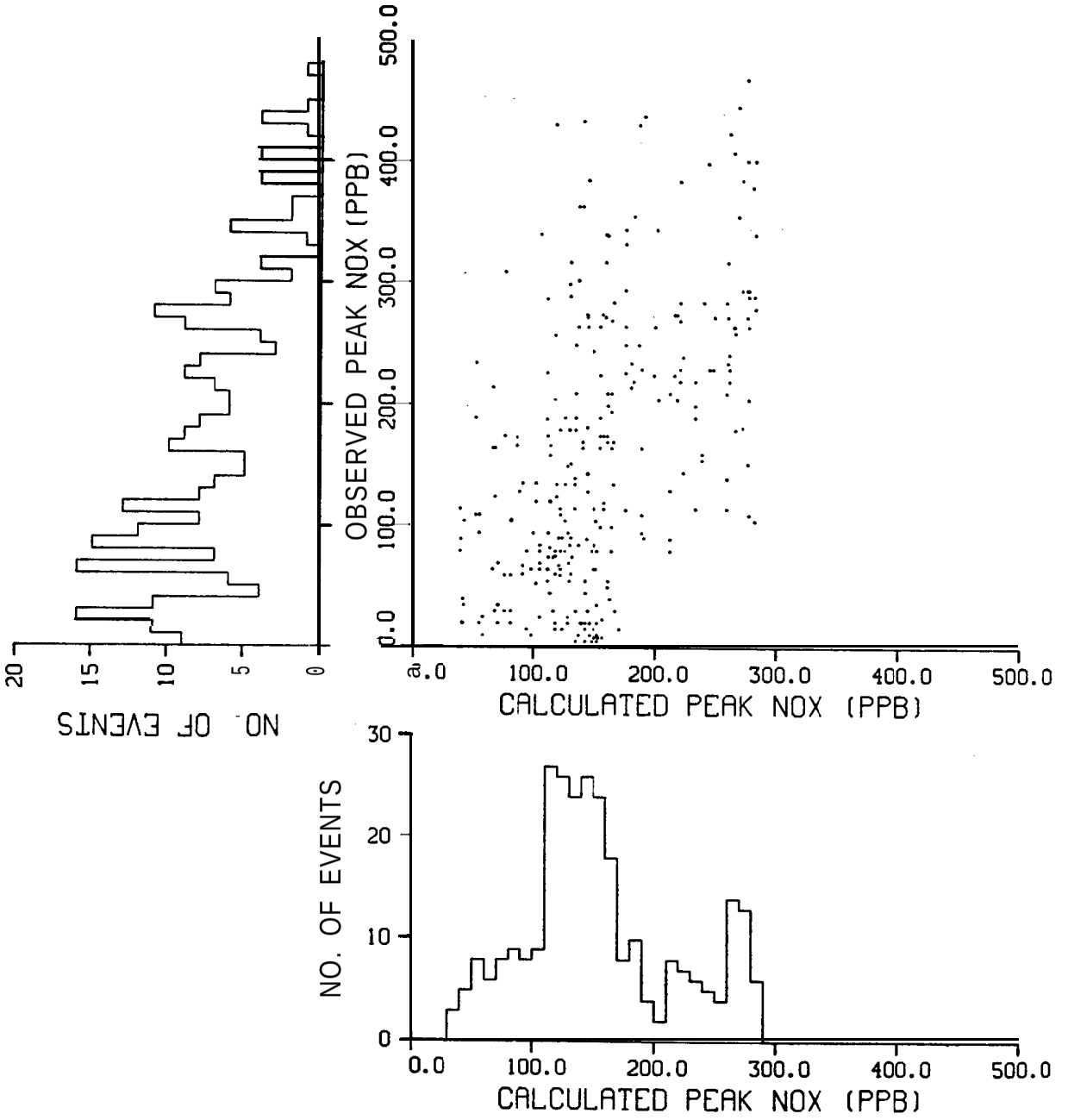

Fig. 3.24 Observed versus Predicted Peak NO_x Concentrations at DCA.

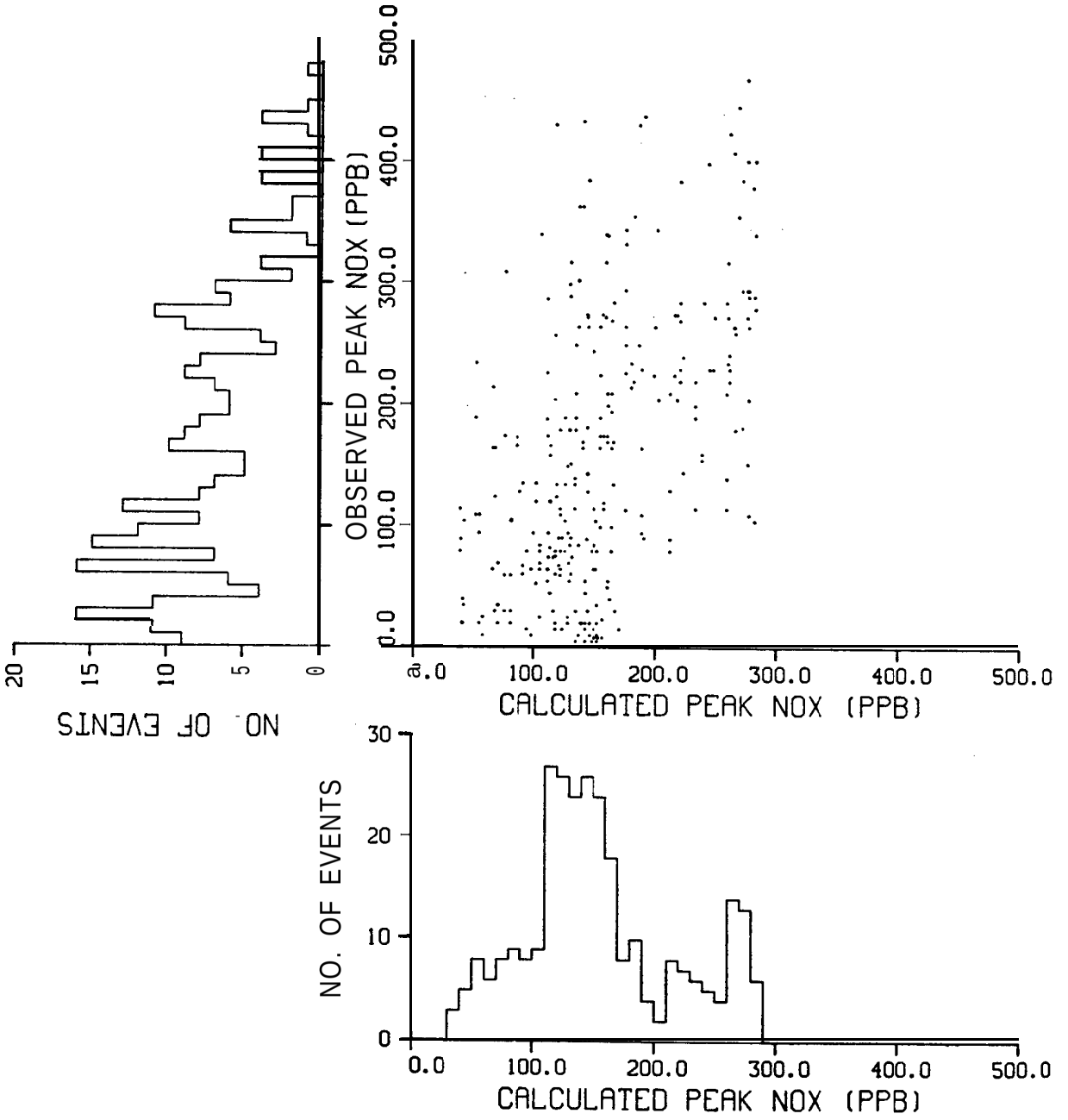

Fig. 3.24 Observed versus Predicted Peak NO_x Concentrations at DCA.

4 ANALYSIS OF EXPERIMENTS AT DULLES INTERNATIONAL AIRPORT

4.1 INTRODUCTION

The measurement program at Dulles International Airport was initiated in 1976 in response to an order by the Secretary of Transportation to monitor pollutant emissions and noise levels associated with Concorde aircraft operations. Three pollutants for which there are engine emission standards (carbon monoxides (CO), nitrogen oxides (NO_x), and hydrocarbons (HC)) were monitored. Measurements were obtained at nearby regional monitoring stations, and these data were analyzed using statistical inference techniques as well as by means of a source finding algorithm; a method designed to locate sources and assess source culpability based on observed concentrations.

Principal effort, both during the experimental program and in subsequent analysis efforts, was devoted to arrays of sensors placed at the airport in the vicinity of aircraft operations. The locations and periods of use for these arrays are detailed elsewhere by Smith et al. (1977)

Early measurements indicated low concentrations that would not be explicable with many conventional airport models, apparently because previous models developed specifically for airports have generally ignored plume rise and initial plume dilution. Although many model applications are not severely limited by this omission, when conservative estimates of airport impact at distances of 2 to 10 miles are at issue, it is essential to consider both the direct and indirect (augmentation of σ_z) effects of plume rise for validating model predictions at closer distances. Thus, the early results led to a design of a progressively more sophisticated experiment, using first one, then two, and finally three towers instrumented at three to five levels with CO sensor probes. Meteorological data included two levels of wind direction and speed and temperature and its gradient. These data have been analyzed in detail to provide information on jet plume rise, actual atmospheric dispersion parameters, and vertical and horizontal "profiles" of exhaust-plume pollutant concentrations for individual aircraft in actual service.

4 ANALYSIS OF EXPERIMENTS AT DULLES INTERNATIONAL AIRPORT

4.1 INTRODUCTION

The measurement program at Dulles International Airport was initiated in 1976 in response to an order by the Secretary of Transportation to monitor pollutant emissions and noise levels associated with Concorde aircraft operations. Three pollutants for which there are engine emission standards (carbon monoxides (CO), nitrogen oxides (NO_x), and hydrocarbons (HC)) were monitored. Measurements were obtained at nearby regional monitoring stations, and these data were analyzed using statistical inference techniques as well as by means of a source finding algorithm; a method designed to locate sources and assess source culpability based on observed concentrations.

Principal effort, both during the experimental program and in subsequent analysis efforts, was devoted to arrays of sensors placed at the airport in the vicinity of aircraft operations. The locations and periods of use for these arrays are detailed elsewhere by Smith et al. (1977)

Early measurements indicated low concentrations that would not be explicable with many conventional airport models, apparently because previous models developed specifically for airports have generally ignored plume rise and initial plume dilution. Although many model applications are not severely limited by this omission, when conservative estimates of airport impact at distances of 2 to 10 miles are at issue, it is essential to consider both the direct and indirect (augmentation of σ_z) effects of plume rise for validating model predictions at closer distances. Thus, the early results led to a design of a progressively more sophisticated experiment, using first one, then two, and finally three towers instrumented at three to five levels with CO sensor probes. Meteorological data included two levels of wind direction and speed and temperature and its gradient. These data have been analyzed in detail to provide information on jet plume rise, actual atmospheric dispersion parameters, and vertical and horizontal "profiles" of exhaust-plume pollutant concentrations for individual aircraft in actual service.

Fig. 4.1. Regional Air Quality Monitoring Stations

Fig. 4.1. Regional Air Quality Monitoring Stations

a) an independent means of checking source inventories and determining source culpability,

b) the ability to locate inadvertent leaks of hazardous effluents into the atmosphere, and

c) as an enforcement tool for air pollution regulatory agencies.

One possible approach to this problem is to develop a technique for relating the aerometric data obtained from a monitoring network under a wide range of meteorological conditions to the spatial distribution and strengths of emissions sources via the use of existing air quality dispersion algorithms. The approach may be envisioned, quite literally, as the running of an air quality dispersion model "in reverse"; where an effective emission density map is determined from knowledge of the concentrations at the receptors of a network and the values of a few relevant meteorological parameters over the area of interest.

The regional data base available from the Dulles monitoring program can, therefore, be used as input to this source finding algorithm in an attempt to determine the significance of local or on-site sources on the overall measured concentrations.

4.3.2 Model Development

Air quality dispersion models are most often concerned with the determination of pollutant concentrations at a receptor given known source strengths and locations. Assuming steady state conditions have been achieved, the concentration, C_{kt}, at the k^{th} receptor during the t^{th} time interval can be expressed as

$$C_{kt} = \sum_{j} R_{jkt} \; Q_j \; ,$$

where Q_j is the time independent strength of the j^{th} source and R_{jkt} is the transport coupling coefficient between the j^{th} source and k^{th} receptor for the meteorological conditions existent during the t^{th} time interval. The solution of the simple inverse problem

$$Q_j = \sum R^{-1}_{jkt} \; C_{kt}$$

is not of particular interest as a unique solution might exist only if the number of receptors, K, equalled the number of source candidates, J. A

more reasonable problem would consist of determining the set of Q_j values leading to the minimization of the quantity χ^2, defined as

$$\chi^2 = \sum_{t,k} \frac{\left(C_{kt} - \sum_{i=1}^{J} R_{ikt} \; Q_i \right)^2}{(\Delta C_{kt})^2} \qquad (1)$$

where ΔC_{kt} is the uncertainty in C_{kt}, i is a dummy index, and a summation over both t and k is required. This problem will generally lead to a unique set of J source strengths provided the number of measurements M (nominally KT, where T is the number of time periods of data available) exceeds J, and secondly, that the sources Q_j of interest actually couple to the data in hand (i.e., $R_{jkt} \neq 0$ for all j and some k, t). Given these conditions, one may write down the set of J equations generated by the relations

$$\frac{\partial \chi^2}{\partial Q_j} = 0.$$

These equations are of the form:

$$\sum_j A_{ij} \; Q_j = B_i \qquad (2)$$

where

$$A_{ij} \equiv \sum_{t,k} \frac{R_{ikt} \; R_{jkt}}{(\Delta C_{kt})^2}$$

and

$$B_i \equiv \sum_{t,k} \frac{C_{kt} \; R_{ikt}}{(\Delta C_{kt})^2}$$

and upon obtaining the inverse A^{-1} of the positive definite matrix A, one arrives at the solution

$$Q_j = \sum_i A_{ji}^{-1} \; B_i \qquad (3)$$

This approach, with no constraint on the Q_j, is quite acceptable provided the number of candidate source locations J is small (e.g., J<100) and source candidate locations are well separated; however, if nothing is known about the source locations, and instead, an array of point or area sources is conjectured to exist on an X-Y-grid of size n x m, then one must

more reasonable problem would consist of determining the set of Q_j values leading to the minimization of the quantity χ^2, defined as

$$\chi^2 = \sum_{t,k} \frac{\left(C_{kt} - \sum_{i=1}^{J} R_{ikt} \; Q_i \right)^2}{(\Delta C_{kt})^2} \qquad (1)$$

where ΔC_{kt} is the uncertainty in C_{kt}, i is a dummy index, and a summation over both t and k is required. This problem will generally lead to a unique set of J source strengths provided the number of measurements M (nominally KT, where T is the number of time periods of data available) exceeds J, and secondly, that the sources Q_j of interest actually couple to the data in hand (i.e., $R_{jkt} \neq 0$ for all j and some k, t). Given these conditions, one may write down the set of J equations generated by the relations

$$\frac{\partial \chi^2}{\partial Q_j} = 0.$$

These equations are of the form:

$$\sum_j A_{ij} \; Q_j = B_i \qquad (2)$$

where

$$A_{ij} \equiv \sum_{t,k} \frac{R_{ikt} \; R_{jkt}}{(\Delta C_{kt})^2}$$

and

$$B_i \equiv \sum_{t,k} \frac{C_{kt} \; R_{ikt}}{(\Delta C_{kt})^2}$$

and upon obtaining the inverse A^{-1} of the positive definite matrix A, one arrives at the solution

$$Q_j = \sum_i A_{ji}^{-1} \; B_i \qquad (3)$$

This approach, with no constraint on the Q_j, is quite acceptable provided the number of candidate source locations J is small (e.g., J<100) and source candidate locations are well separated; however, if nothing is known about the source locations, and instead, an array of point or area sources is conjectured to exist on an X-Y-grid of size n x m, then one must

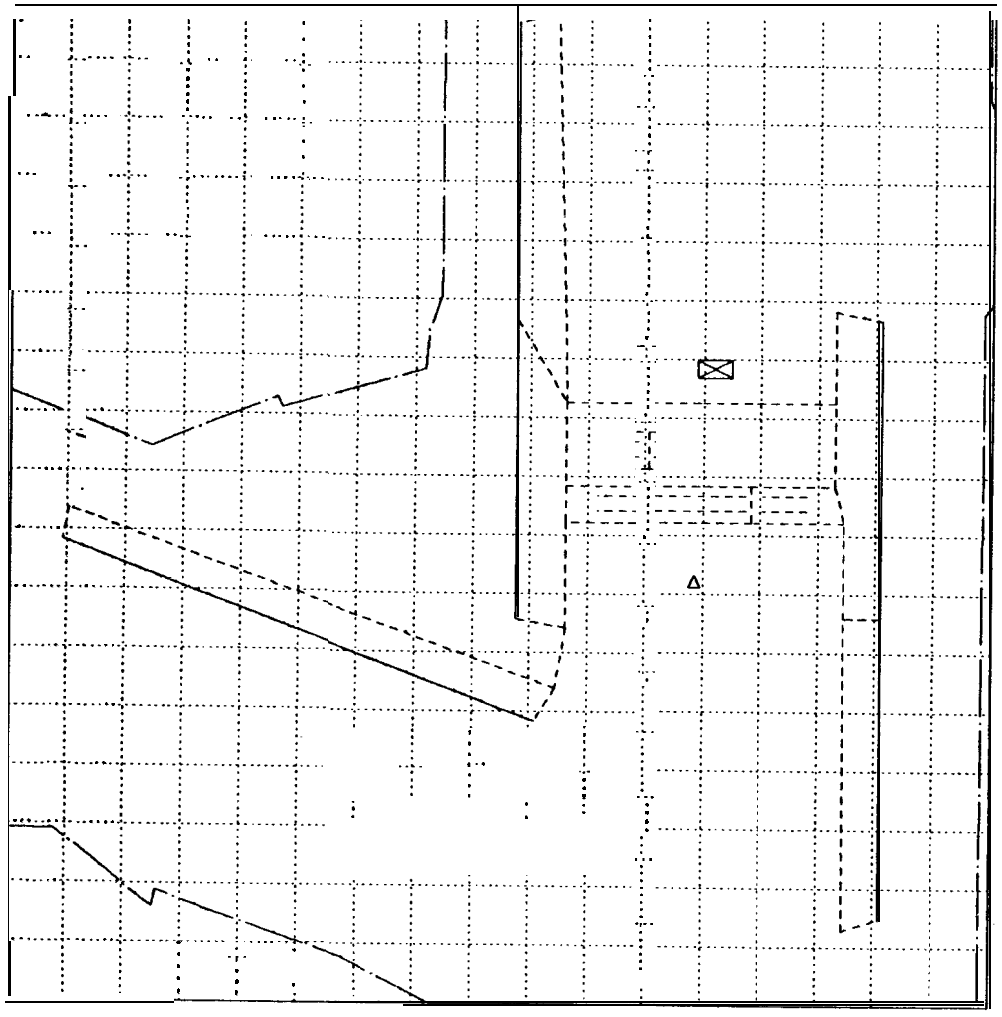

Fig. 4.3. Computational Grid Superimposed on Map of Dulles International Airport

⊠ Terminal

△ South Ramp Monitoring Station

——— runway

- - - taxiway

- · - airport property line

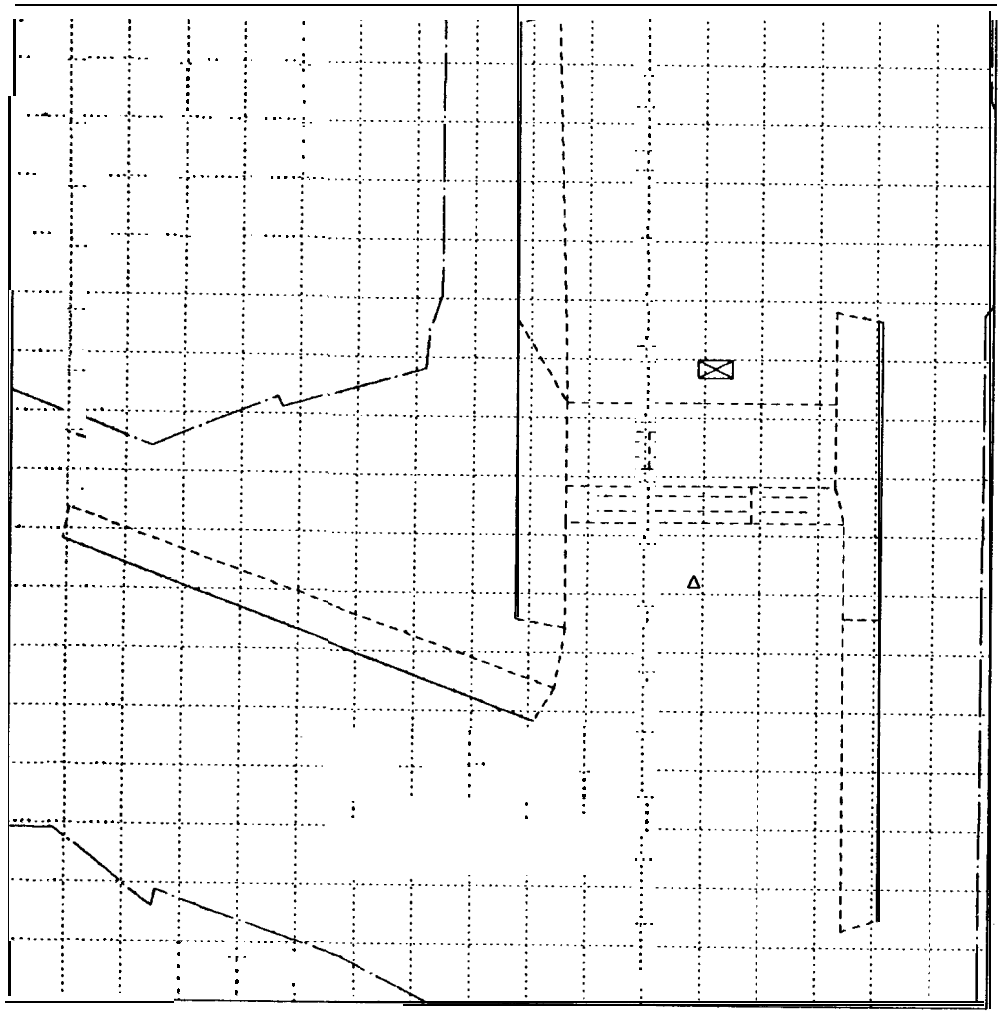

Fig. 4.3. Computational Grid Superimposed on Map of Dulles International Airport

⊠ Terminal

△ South Ramp Monitoring Station

——— runway

- - - taxiway

- · - airport property line

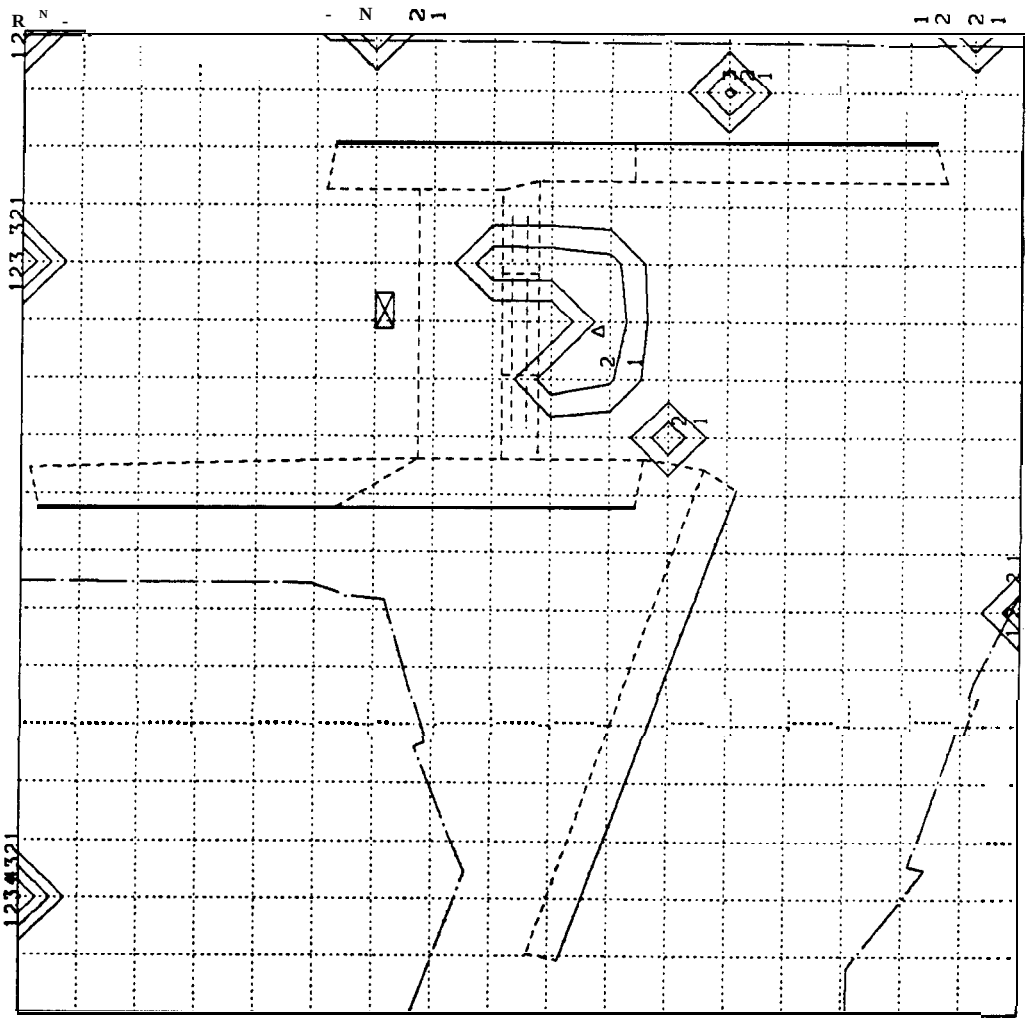

Fig. 4.4. Source Finding Solution Contours for CO. Isopleths are proportional to the $\log_{10}$ of the CO emission density fuction found to give a best χ^2 fit to observed concentrations.

problem is best treated exactly for the case of J source candidates via solution of the coupled equations

$$\sum_j A_{ij} Q_j = B_i$$

subject to the condition $Q_j \geq 0$ for all j.

Application of this source finding algorithm to the CO data obtained from the regional network at and around Dulles International Airport, correctly locates the leading aircraft CO emission zone but further indicates the presence of substantially stronger off-airport sources.

4.4 THREE TOWER MEASUREMENTS OF CO

The Concorde air quality monitoring and analysis program conducted at Dulles International Airport during 1976-77 provided a unique opportunity to measure CO plumes from taxiing aircraft. The transport and dispersion of these CO plumes was monitored at 13 points on the three tower array shown in Fig. 4.5, measured with Ecolyzers, and recorded on high-speed strip chart recorders. CO values were extracted from measurements of strip chart records. A sample set of CO traces is also seen in Fig. 4.5. Wind speed and direction were measured at the 80' and 14' levels on the first tower. Temperature gradient was measured between 67' and 14' on the same tower. Several hundred plumes were observed under neutral/unstable daytime conditions during the one-, two-, and three-tower phases of the experiment. Commercial aircraft types monitored included the Concorde, 707, 727, 737, 747, DC8, DC9, DC10, and L1011. Though peak instantaneous CO levels reached 10 ppm at the first tower (only 215 ft from the taxiway centerline), maximum aircraft contribution to the hourly average, ground level, CO concentration remained below 0.06 ppm per aircraft. Extrapolations to 1000 ft from the taxiway indicate a maximum hourly average concentration of 0.03 ppm CO per aircraft. Thus, hourly concentrations in excess of several ppm, adjacent to a busy taxiway, would be unlikely to occur.

Though maximum CO impacts are expected from queueing operations rather than taxi, the data from the taxi mode provide interesting information on initial plume dimensions and buoyant plume rise. These plume parameters may then be used in airport air quality models to increase their accuracy and predictive power.

problem is best treated exactly for the case of J source candidates via solution of the coupled equations

$$\sum_j A_{ij} Q_j = B_i$$

subject to the condition $Q_j \geq 0$ for all j.

Application of this source finding algorithm to the CO data obtained from the regional network at and around Dulles International Airport, correctly locates the leading aircraft CO emission zone but further indicates the presence of substantially stronger off-airport sources.

4.4 THREE TOWER MEASUREMENTS OF CO

The Concorde air quality monitoring and analysis program conducted at Dulles International Airport during 1976-77 provided a unique opportunity to measure CO plumes from taxiing aircraft. The transport and dispersion of these CO plumes was monitored at 13 points on the three tower array shown in Fig. 4.5, measured with Ecolyzers, and recorded on high-speed strip chart recorders. CO values were extracted from measurements of strip chart records. A sample set of CO traces is also seen in Fig. 4.5. Wind speed and direction were measured at the 80' and 14' levels on the first tower. Temperature gradient was measured between 67' and 14' on the same tower. Several hundred plumes were observed under neutral/unstable daytime conditions during the one-, two-, and three-tower phases of the experiment. Commercial aircraft types monitored included the Concorde, 707, 727, 737, 747, DC8, DC9, DC10, and L1011. Though peak instantaneous CO levels reached 10 ppm at the first tower (only 215 ft from the taxiway centerline), maximum aircraft contribution to the hourly average, ground level, CO concentration remained below 0.06 ppm per aircraft. Extrapolations to 1000 ft from the taxiway indicate a maximum hourly average concentration of 0.03 ppm CO per aircraft. Thus, hourly concentrations in excess of several ppm, adjacent to a busy taxiway, would be unlikely to occur.

Though maximum CO impacts are expected from queueing operations rather than taxi, the data from the taxi mode provide interesting information on initial plume dimensions and buoyant plume rise. These plume parameters may then be used in airport air quality models to increase their accuracy and predictive power.

As indicated in Fig. 4.5, CO was measured by pumping air samples continuously through identical volume sampling lines into individual Ecolyzer units. These units were housed in an air conditioned shelter. They were periodically calibrated by sequential switching of the intakes to the same 18 ppm concentration. The calibration system was designed to allow precise timing of sensor exposure to calibration gases of different concentrations so that response time constraints and linearity of signal amplitude could be determined. Since an aircraft passage "event" was expected to produce a pulse representing concentration versus time (as shown if Fig. 4.6), the measurement of sensor system time characteristics was deemed important. The time constant of the Ecolyzers averaged 12 seconds, and their threshold sensitivity averaged 0.25 ppm.

The concentration shown in Fig. 4.5 represent the instantaneous peak values from the relatively high speed chart records. Figure 4.6 is idealized in the sense that the skew (to the right) observed as a result of the time response, and potentially the pollutant distribution, is not shown. When the data was reduced, both the time-to-peak and the time-to-half-peak were recorded in addition to the peak CO value, the full-width-at-half-maximum time, and the background CO so that skewness could be accounted for in future modeling. Details of the method for correcting the peak concentrations when one uses an event modeling technique are given by Smith (1977).

In addition to concentration measurements, documentation for each event included event time, direction of aircraft travel, departure or arrival made, time to travel 50 m, and meteorological conditions. Wind direction and speed were averaged over three minutes. The value of σ_θ for the same averaging time was found from 30 six-second samples for each event, commencing at the recorded event time. The specific ranges of meteorological conditions are given with the results below. All selected tests were conducted in the daytime and had winds between 290° and 70°. The taxiing activity pattern, the orientation of the towers at Dulles, and simplicity for modeling were factors leading to this selection.

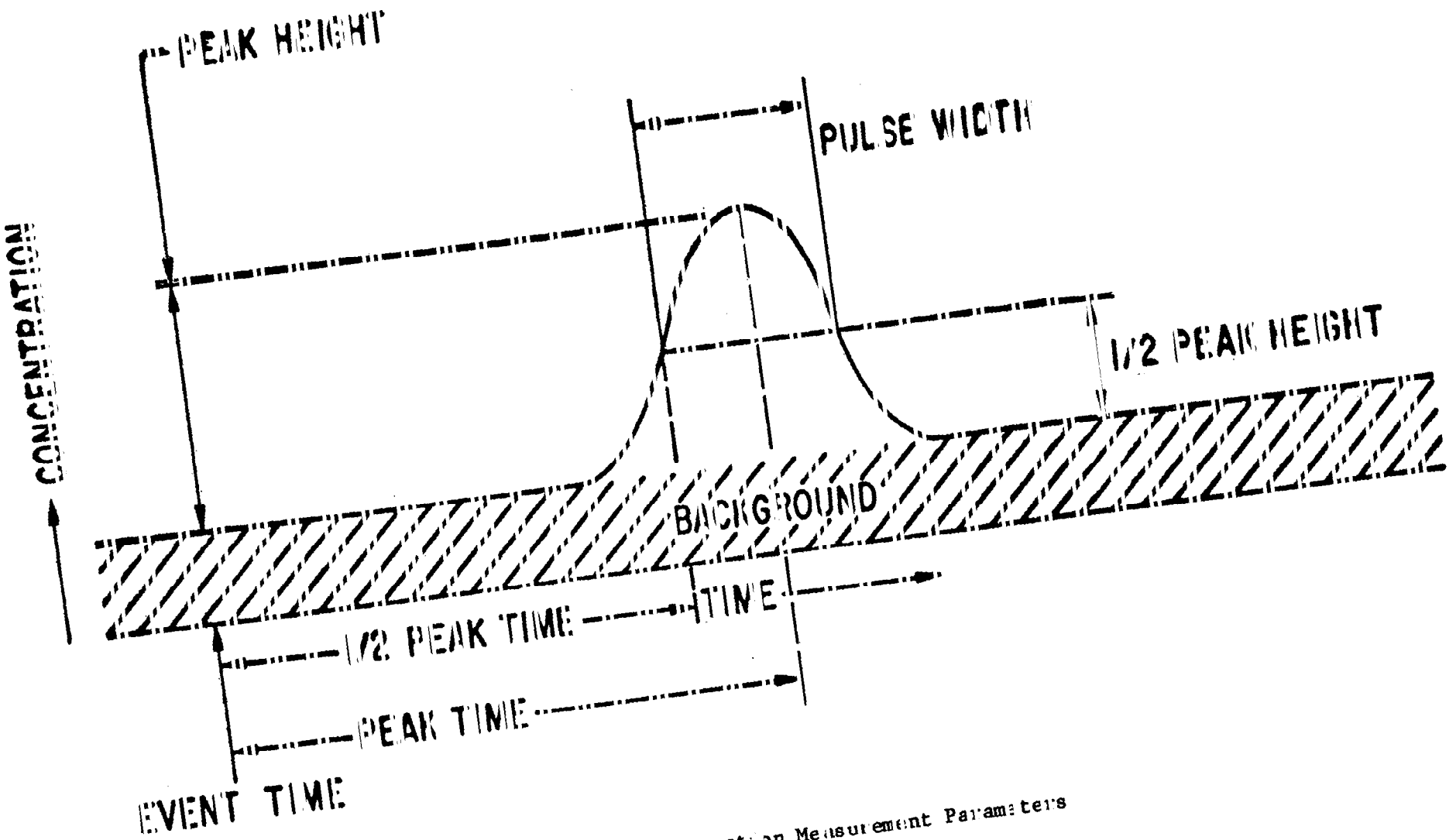

Fig. 4 6. Concentration Measurement Parameters

4.5 PLUME RISE FROM JET AIRCRAFT DURING THE TAXI MODE

4.5.1 Introduction

This section discusses the results of an investigation of the behavior of buoyant jet engine exhaust plumes in a crosswind; it attempts to identify the degree to which the plume rise can be described by relationships developed for other types of sources.

At least four factors affecting the rate of dilution of jet exhaust before it reaches receptor adjacent to taxi-ways or runways have been previously identified [Heywood et al. (1971)]:

1. turbulent mixing of the jet exhaust at the engine exit
2. buoyant plume rise
3. advective dilution
4. dispersion by ambient turbulence

Observational studies of plumes generally allow only one or two separate processes to be measured (plume rise and total dispersion rate). Although the bending of an exhaust plume from its original release axis until it is aligned with the prevailing wind direction is also observable (particularly from above). This change in orientation or "bending" may also be viewed as the transition from plume dilution dominated by the first mechanism to dilution controlled by the latter three. For this reason, the maximum length of the highly turbulent jet trail as a function of wind speed is of interest.

The assumption is made that the two phenomena, plume bending and plume rise, can be treated independently as a first approach. Both theoretical and empirical models are available to describe plume bending in a perpendicular wind [e.g. Abramovich (1963)]. Estimates of the maximum distances of dominance of jet exhaust mechanical turbulence are made for taxiing aircraft. The estimates here are restricted to perpendicular winds for simplicity.

Analysis of the experimental data revealed that the precision of measurement of the initiation time of each aircraft passage "event" was not adequate for analysis of differences between expected arrival times for CO at the first tower under alternate plume bending hypothesis. Thus, although

these alternative descriptions of aircraft plume bending are given, the present comparisons with experimental evidence are restricted to the phenomenon of plume rise. It is this mechanism for aircraft plume dilution that was of primary concern in the Dulles experiments [Smith (1977)], although the other three mechanisms listed were also considered.

4.5.2 Modeling Turbulent Jet Exhausts without Plume Rise

Aircraft jet exhausts discharged horizontally into a uniform crosswind may be described in two stages: the momentum-dominant 'stage and the buoyancy-dominant stage. In the momentum-dominant stage, the horizontal velocity of the jet plume decays through turbulent mixing with ambient air, and plume rise is suppressed. In the buoyancy-dominant stage, the plume rises and is entrained by the vertical motion. If it is assumed that there are no interactions between adjacent engine plumes and plume rise ignored, the benching path of a nonbuoyant momentum jet in a crosswind may be estimated from Eq. (1):

$$\hat{y} = 1.5\ V_r^{2/3}\ \hat{x}^{1/3} \qquad (1)$$

where the coordinate system is that shown in Fig. 4.7, with B (angle between the y-axis and aircraft path) equal to zero [see Briggs (1969)].

$V_r = Ve/u$
V_e = exhaust velocity
u = windspeed
$\hat{y} \equiv y/D$
$\hat{x}$ x/D
D = exit diameter

the maximum penetration length of the exhaust plume behind the aircraft can be estimated from:

$$\hat{y}_{max} = 3V_r \text{ and } \hat{x}_{max} = 8V_r \qquad (2)$$

At this y_{max} distance behind the aircraft, the angle between the plume centerline and the y-axis may be found from Eq. (3):

$$\Theta = \tan(dy/dx) = \tan^{-1}\left[1/2\left(\frac{Vr}{x}\right)^{2/3}\right] \qquad (3)$$

therefore, Θ_{max} 7°.

these alternative descriptions of aircraft plume bending are given, the present comparisons with experimental evidence are restricted to the phenomenon of plume rise. It is this mechanism for aircraft plume dilution that was of primary concern in the Dulles experiments [Smith (1977)], although the other three mechanisms listed were also considered.

4.5.2 Modeling Turbulent Jet Exhausts without Plume Rise

Aircraft jet exhausts discharged horizontally into a uniform crosswind may be described in two stages: the momentum-dominant 'stage and the buoyancy-dominant stage. In the momentum-dominant stage, the horizontal velocity of the jet plume decays through turbulent mixing with ambient air, and plume rise is suppressed. In the buoyancy-dominant stage, the plume rises and is entrained by the vertical motion. If it is assumed that there are no interactions between adjacent engine plumes and plume rise ignored, the benching path of a nonbuoyant momentum jet in a crosswind may be estimated from Eq. (1):

$$\hat{y} = 1.5\ V_r^{2/3}\ \hat{x}^{1/3} \qquad (1)$$

where the coordinate system is that shown in Fig. 4.7, with B (angle between the y-axis and aircraft path) equal to zero [see Briggs (1969)].

$V_r = Ve/u$
V_e = exhaust velocity
u = windspeed
$\hat{y} \equiv y/D$
$\hat{x}$ x/D
D = exit diameter

the maximum penetration length of the exhaust plume behind the aircraft can be estimated from:

$$\hat{y}_{max} = 3V_r \text{ and } \hat{x}_{max} = 8V_r \qquad (2)$$

At this y_{max} distance behind the aircraft, the angle between the plume centerline and the y-axis may be found from Eq. (3):

$$\Theta = \tan(dy/dx) = \tan^{-1}\left[1/2\left(\frac{Vr}{x}\right)^{2/3}\right] \qquad (3)$$

therefore, Θ_{max} 7°.

To evaluate $\hat{y}_{max}$ and $\hat{x}_{max}$ for engines of the specific aircraft, Table 4.1 should be consulted. Also presented in Table 4.1 are appropriate values of the exit velocities and temperatures for calculation of effective velocity ratio:

$$V_r' \equiv \left[\frac{\rho' u^2}{\rho u^2}\right]^{1/2} \qquad (4)$$

where ρ = density of the ambient air
ρ' = density of the jet exhaust

It is expected that substitution of V_r' in the Eq. (1) through (3) will yield more accurate estimates for jet exhausts. In Table 4.1, the exhaust diameter, exit velocity, and exit temperature is given for the JT-3 and JT-8 engine during taxi/idle mode operation. Thrust values and mass emission rates are also given for comparison. For average surface winds of 5 m/sec, V_r would range from 15 for the JT3s to 23 for the JT-8s during taxiing operations. For the range of $8 < V_r' < 54$ and $x \leq 34$, experimental evidence [Patrick (1967)] indicates:

$$\hat{Y} = (V_r')^{0.85} (x)^{0.38} \text{ and } y_{max} = 2.3 (V_r')^{1.37} \qquad (5)$$

These relationships yield similar results to those obtained from Eqs. (1) and (2). Thus, for taxiing B707s, $y_{max} \simeq 40$ m and for B727s $y_{max} \simeq 53$ m, and corresponding x_{max} values of 108 m and 138 m (with wind speeds of 5 m/sec). For sensors near the edge of the taxiway, the value of x_{max} would determine whether dilution of the plume reaching those sensors was dominated by jet trail turbulence or ambient turbulence.

Table 4.1. Aircraft Engine Emission Parameters

Aircraft Type	B707	B727
Engine Type	JT-3	JT-8
Diameter, Exit (m)	0.9	0.75
Ve (m/sec)	76	114
Te (°K)	386	440
Mass Rate (Kg/sec)	45	40
Thrust (Nt)	270	250

Source: Goldberg (1978)

4.5.3 Plume Rise Modeling

To obtain a simple plume rise equation for a buoyant plume it is necessary to make some basic assumptions:

1. The flow is fully turbulent, thus the effect of molecular viscosity or Reynolds number is negligible.

2. Boussinesq approximation is valid, i.e., local density variations are neglected except when multiplying by gravity.

3. The buoyancy is assumed to be conserved.

4. The fluids are quasi-incompressible.

This theory or the 2/3 power relation was obtained by Slawson and Csanady (1967) and substantiated by Briggs (1969) and Hoult, Fay and Forney (1969).

Using the entrainment hypothesis given by Morton, Taylor, and Turner (1956), one may express the rise of the buoyant plume from jet aircraft as:

$$z - z_o = \left[\frac{3}{2\alpha^2}\right]^{1/3} F^{1/3} u^{-1} (x - x_o)^{2/3} \qquad (6)$$

where

z_o = initial height
x_o = initial downwind distance
F = bouyancy flux
a = entrainment constant
u = windspeed

Although this 2/3 power law relation was developed originally for stationary sources with lower exit plumes than jet exhaust, its use as a first estimate for the present application is encouraged two factors:

1. The heat flux from a jet engine is similar in magnitude to a small stationary source ($F \simeq 10^2 m^4/sec^3$).

2. This same power law has been successful in describing plumes from high temperature has turbine stacks located in a region of high ambient turbulence [Hoult (1975) and Egan (1975)].

4.5.4 Event Modeling

Several distinct approaches were attempted in the analysis of the Dulles three-tower data. The most straight-forward involved fitting a gaussian vertical profile, plus ground reflection term to the concentration measurements at each tower to obtain the plume's centerline location and vertical spread for each event. After this individual fitting, the dynamical plume rise and growth equations were fitted to the earlier obtained values for the plume centerline and σ_z. The advantage of this approach was that plume successful for the first tower (i.e., closest to the taxiway), but it proved unreliable at the more distant towers where plume centerlines were often above the highest receptor and/ or where rapid vertical dispersion produced nearly uniform vertical concentration profiles.

At the other extreme lies the ensemble-fit method, where the entire set of observations of a single aircraft type under the full range of meteorological conditions is applied to a single comprehensive theory containing a number of adjustible parameters. This method provides a starting point for investigating single event deviations from the ensemble predictions but may obscure interesting dynamical effects not built explicitly into the model. This method was chosen above the single event method because of the fact that many events had a "non-ideal" distribution where a centerline maximum was not observable at even the first tower. Figure illustrates the plume rise at tower 1.

Other methods like alternate multiparameter schemes for assessing individual events were considered but abandoned as their numerous parameters could not be adequately determined by the data accompanying each event.

4.5.5 The Ensemble Model

Consider the case of a source with emission rate q moving at velocity V along an infinite line orientated at an angle θ' with respect to the positive y direction (see Fig. 4.7). If the wind, u, defines the positive x direction, the receptor is located at (x, o, z) and t = 0 corresponds to the source position (0,0), then the instantaneous concentration at the receptor is given by Eq. 7.

$$c(t) = \frac{q \exp\left\{-\frac{1}{2}\left(\frac{x - ut}{\sigma}\right)^2 \left(\frac{V\cos\theta'}{V_e}\right)^2\right\} S(z,H,\sigma_z)}{2\pi\sigma\sigma_z V_e} \qquad (7)$$

4.5.4 Event Modeling

Several distinct approaches were attempted in the analysis of the Dulles three-tower data. The most straight-forward involved fitting a gaussian vertical profile, plus ground reflection term to the concentration measurements at each tower to obtain the plume's centerline location and vertical spread for each event. After this individual fitting, the dynamical plume rise and growth equations were fitted to the earlier obtained values for the plume centerline and σ_z. The advantage of this approach was that plume successful for the first tower (i.e., closest to the taxiway), but it proved unreliable at the more distant towers where plume centerlines were often above the highest receptor and/ or where rapid vertical dispersion produced nearly uniform vertical concentration profiles.

At the other extreme lies the ensemble-fit method, where the entire set of observations of a single aircraft type under the full range of meteorological conditions is applied to a single comprehensive theory containing a number of adjustible parameters. This method provides a starting point for investigating single event deviations from the ensemble predictions but may obscure interesting dynamical effects not built explicitly into the model. This method was chosen above the single event method because of the fact that many events had a "non-ideal" distribution where a centerline maximum was not observable at even the first tower. Figure illustrates the plume rise at tower 1.

Other methods like alternate multiparameter schemes for assessing individual events were considered but abandoned as their numerous parameters could not be adequately determined by the data accompanying each event.

4.5.5 The Ensemble Model

Consider the case of a source with emission rate q moving at velocity V along an infinite line orientated at an angle θ' with respect to the positive y direction (see Fig. 4.7). If the wind, u, defines the positive x direction, the receptor is located at (x, o, z) and t = 0 corresponds to the source position (0,0), then the instantaneous concentration at the receptor is given by Eq. 7.

$$c(t) = \frac{q \exp\left\{-\frac{1}{2}\left(\frac{x - ut}{\sigma}\right)^2 \left(\frac{V\cos\theta'}{V_e}\right)^2\right\} S(z,H,\sigma_z)}{2\pi\sigma\sigma_z V_e} \qquad (7)$$

where

σ_θ = 3 min average measurement of the standard deviation of wind direction,

$\sigma_x(0)$ = initial along-wing plume spread,

$\sigma_z(0)$ = initial vertical plume spread,

b_x, b_z = plume growth parameters. They describe the growth of the plume relative to σ_θ,

H = plume centerline height at distance x,

H_o = initial plume centerline height.

The addition of the term $\frac{(H - H_o)^2}{10}$ is suggested by Pasquill.

The Eq. (14) used for plume rise is somewhat more general than the equation suggested theoretically in that the powers p and q are free parameters. Fits were done with p and q free and with these parameters fixed at p = 2/3 and q = 1 as given by the 2/3 power law relation.

Equation 15, $H_o = 1.2\ \sigma_z(0)$ is dictated by the assumption of zero vertical concentration gradient which causes an uniform concentration profile near the ground.

With these Eq. (9-14) we can define a measure of "goodness-of-fit" χ^2 and via minimization of χ^2 the eight free parameters $\sigma_x(0)$, $\sigma_z(0)$, b_x, b_z, h, t_o, p, and q are to be determined. The equation for χ^2 is given by:

$$\chi^2 = \frac{1}{(\delta C)^2}\sum\left(C^T_{peak} - C^M_{peak}\right)^2 + \frac{1}{(\delta\Gamma)^2}\sum\left(\Gamma^T - \Gamma^M\right)^2 \qquad (16)$$

where ΓC and $\delta\Gamma$ denote the approximate measurement errors of 0.25 ppm and 10 seconds. The superscripts T and M denote theory and measurement respectively. The indicated summation is over all measurements for a single aircraft type.

The preceding expression for χ^2 should actually be normalized by the total expected variances in C_{peak} and (i.e., the statistical plus the measurement component) and not merely by the measurement variances. However, the statistical variances are not determinable from these data alone. This shortcoming preclude determination of overall model confidence level and parameter errors. Some additional insight into potential model improvements is provided by alternate consideration of the linear correlation coef-

ficients, for predicted versus observed C_{peak} and τ, and the associated confidence bounds on these correlations.

4.5.6 Results

Table 4.2 shows the number of events for the different aircraft types. The results are based on a somewhat smaller selection because of the constraint that the wind direction was within 70° of being perpendicular to the taxiway. All events were observed under near neutral to unstable atmospheric conditions, with bulk Richardson numbers ranging from $-1.0 * 10^{-4}$ to -0.02, windspeeds in the range from 1.2 to 13.4 m/sec, and 3-minute σ_θ from 4.7 to 37.0 degrees. Average taxi speeds ranged from 7.6 to 11.8 m/sec.

Fixing the values of p and q as 2/3 and 1 respectively, the ensemble fit yields the parameters given in Table 4.3. The correlation values for the concentration values and their 95% confidence limits are also given.

The correlation values for the pulse duration is not given. The theory is quite poor in predicting τ, the pulse duration. This is partially attributable to the fact that τ is predicted to be independent of height but considerable fluctuation is observed experimentally. Another factor contributing to this poor correlation is that, contrary to theoretical expectations, the observed pulse duration increases very little between the first and third tower and is, in fact, consistent with zero along wind plume growth (i.e., $b_x = 0$). Thus, the differences in horizontal growth rate factor b_x between aircraft types cannot be considered significant. The value of b_z is found to be highly correlated with the H parameter, which establishes the rate of plume rise and the associated vertical dispersion due to entrainment. In addition, despite significant differences in engine placement on the B707, B727, and DC8 aircraft, the initial along wind and vertical plume dimensions are nearly identical.

The rather poor value of the correlation coefficient r is thought to be due to large variations in ambient air stratification and its effect on buoyancy. Evidence for this is obtained when each event is optimized separately with h, the parameter which describes the buoyancy, as the only free parameter . The other parameters were fixed to their values, found in the ensemble fit. Figure 4.8 shows the wide variety of h values for the B707 when calculated as described above. Significant variations about the ensemble

ficients, for predicted versus observed C_{peak} and τ, and the associated confidence bounds on these correlations.

4.5.6 Results

Table 4.2 shows the number of events for the different aircraft types. The results are based on a somewhat smaller selection because of the constraint that the wind direction was within 70° of being perpendicular to the taxiway. All events were observed under near neutral to unstable atmospheric conditions, with bulk Richardson numbers ranging from $-1.0 * 10^{-4}$ to -0.02, windspeeds in the range from 1.2 to 13.4 m/sec, and 3-minute σ_θ from 4.7 to 37.0 degrees. Average taxi speeds ranged from 7.6 to 11.8 m/sec.

Fixing the values of p and q as 2/3 and 1 respectively, the ensemble fit yields the parameters given in Table 4.3. The correlation values for the concentration values and their 95% confidence limits are also given.

The correlation values for the pulse duration is not given. The theory is quite poor in predicting τ, the pulse duration. This is partially attributable to the fact that τ is predicted to be independent of height but considerable fluctuation is observed experimentally. Another factor contributing to this poor correlation is that, contrary to theoretical expectations, the observed pulse duration increases very little between the first and third tower and is, in fact, consistent with zero along wind plume growth (i.e., $b_x = 0$). Thus, the differences in horizontal growth rate factor b_x between aircraft types cannot be considered significant. The value of b_z is found to be highly correlated with the H parameter, which establishes the rate of plume rise and the associated vertical dispersion due to entrainment. In addition, despite significant differences in engine placement on the B707, B727, and DC8 aircraft, the initial along wind and vertical plume dimensions are nearly identical.

The rather poor value of the correlation coefficient r is thought to be due to large variations in ambient air stratification and its effect on buoyancy. Evidence for this is obtained when each event is optimized separately with h, the parameter which describes the buoyancy, as the only free parameter . The other parameters were fixed to their values, found in the ensemble fit. Figure 4.8 shows the wide variety of h values for the B707 when calculated as described above. Significant variations about the ensemble

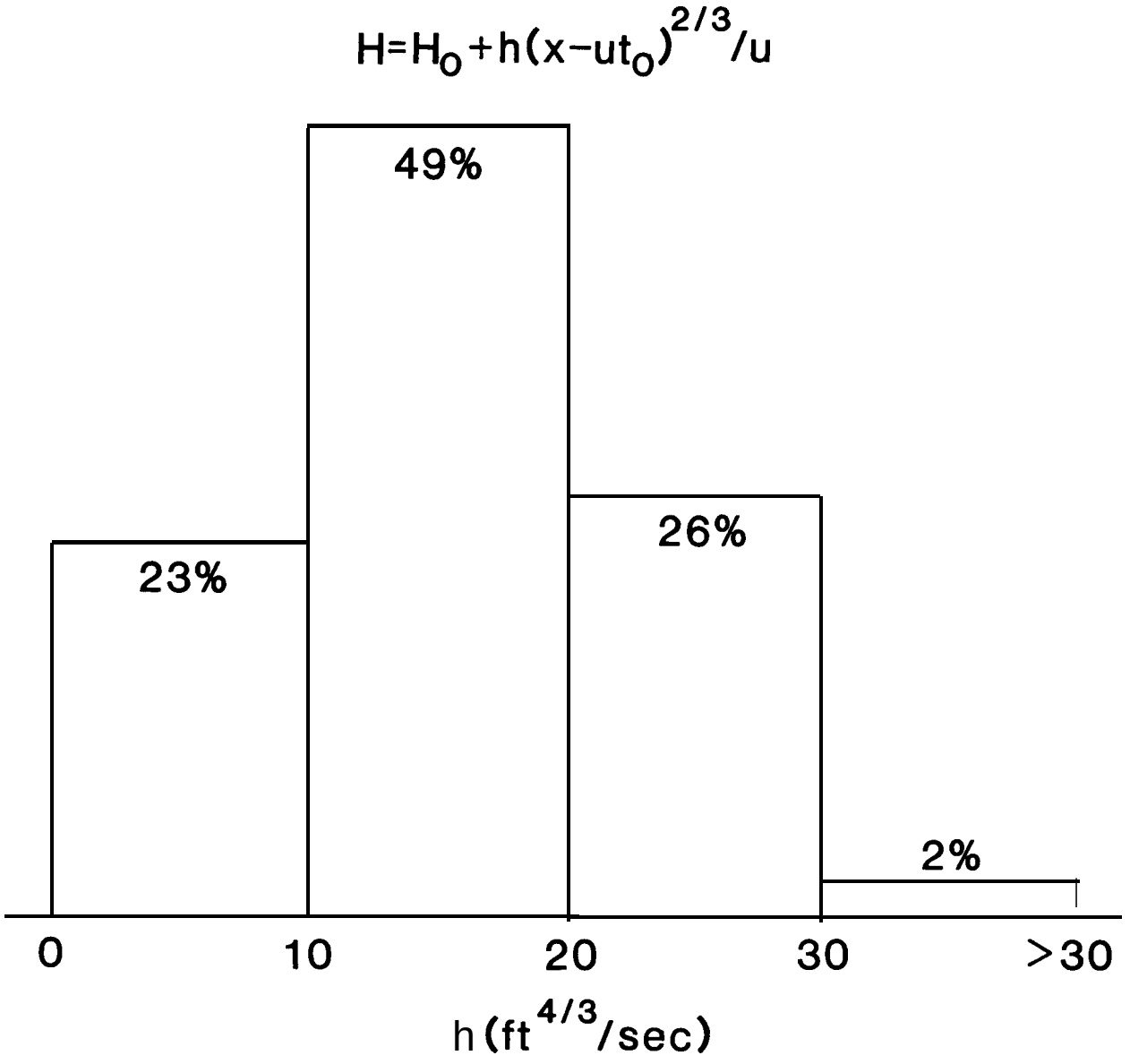

Fig. 4.8. Frequency Distribution of Plume Rise Coefficient

value of 16 are seen. The correlation coefficient of jumps from 0.53 to 0.81 when this event-by-event freedom is permitted.

Another insight into event-by-event deviation from the predicted $x^{2/3}$ plume rise behavior can be seen in Fig. 4.9. It shows the wide variety of p-values (the plume rise trajectories) one obtains when p is determined on an event-by-event basis. Ensemble optimizations in which p and q were allowed to be free indicated somewhat higher values for p and q of 1.25 and 1.75, respectively; however, the resulting improvements in r were insignificant.

The plume rise equation used in the above analysis does not predict final plume height and thus is of limited usefulness in terms of airport air quality models. A simpler model, described briefly below has been applied to the 3-tower data and the results indicate the importance of initial plume dilution and rise on observed concentrations.

Assume that plume growth is governed by the equations

$$\sigma_x = \sigma_y = \sigma_x(0) + b_x \sigma_{yT}(x) \qquad (17)$$

and

$$\sigma_z = \left[\left(\sigma_z(0) + b_z \sigma_{zT}(x) \right)^2 + 0.1 (H - H_o)^2 \right]^{1/2} , \qquad (18)$$

where $\sigma_x(0)$ and $\sigma_z(0)$ are the initial horizontal and vertical plume dimensions, $\sigma_{yT}(x)$ and $\sigma_{zT}(x)$ are the dispersion coefficients taken from Turner (1970) and $b_x = b_z = 0.7$ is a correction for averaging time. Further assume that the final plume rise is given by the equation

$$H = H_o + h/u, \qquad \text{where } H_o \equiv 1.2 \sigma_z(0) \qquad (19)$$

u is the wind speed, and h is the plume rise factor to be determined. Taking the dynamical behavior of the plume rise into account and applying these equations to a sample of 121 cases, encompassing all the aforementioned aircraft types except Concorde, one obtains the optimized parameters

$$\sigma_x(0) = 60 \text{ ft}$$
$$\sigma_z(0) = 26 \text{ ft}$$
$$h = 386 \text{ ft}^2/\text{sec}$$

For ground level data points ($z = 6$ ft) the regression equation

$$C_{OBSERVED} = m\, C_{THEORY} + b$$

value of 16 are seen. The correlation coefficient of jumps from 0.53 to 0.81 when this event-by-event freedom is permitted.

Another insight into event-by-event deviation from the predicted $x^{2/3}$ plume rise behavior can be seen in Fig. 4.9. It shows the wide variety of p-values (the plume rise trajectories) one obtains when p is determined on an event-by-event basis. Ensemble optimizations in which p and q were allowed to be free indicated somewhat higher values for p and q of 1.25 and 1.75, respectively; however, the resulting improvements in r were insignificant.

The plume rise equation used in the above analysis does not predict final plume height and thus is of limited usefulness in terms of airport air quality models. A simpler model, described briefly below has been applied to the 3-tower data and the results indicate the importance of initial plume dilution and rise on observed concentrations.

Assume that plume growth is governed by the equations

$$\sigma_x = \sigma_y = \sigma_x(0) + b_x \sigma_{yT}(x) \qquad (17)$$

and

$$\sigma_z = \left[\left(\sigma_z(0) + b_z \sigma_{zT}(x) \right)^2 + 0.1 (H - H_o)^2 \right]^{1/2} , \qquad (18)$$

where $\sigma_x(0)$ and $\sigma_z(0)$ are the initial horizontal and vertical plume dimensions, $\sigma_{yT}(x)$ and $\sigma_{zT}(x)$ are the dispersion coefficients taken from Turner (1970) and $b_x = b_z = 0.7$ is a correction for averaging time. Further assume that the final plume rise is given by the equation

$$H = H_o + h/u, \qquad \text{where } H_o \equiv 1.2 \sigma_z(0) \qquad (19)$$

u is the wind speed, and h is the plume rise factor to be determined. Taking the dynamical behavior of the plume rise into account and applying these equations to a sample of 121 cases, encompassing all the aforementioned aircraft types except Concorde, one obtains the optimized parameters

$$\sigma_x(0) = 60 \text{ ft}$$
$$\sigma_z(0) = 26 \text{ ft}$$
$$h = 386 \text{ ft}^2/\text{sec}$$

For ground level data points ($z = 6$ ft) the regression equation

$$C_{OBSERVED} = m\, C_{THEORY} + b$$

fit to the peak concentrations yields a correlation coefficient of 0.56, a slope of m = 0.96, and an intercept of b = 0.11 ppm. A scatter plot of observed versus peak concentrations is shown in Fig. 4.10.

If the parameters describing the initial plume dimensions and plume rise are instead taken as $\sigma_x(0) = \sigma_z(0) = h = 0$, the resulting regression parameters are m = 0.11 and b = 0.52, which implies that for the highest observed concentrations, the theory is overpredicting by a factor of 9. Hence the assumptions about initial plume size and rise can have serious air quality modeling consequences. For example, the initial vertical dispersion of 26 ft is equivalent to the amount of dispersion realized by 1500 ft of downwind transport under F stability conditions.

4.5.7 Conclusions

Preliminary analysis of measurements of the CO exhaust plume from taxiing aircraft suggest that the rise of these horizontally injected, buoyant plumes is not inconsistent with the 2/3 power law relation over the distance range of 65 m to 165 m, but large event-by-event fluctuations from this average behavior lead to rather mediocre correlations between theoretically predicted and observed pollutant concentrations.

There is an evidence for about a 10 second delay in plume rise. The present analysis suggests that the plume rise delay time, t_o is significant and at the highest wind speed has the effect of suppressing plume rise at the first tower.

Recalling the comparison between the B707, B727, and DC8, the initial plume rise during taxi was found to be characteristic of aircraft dimensions. The significance of engine geometry one might expect was not observed.

The average value of h, which describes the buoyancy, determined here is about equal to one-half the value found from

$$\left(\frac{3}{2\alpha^2}\right)^{1/3} F^{1/3},$$

where the total buoyancy flux F for the B707 and B727 aircraft types while taxiing is about 150 m^4/sec^3 [Goldberg (1978)]. A value of 0.6 for a was used in this calculation. In the case of jet aircraft plumes a larger value for the entrainment constant might be expected.

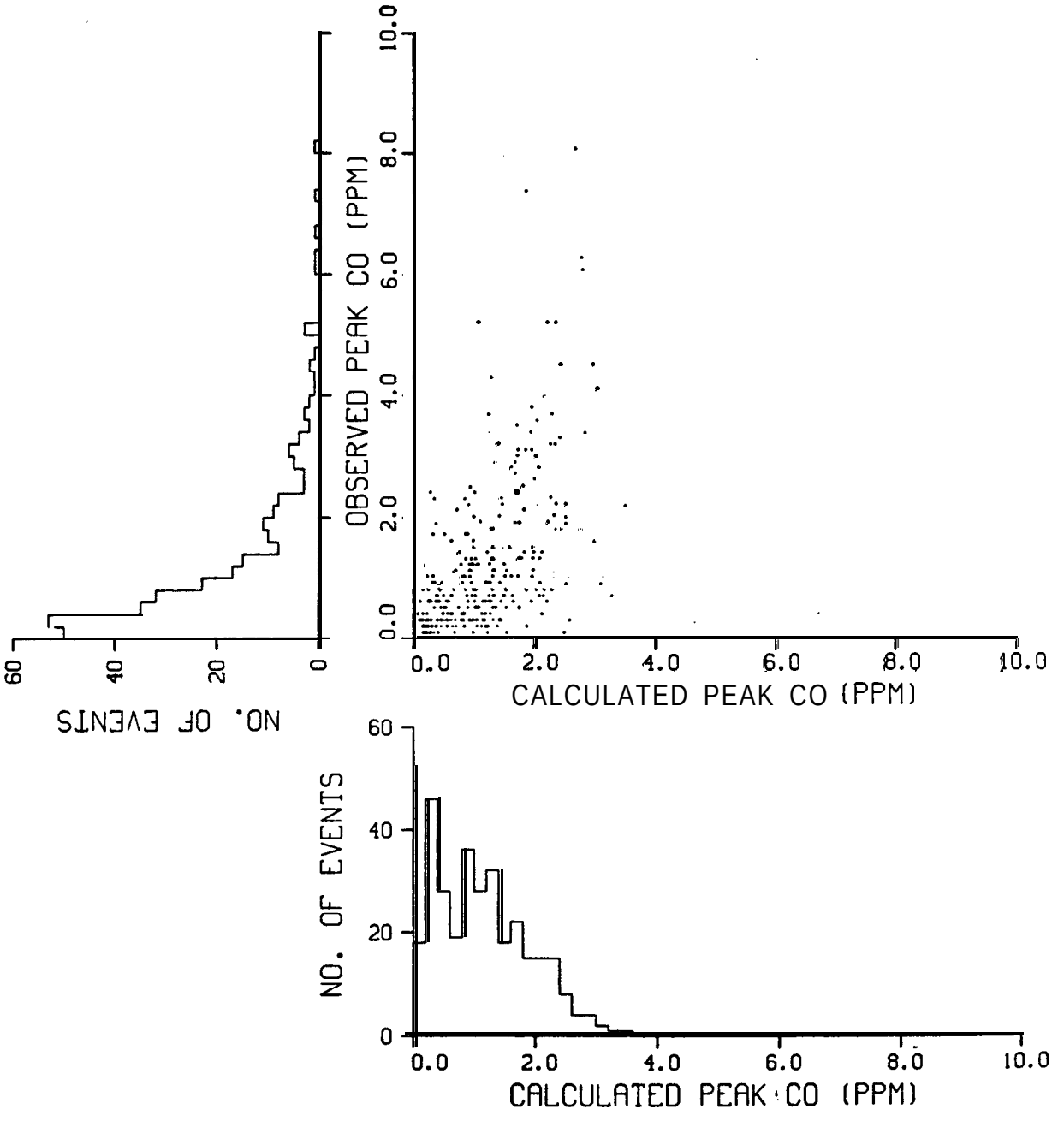

Fig. 4.10. Scatter Plot Plus Projection Histograms for Observed Versus Calculated Peak CO at Ground Level Receptors (z = 6 ft.). The calculation uses equations 17-19 and the optimal parameters given in the text.

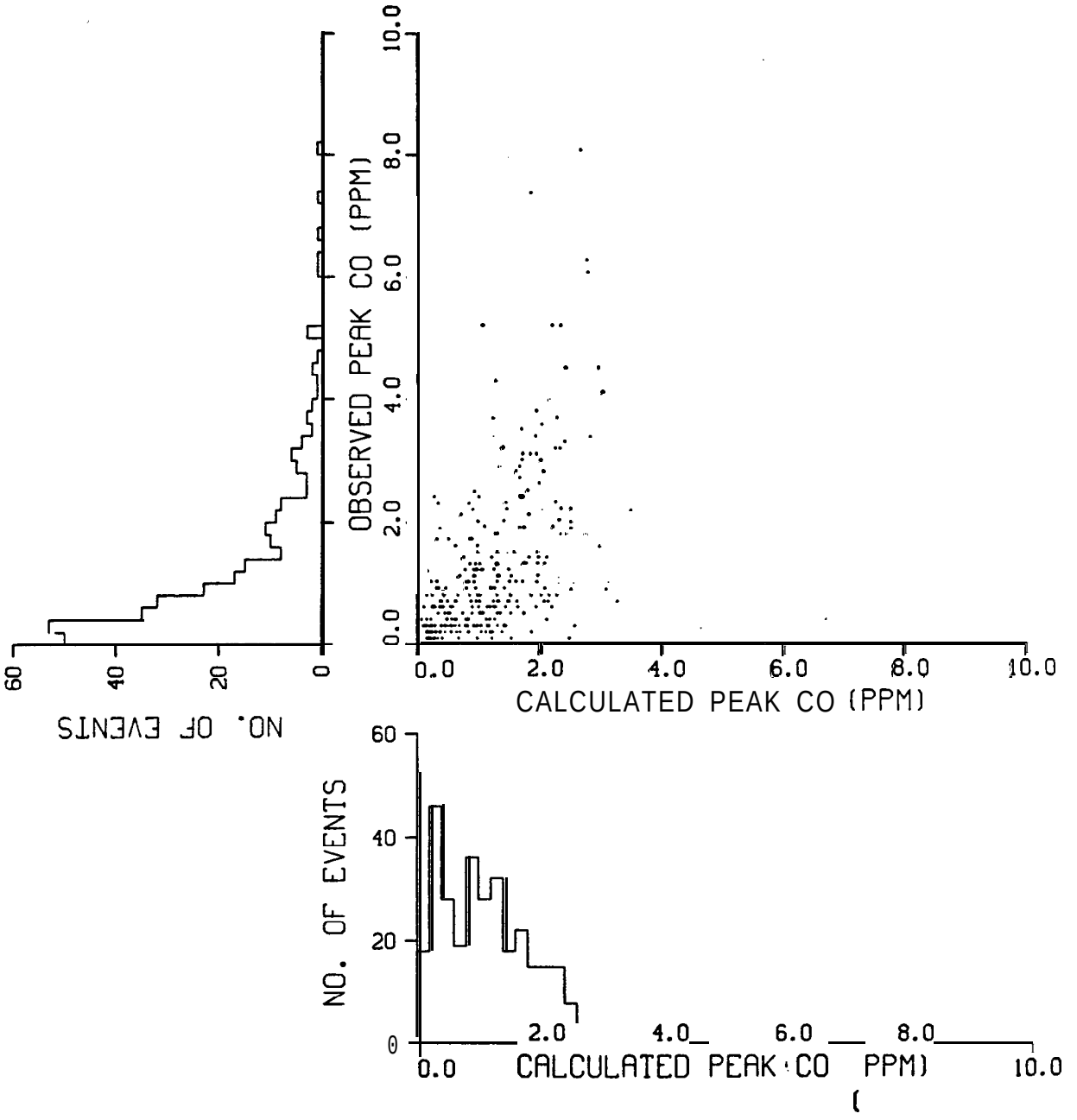

Fig. 4.10. Scatter Plot Plus Projection Histograms for Observed Versus Calculated Peak CO at Ground Level Receptors (z = 6 ft.). The calculation uses equations 17-19 and the optimal parameters given in the text.

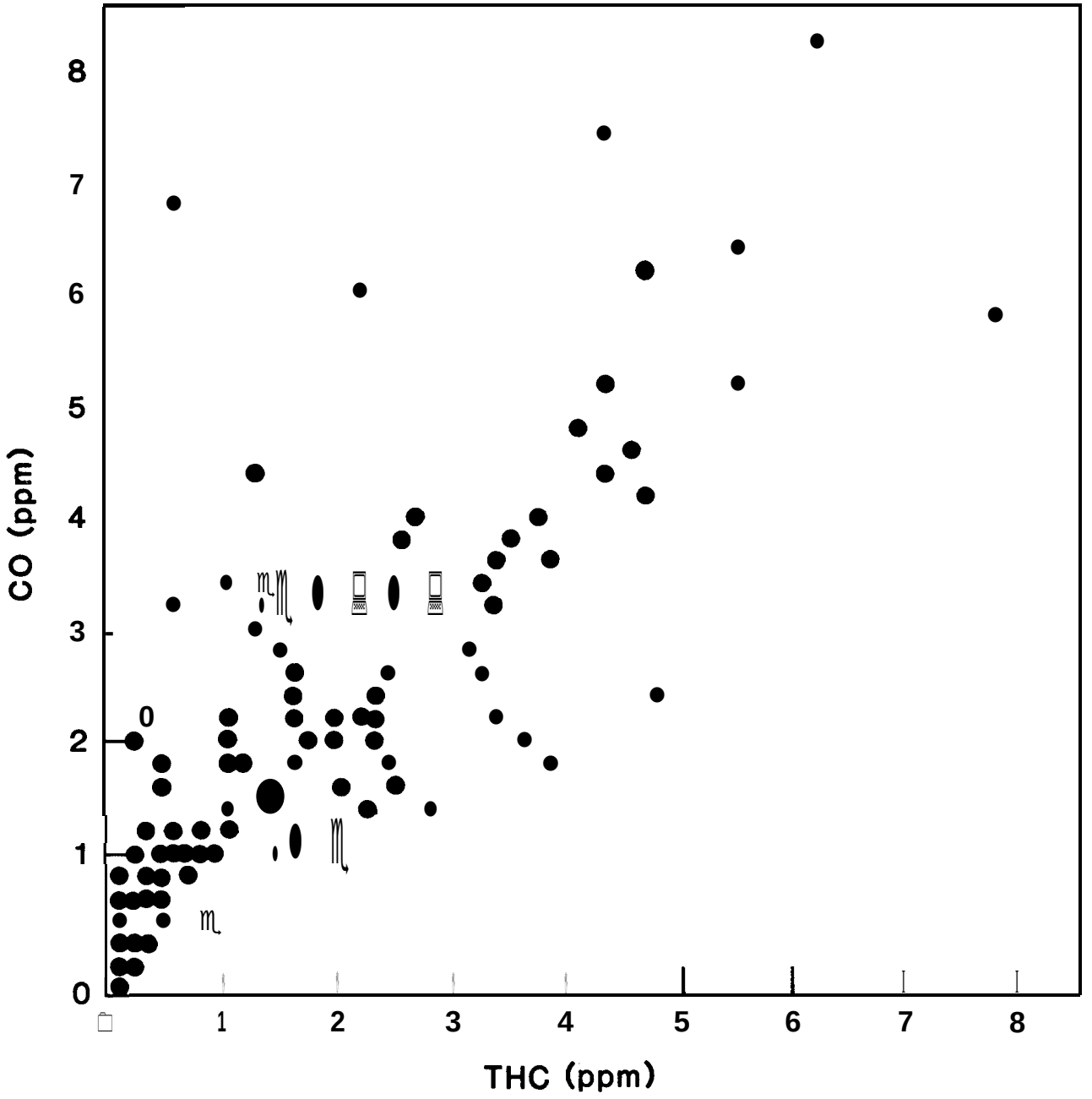

Fig. 4.11. Concentration Crossplot of CO vs THC from Taxiing Aircraft

(i.e., engine) types, are seen to agree in the mean with the engine emission ratios of CO to THC. From these single station comparisons it appears that estimation of THC through scaling of CO concentrations is viable for such near-field experiments where the background may be separately identified.

5 CARBON MONOXIDE MEASUREMENTS AT A HIGH ACTIVITY FLY-IN AT LAKELAND AIRPORT, FLORIDA+

5.1 INTRODUCTION

Carbon Monoxide (CO) concentrations were measured during a major fly-in of general aviation (GA) and experimental aircraft at Lakeland Airport, Florida from January 23 thru 29, 1978. Over 3000 aircraft participated in this fly-in, where in excess of 250 aircraft operations per hour were experienced. The purpose of the measurements was to quantify the effect of emissions from GA aircraft on air quality under extreme conditions of airport activity. The Federal Aviation Administration (FAA), in conjunction with the Environmental Protection Agency (EPA), planned the measurement activity. Three FAA-owned Energetic Sciences "Ecolysers" (CO monitors) were used. EPA personnel participated in the field program and assisted in data gathering.

Figure 5.1 is an aerial view of the airport and the lightly populated surrounding countryside and Figures 5.2 and 5.3 show the operating pattern at the airport during easterly and westerly winds, respectively. Figure 5.4 shows the location of the 25 monitoring sites used at one time or another in the course of the data gathering. Measurements were made during aircraft landing, takeoff and taxi modes. Additionally, an instrument was set up in an auto which was periodically driven around the entire airfield at the periphery, in attempts to detect gross airport contributions to the local CO "background." Within the discriminating capability of the equipment this was not possible, nor were significant observable levels of CO measured during any of some 50 observed landings.

From all these measurements taken under a variety of airplane activity, and meteorological conditions, the maximum projected one-hour average concentration measured at positions where people might be expected to be located was less than 2 parts per million (ppm) by volume. This concentration is insignificant (Federal Register, June 19, 1978) when compared to the one-hour National Ambient Air Quality Standard (NAAQS) of 35 ppm. These measurements constituted one consideration in the formal recommendation by the EPA to withdraw GA engine emission standards (Federal Register, March 24, 1978).

+Adapted from "Pollution Dispersion Measurements at High-Activity Fly-In of General Aviation, Military, and Antique Aircraft" by H.M. Segal, 1978

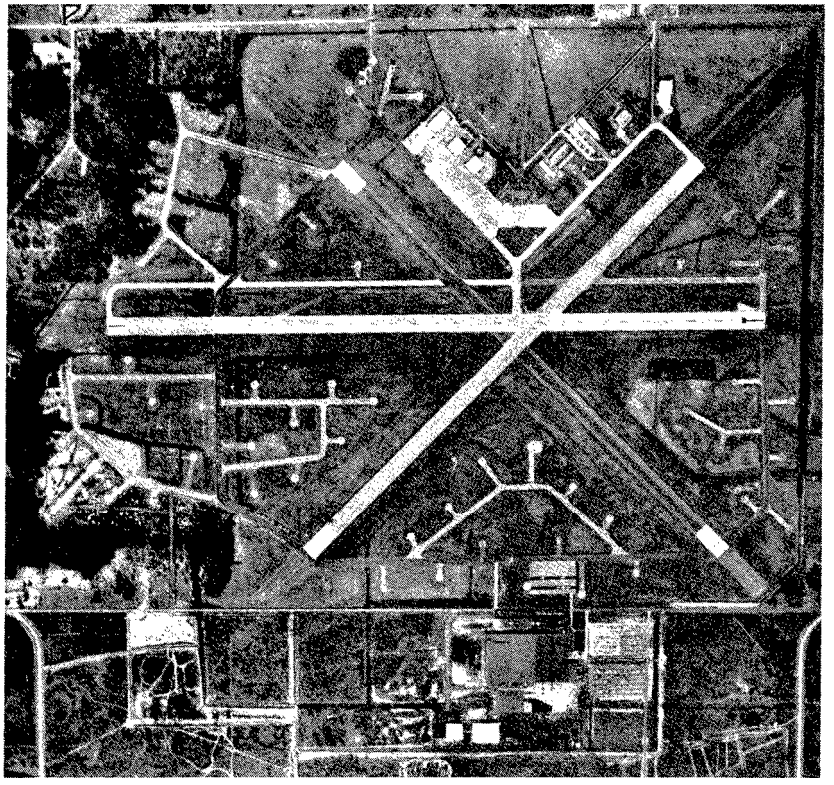

Fig. 5.1. Aerial View of Lakeland Airport, Fla.

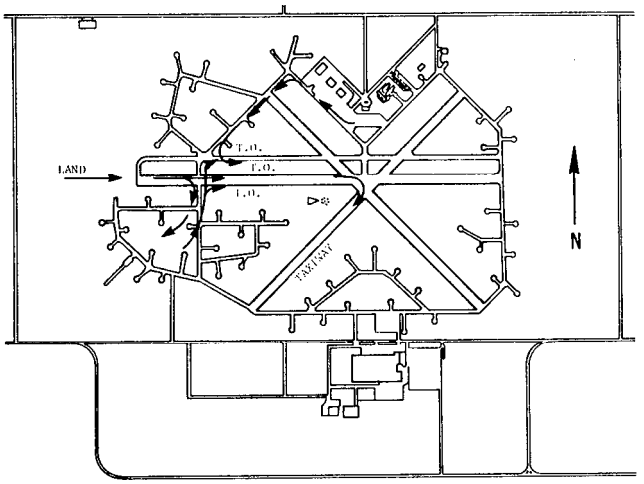

Fig. 5.2. Airport Operations During Easterly Winds - Lakeland Airport

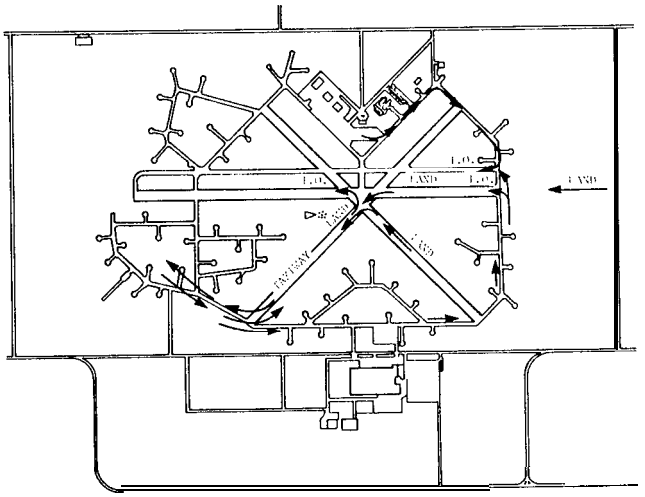

Fig. 5.3. Airport Operations During Westerly Winds - Lakeland Airport

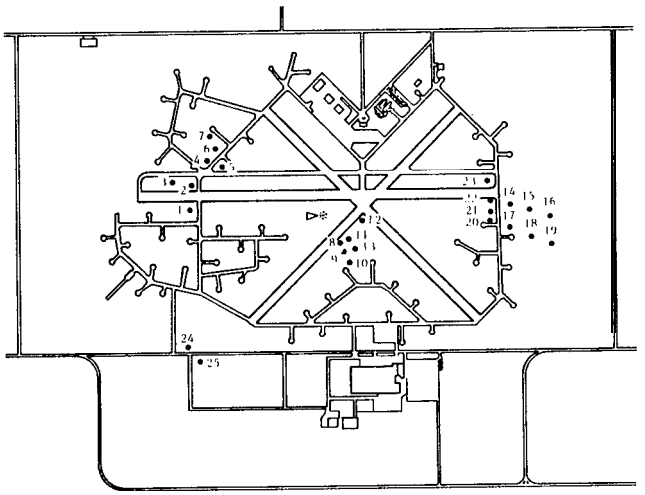

Fig. 5.4. Monitoring Sites - Lakeland Airport January 23-30, 1978

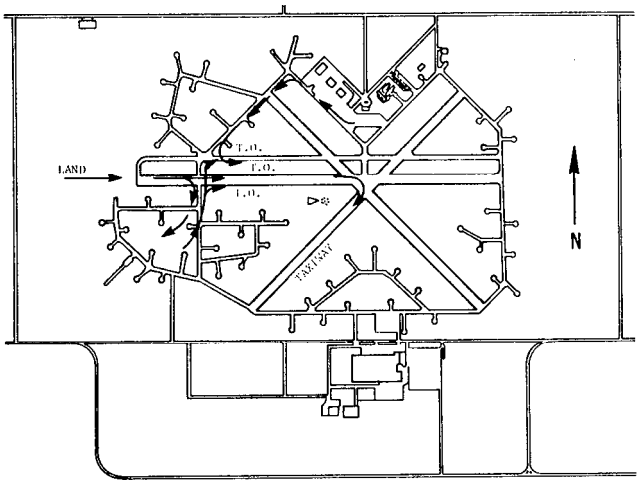

Fig. 5.2. Airport Operations During Easterly Winds - Lakeland Airport

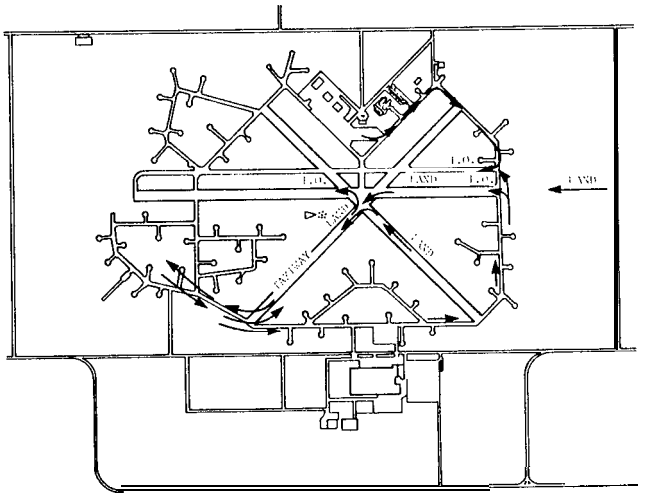

Fig. 5.3. Airport Operations During Westerly Winds - Lakeland Airport

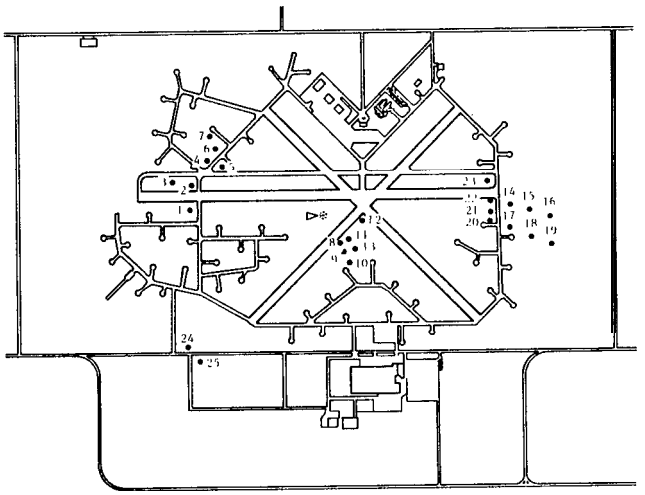

Fig. 5.4. Monitoring Sites - Lakeland Airport January 23-30, 1978

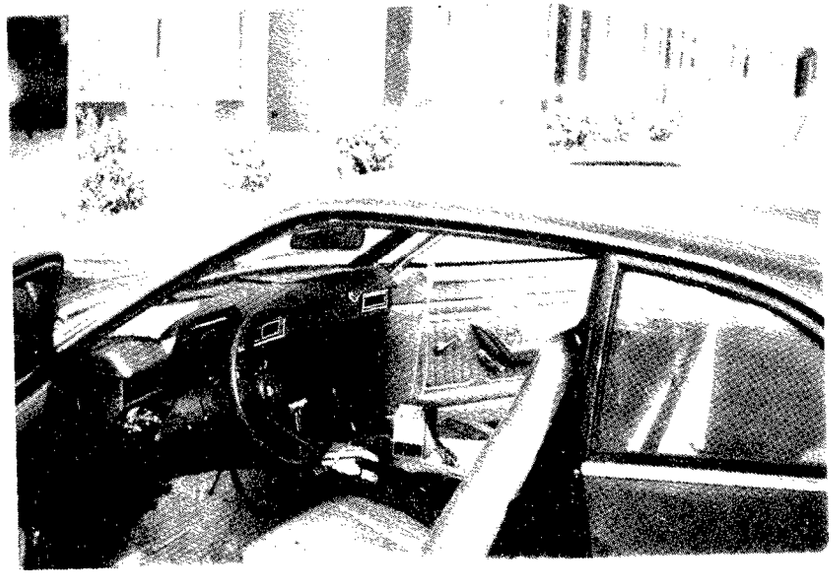

Fig. 5.5. Monitoring Installation - Inside Automobile

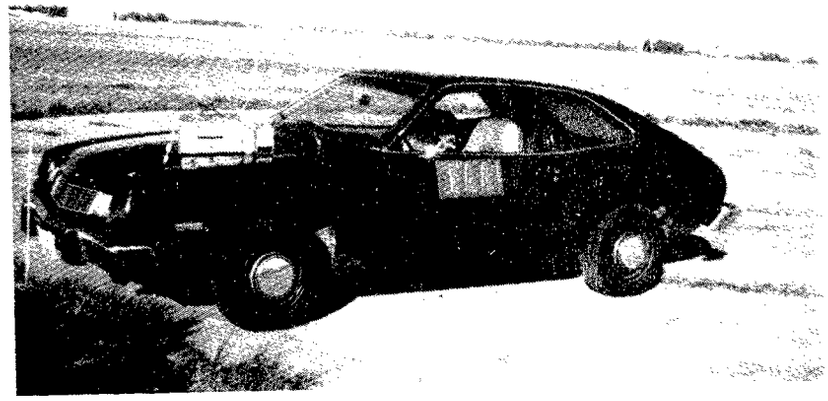

Fig. 5.6. Monitoring Installation - Outside Automobile

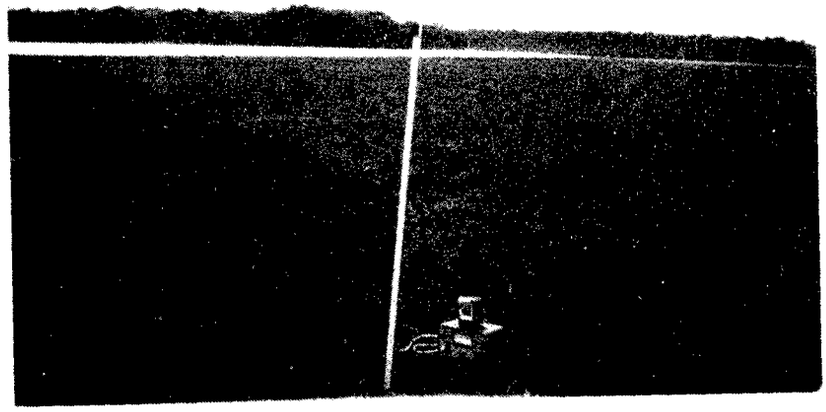

Fig. 5.7. Monitoring Installation - Non-mobile

Takeoff Measurements - On January 29, emissions from over 30 taking-off aircraft were measured at sites 20, 21, and 22. (Figure 5.4). Wind was from 330° at 12 mph and a "B" stability was estimated.

The strip chart trace from a typical taking-off GA aircraft is shown in Figure 5.8. Emissions from this modern GA aircraft are quite low.

However, at sites 20, 21, and 22, the highest pollution levels of the entire week was also recorded. This occurred when a World War II vintage B-25 took off. The CO strip chart trace of this take-off is shown in Figure 5.9. The high emission levels from this aircraft's large radial engines, characteristic of both military and commercial aircraft engines of that time period are to be compared with the almost undetectable pollution produced by the turbine engines used in present day commercial aircraft (Segal, 1977 and Smith et al, 1977). This comparison indicates that pollutant emissions have been drastically reduced by the aircraft industry in developing the gas turbine engine technology of the present era.

Dispersion measurements permit determination of a power law exponent by which atmospheric dispersion may be parameterized. This dispersion rate exponent has been measured during airplane taxi and takeoff assuming that the relationship between concentration and downwind distance can be expressed as:

$$C \quad X^{-K} \qquad (1)$$

where C is the concentration at downwind distance X. The rate exponent at which the pollutant disperses is defined as K. Peak concentrations of those takeoff events having adequate signal to background ratio were averaged and were found to disperse as $X^{-1.9}$ in the power law expression listed above. This exponent which is derived from measurement data will be compared with the theoretical value of this exponent in Section 5.4.

Taxi Measurements (Low Activity) - On January 26, emissions from over 40 taxiing aircraft were recorded. Wind was from 340° at 15 mph and a "C" stability was estimated. Pollution from this mode dispersed as $X^{-1.0}$ in the previously mentioned power law relationship.

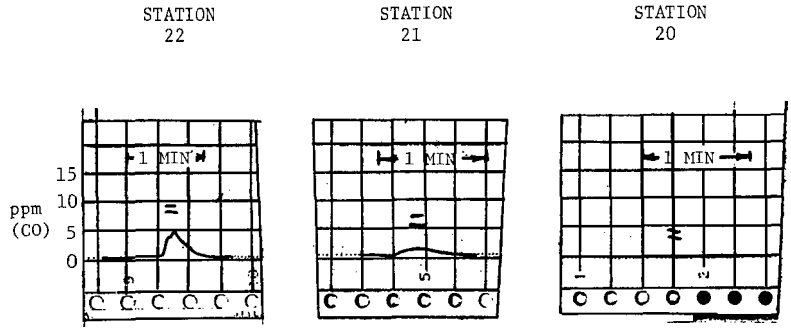

Fig. 5.8. Trace of General Aviation Takeoff

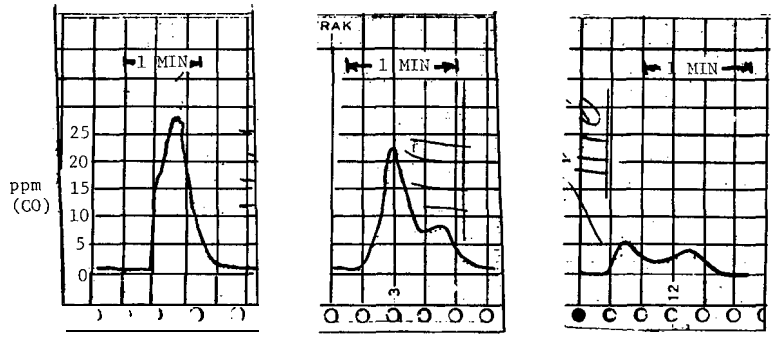

Fig. 5.9. Trace of B-25 Takeoff

Taxi Measurements (High Activity) - The most note-worthy data were obtained at station 17, 18 and 19 between 1700 and 1740 hours on January 28, when a continuous queue of over 30 aircraft stretched down the taxiway for more than 1/2 mile. Wind was from 345° at 12 mph and "D" stability was estimated. During peak activity one airplane taxied by the monitoring station every ten seconds. As they approached the end of the taxiway, these aircraft were almost continuously dispatched down the two takeoff runways at the rate of 278 aircraft per hour.

Because both taxi and takeoff emissions impacted at the three monitoring stations downwind of the taxiing aircraft, it was necessary to devise a method for measuring emissions from the taking-off aircraft only. This was accomplished by moving the instrumented auto at site 18 to site 20 which is directly upwind of the taxiing aircraft. Takeoff concentrations were measured at this location. This move was made after sufficient data had been collected at site 18.

The contribution of takeoff emissions to concentrations at sites 17, 18, 19, and 20 was modeled and calibrated with measurements taken at site 20. This takeoff contribution was then subtracted from the total concentrations measured at sites 17, 18, and 19 to identify concentrations directly attributable to the taxiing aircraft. These data are plotted in Figure 5.10. These multiple event taxi emissions are the found to disperse as $X^{-0.4}$ in the power law relationship $C_{\alpha}X^{-K}$.

5.4 CONCLUSIONS

The following conclusions may be drawn from the concentration summary of Table 5.1:

1. From all measurements taken under extreme aircraft activity conditions, the maximum recorded concentration for CO at the closest position where people might be expected to be located, was less than 2 ppm for a projected one-hour time period. This concentration is insignificant when compared to the one-hour NAAQS of 35 ppm.
2. The highest CO concentration ever recorded of the dispersing plumes of a taking-off airplane (22 ppm at 335 ft. from the runway centerline) was measured at Lakeland Airport on January 29, 1978. This measurement, which was from a World War II vintage B-25, indicates that airplanes have been significant sources of CO pollution in the past.

Taxi Measurements (High Activity) - The most note-worthy data were obtained at station 17, 18 and 19 between 1700 and 1740 hours on January 28, when a continuous queue of over 30 aircraft stretched down the taxiway for more than 1/2 mile. Wind was from 345° at 12 mph and "D" stability was estimated. During peak activity one airplane taxied by the monitoring station every ten seconds. As they approached the end of the taxiway, these aircraft were almost continuously dispatched down the two takeoff runways at the rate of 278 aircraft per hour.

Because both taxi and takeoff emissions impacted at the three monitoring stations downwind of the taxiing aircraft, it was necessary to devise a method for measuring emissions from the taking-off aircraft only. This was accomplished by moving the instrumented auto at site 18 to site 20 which is directly upwind of the taxiing aircraft. Takeoff concentrations were measured at this location. This move was made after sufficient data had been collected at site 18.

The contribution of takeoff emissions to concentrations at sites 17, 18, 19, and 20 was modeled and calibrated with measurements taken at site 20. This takeoff contribution was then subtracted from the total concentrations measured at sites 17, 18, and 19 to identify concentrations directly attributable to the taxiing aircraft. These data are plotted in Figure 5.10. These multiple event taxi emissions are the found to disperse as $X^{-0.4}$ in the power law relationship $C_{\alpha}X^{-K}$.

5.4 CONCLUSIONS

The following conclusions may be drawn from the concentration summary of Table 5.1:

1. From all measurements taken under extreme aircraft activity conditions, the maximum recorded concentration for CO at the closest position where people might be expected to be located, was less than 2 ppm for a projected one-hour time period. This concentration is insignificant when compared to the one-hour NAAQS of 35 ppm.
2. The highest CO concentration ever recorded of the dispersing plumes of a taking-off airplane (22 ppm at 335 ft. from the runway centerline) was measured at Lakeland Airport on January 29, 1978. This measurement, which was from a World War II vintage B-25, indicates that airplanes have been significant sources of CO pollution in the past.

Table 5.1. Carbon Monoxide Concentrations During Different Operational Modes

MODE	STABILITY CLASS	WIND SPEED (MPH)	CHARACTERISTICS PEAK CONCENTRATIONS PPM ABOVE BACKGROUND		
			SINGLE EVENT		1 HOUR AVERAGE
			DIST. 450 FT.	DIST. 335 FT.	DISTANCE 385 FT.
LANDING (SINGLE EVENT)	C	18	<1 PPM		
TAKEOFF (SINGLE EVENT)	B	12	<1 PPM*	23 PPM (B-25) 2 PPM (GA)	
TAXI (SINGLE EVENT)	C	15		< 1 PPM	
TAXI (DURING QUEUE)	D	12			~2 PPM

*(Commercial Jet from Dulles Data, Ref. Smith et al, 1977)

The measured dispersion rate exponents during taxi and takeoff in some cases do not coincide with expectations based on dispersion rate curves (Turner, 1970) that are used in most airport models. This inconsistency is important to recognize, since it may contribute to errors in receptor concentrations calculated from airport pollution models. While this short term measurement program was not designed to develop a large data base or to explain dispersion inconsistencies (m.b., that no measurements of the vertical dispersion of the emission plume were made), the listing of the dispersion parameters in Table 5.2 represents an initial quantification of previously unmeasured dispersion characteristics of several types of aircraft exhaust plumes.

Factors contributing to the inconsistency between measurement and theory may be traced to the inability of the theory to effectively account for:

a. Plume rise

b. Extensive initial dispersion related to the turbulence field created by the high velocity fan action of the propeller. (The extent and duration of this turbulent field is unknown at the present time.>

c. Different emission densities and turbulence intensity along the takeoff path of an accelerating aircraft.

Table 5.2. Measured versus Theoretical Aircraft Plume Dispersion Rates

Mode	Approximate Aircraft Speed	Propeller Speed	Measured Power Law Exponent, K.	Theoretical* Power Law Exponent, K.
Taxi (Single Event)	15 MPH (Constant)	Low	1.0	1.8
Taxi (During Queue>	5 MPH (Constant)	Low	0.4	0.9
Takeoff	25 (Accelerating)	High	1.9	1.8

*Derived from Turner, 1970

a. Plume rise

b. Extensive initial dispersion related to the turbulence field created by the high velocity fan action of the propeller. (The extent and duration of this turbulent field is unknown at the present time.>

c. Different emission densities and turbulence intensity along the takeoff path of an accelerating aircraft.

Table 5.2. Measured versus Theoretical Aircraft Plume Dispersion Rates

Mode	Approximate Aircraft Speed	Propeller Speed	Measured Power Law Exponent, K.	Theoretical* Power Law Exponent, K.
Taxi (Single Event)	15 MPH (Constant)	Low	1.0	1.8
Taxi (During Queue>	5 MPH (Constant)	Low	0.4	0.9
Takeoff	25 (Accelerating)	High	1.9	1.8

*Derived from Turner, 1970

6 THE MEASUREMENT OF CO CONCENTRATIONS FROM QUEUING AIRCRAFT AT LOS ANGELES INTERNATIONAL AIRPORT+

6.1 INTRODUCTION

Carbon monoxide (CO) emissions from queuing aircraft were monitored at Los Angeles International Airport (LAX) from April 16 to April 20, 1979. Carbon monoxide was selected as the pollutant of concern because it is stable, easily measured and predominant during aircraft queuing. LAX was selected for this experiment because:

1. It is a busy airport.
2. High data accumulation is possible under the influence of the predominant sea breeze which blows emissions directly down the main queueing taxiway.
3. The airport authority was very cooperative and permitted equipment positioning directly on the taxiways.
4. A National Climatic Weather Station which records wind direction, speed and vertical temperature profiles is located within 1500 meters of the monitoring sites.
5. Data from this program could be compared with similar data generated in the early 1970s and which was used as a justification for the aircraft engine emission standards.

6.2 APPROACH

The approach of this program is to measure and model the emissions of aircraft that are lined up (or queued) along a taxiway just prior to takeoff. Queuing was measured at both the north and south runway complexes (Figure 6.1) from April 16 to April 20, 1979. Monitoring and wind measurement equipment were positioned directly downwind of the queuing aircraft.

Two Energetic Sciences Model 2000 "Ecolysers" were employed in this program. These instruments were calibrated with 20 parts per million (ppm) calibration gas before and after each intensive measurement period.

Equipment was placed in a Federal Aviation Administration vehicle with the pollution sampling tube extending outside the vehicle where it was attached to a vertical probe. Air intake height was 1.7 meters. A second

---

+Adapted from "Emissions from Queuing Aircraft" by H.M. Segal, 1980.

monitoring instrument was located 50 meters downwind from the first monitoring location. Its air intake tube was attached to a tripod and elevated to a height of 1.7 meters. (Results from this second monitoring location are not reported.) Figure 6.2 shows instrument layout. Equipment was lined up in the direction of the prevailing wind which, because of its westerly direction, transported a line of aircraft emissions directly over the receptors. This arrangement provided the desired worst case pollution geometry. Wind velocity was measured every 15 minutes at the monitoring sites.

Air quality was recorded during 162 minutes of aircraft activity during a five-day time period. Queue lengths varied from 1 to 8 aircraft. (Figure 3 shows the configuration of one 7 aircraft queue that was monitored.) Distance from the first queuing aircraft to the nearest receptor was 220 meters from the south runway and 320 meters for the north runway. Air quality was recorded for wind speeds of 2.8 to 8.6 meters per second under Pasquill-Gifford stability classes of B, C, D, and E. Airplane entrance to and exit from the various queue positions was recorded to the nearest second. This precise recording of the time when each aircraft entered and left its queue position and the simultaneous recording of pollutant concentrations at the downwind receptors were essential portions of this program. One person was assigned full time to accomplish these tasks.

Upon completing the monitoring program, the 162 minutes of data were stratified according to wind speed, stability class, and queue length, and a flow diagram such as the one shown in Figure 6.4 was prepared for each of eight different queuing conditions. These conditions reflected measurements taken during different days, wind speeds, and stability conditions. Emissions dispersion during transport to the monitoring sites was then modeled for comparison with measurements. Each airplane was positioned on the taxiway in accordance with its observed location. Data from Tank and Hodder (1978) were used to determine the height of the plume centerline and the initial size of the plume. Pollutant transport times from queue to the receptor location were determined by dividing each source-to-receptor distance by the measured wind speed.

monitoring instrument was located 50 meters downwind from the first monitoring location. Its air intake tube was attached to a tripod and elevated to a height of 1.7 meters. (Results from this second monitoring location are not reported.) Figure 6.2 shows instrument layout. Equipment was lined up in the direction of the prevailing wind which, because of its westerly direction, transported a line of aircraft emissions directly over the receptors. This arrangement provided the desired worst case pollution geometry. Wind velocity was measured every 15 minutes at the monitoring sites.

Air quality was recorded during 162 minutes of aircraft activity during a five-day time period. Queue lengths varied from 1 to 8 aircraft. (Figure 3 shows the configuration of one 7 aircraft queue that was monitored.) Distance from the first queuing aircraft to the nearest receptor was 220 meters from the south runway and 320 meters for the north runway. Air quality was recorded for wind speeds of 2.8 to 8.6 meters per second under Pasquill-Gifford stability classes of B, C, D, and E. Airplane entrance to and exit from the various queue positions was recorded to the nearest second. This precise recording of the time when each aircraft entered and left its queue position and the simultaneous recording of pollutant concentrations at the downwind receptors were essential portions of this program. One person was assigned full time to accomplish these tasks.

Upon completing the monitoring program, the 162 minutes of data were stratified according to wind speed, stability class, and queue length, and a flow diagram such as the one shown in Figure 6.4 was prepared for each of eight different queuing conditions. These conditions reflected measurements taken during different days, wind speeds, and stability conditions. Emissions dispersion during transport to the monitoring sites was then modeled for comparison with measurements. Each airplane was positioned on the taxiway in accordance with its observed location. Data from Tank and Hodder (1978) were used to determine the height of the plume centerline and the initial size of the plume. Pollutant transport times from queue to the receptor location were determined by dividing each source-to-receptor distance by the measured wind speed.

$\sigma_z = K_z x^{0.9}$, $\sigma_y = K_y x^{0.9}$ was assumed,

where K_y, K_z were chosen to match the P-G curves at x = 1.0 km.

This functional form was used in all calculations which emcompassed stability classes B thru E. Such an approximation greatly facilitated calculations and differed negligibly from the P-G-T predictions even at the shortest distances used in this study.

6.5 RESULTS

The results are displayed in Figures 6.5 and 6.6. Figure 6.6 shows the comparison of estimated and measured concentrations during the variety of wind and stability conditions experienced over the entire monitoring period. The average ratio of estimated to measured concentrations for the ensemble of measurement events reduces substantially when finite values for plume height and initial plume size are used. The ratio of 1.7 for the latter condition is within the factor-of-two considered in determining an acceptable level of model performance.

Measurements performed during the longest queue were analyzed separately. The results of this analysis are shown in Figure 6.5. The horizontal bars represent the times during which each airplane occupied a particular queue position. The queue length at any time is determined by summing the number of horizontal bars crossed at any particular time. Between 1742 and 1801 hours on April 18 the queue length increased to eight airplanes. During this time period estimated concentrations were 3 ppm while measured (average) concentrations were 1.5 ppm. A second comparison was then made for the extended averaging time period (70 minutes). Under these conditions, the estimated concentration was 1.3 ppm and the measured concentration was 0.9 ppm. Both of these model test conditions fall within the factor-of-two criteria for determining model performance.

A final model calculation was performed to reflect worst case meteorological conditions for comparison to the NAAQS. Worst case conditions of "E" stability and one meter per second wind speed were assumed. The receptor was relocated 750 meters downwind from the end of the taxiway, a distance which is characteristic of where people might first experience aircraft emissions. The uppermost curve in Figure 6.5 is a plot of these conditions. When this curve

is averaged over the entire 70 minute period, an estimated concentration of 4 ppm results.

6.6 CONCLUSIONS

The model appears to reflect measured concentrations quite well under both the short averaging times of specific queue events and the longer averaging times associated with all types of airplane activity at the end of the taxiway.

It is interesting to note the ability of the model to track the pollution peaks and valleys during the period from 1742 to 1801. This capability is quite impressive considering the number of times the airplane changes its queue position. The time shift between the two curves is in the expected direction and is probably related to the time taken for the high velocity engine exhaust to slow down to ambient conditions prior to atmospheric transport and to the actual slowing down of the ambient wind field by a line of queuing aircraft. (This latter condition has been observed at Washington National Airport).

When the verified Simplex model is used to estimate concentrations at expected populated locations during the highest activity hour monitored, concentrations of only 4 ppm from aircraft alone result. This value is small when compared to the NAAQS limit value of 35 ppm.

This assessment indicates that a simple point source algorithm can successfully accomplish the "verification by parts" procedure suggested by Turner (1979). Parameterizations from this verified model may subsequently be incorporated into a number of more complex models if validation efforts at other airports confirm these results.

The results of this study should apply to other engine exhaust gases and should be particularly useful in defining the queuing concentrations of engine NO, (NO_2 under a high ozone environment). This can be accomplished by merely changing the model inputs to reflect NO, rather then CO emissions.

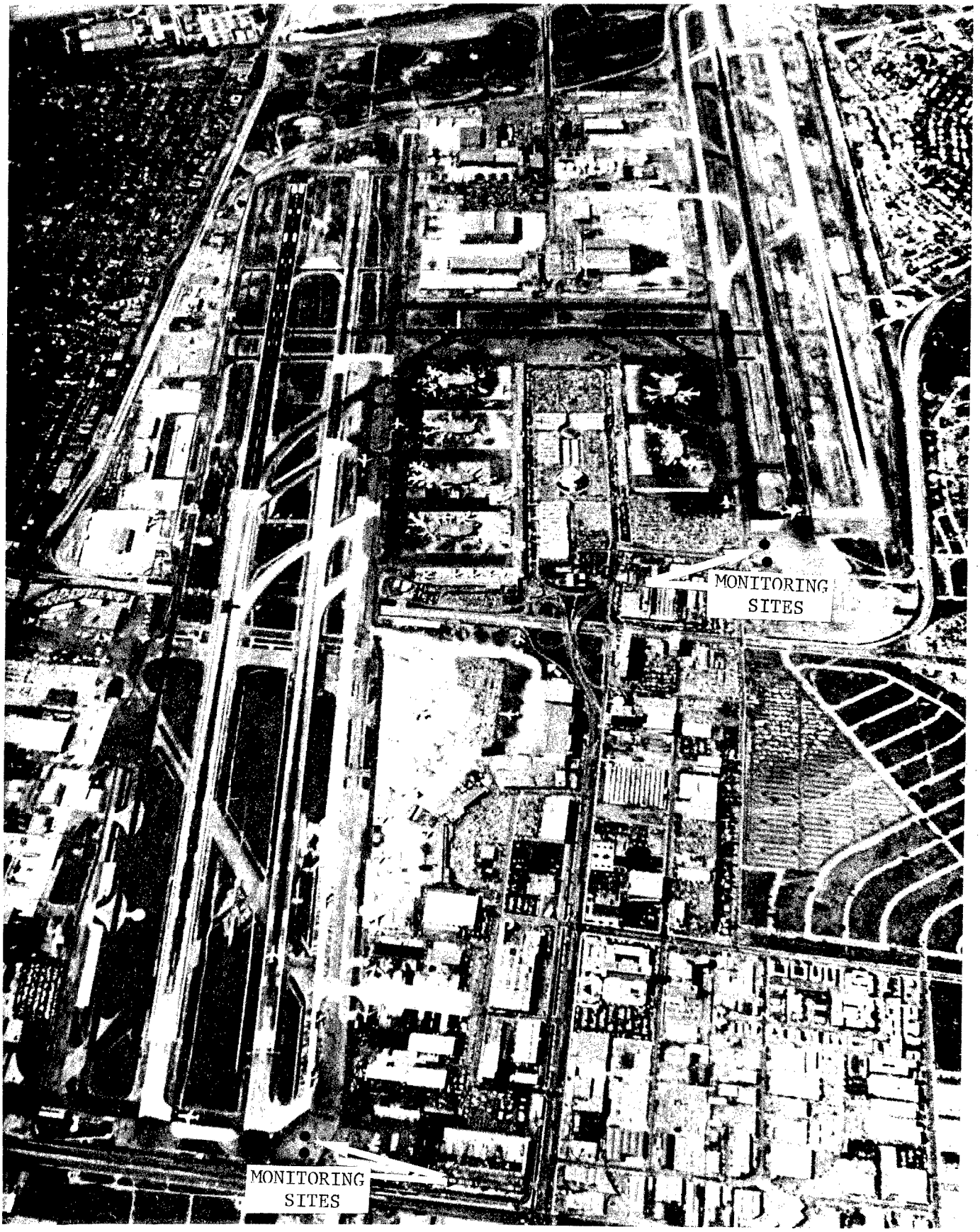

Fig. 6.1. Monitoring Site Locations

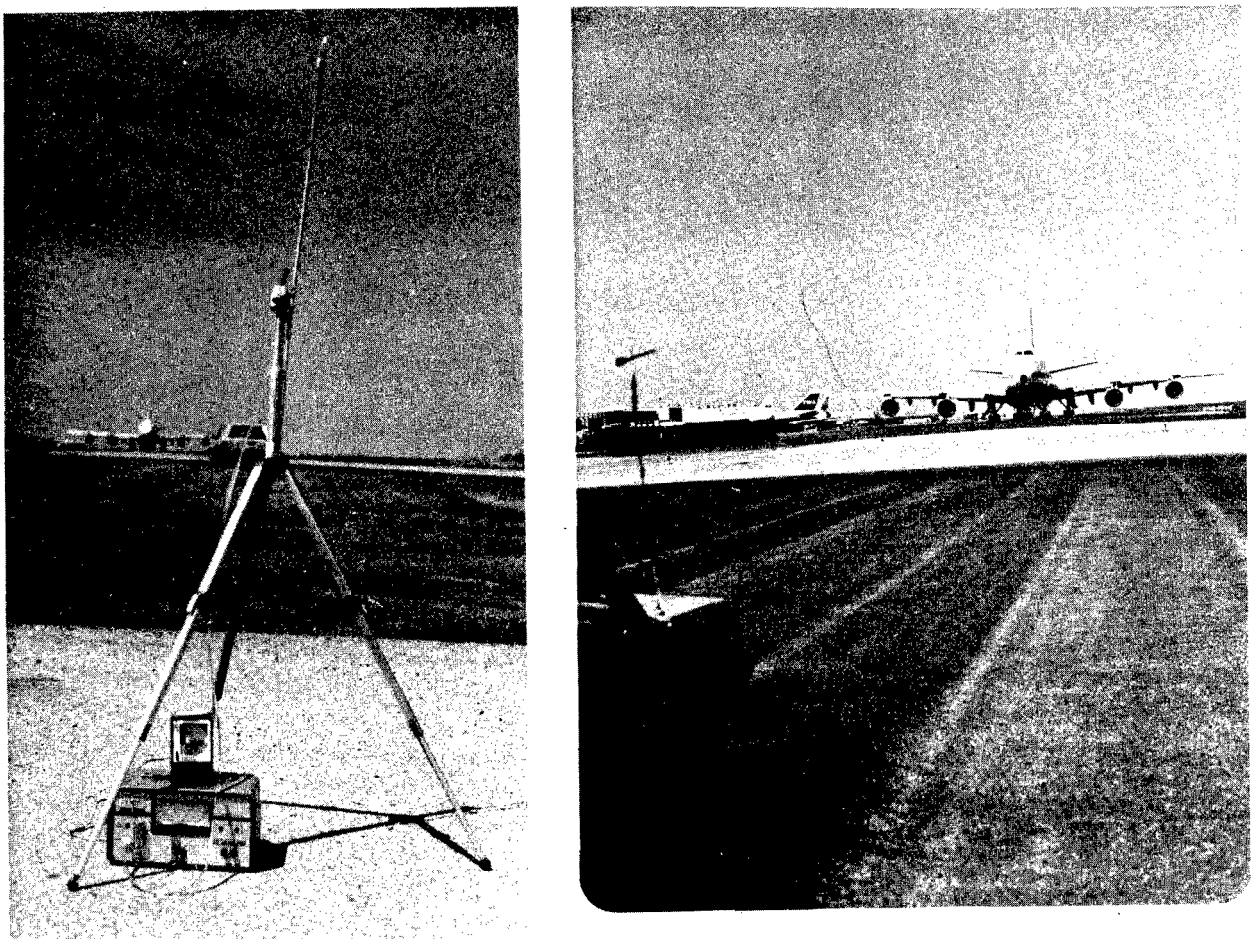

Fig. 6.2. Monitoring Equipment

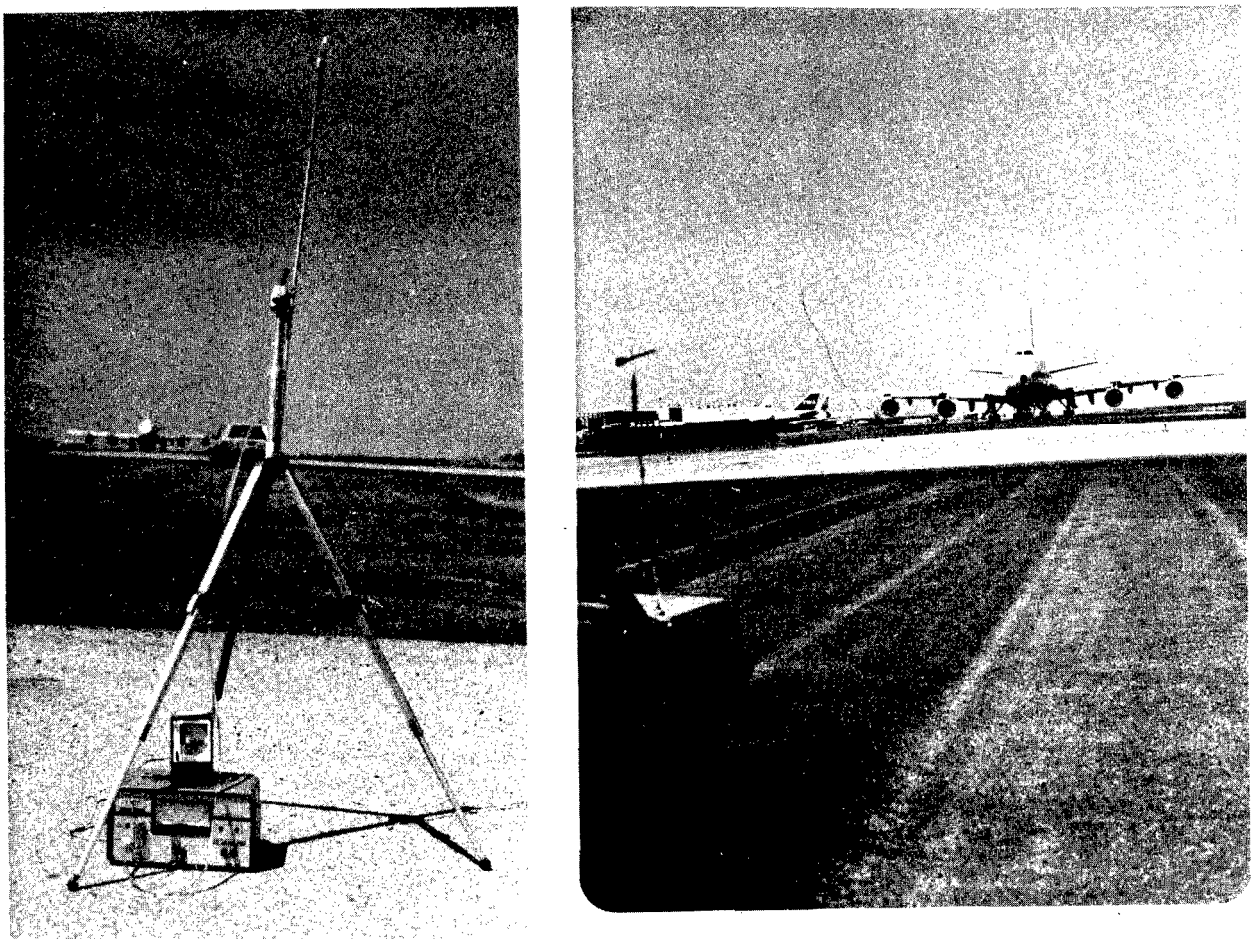

Fig. 6.2. Monitoring Equipment

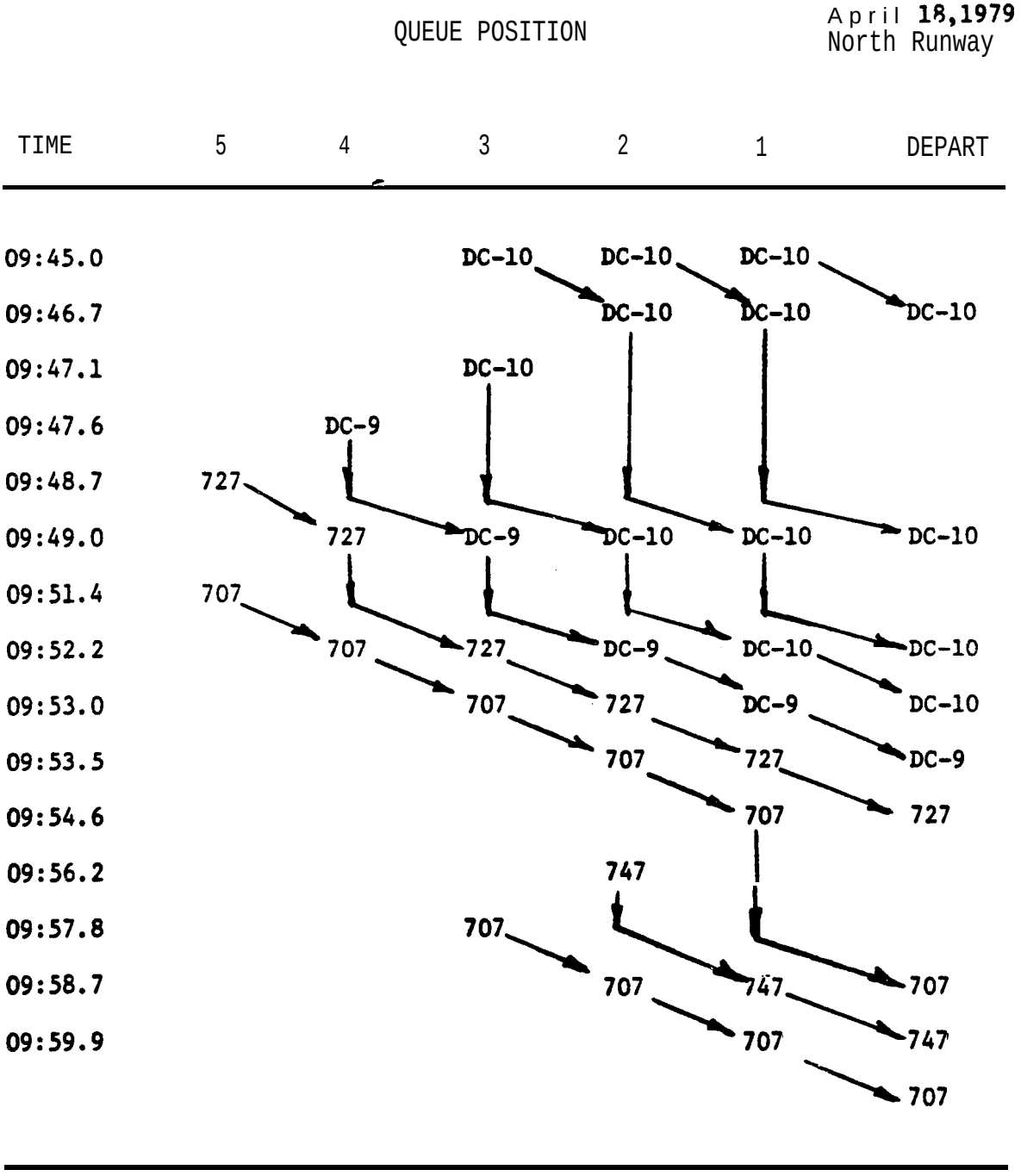

Fig. 6.4. Airplane Flow Diagram

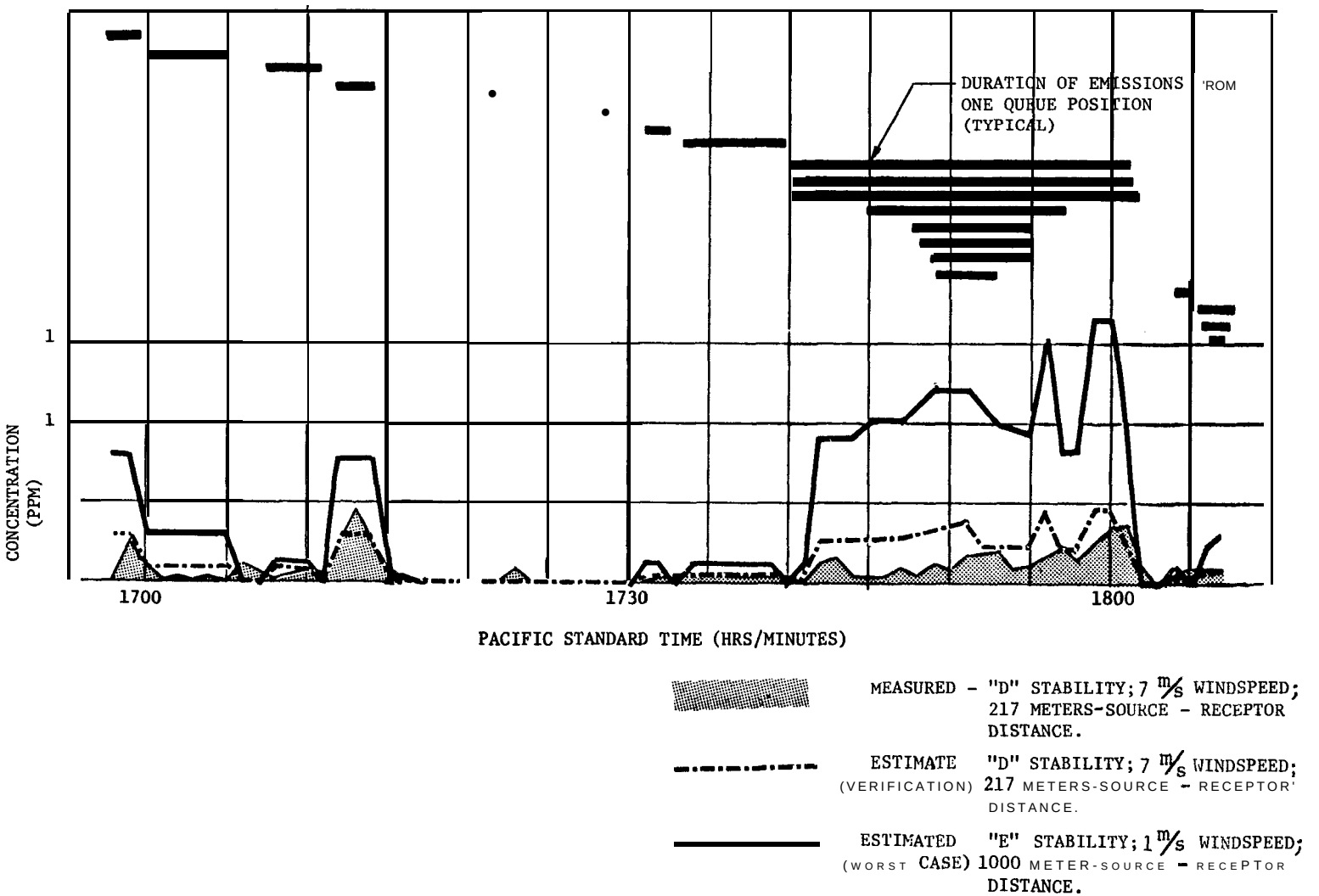

Fig. 6.5. Concentrations and Times in Queue (April 18, 1979)

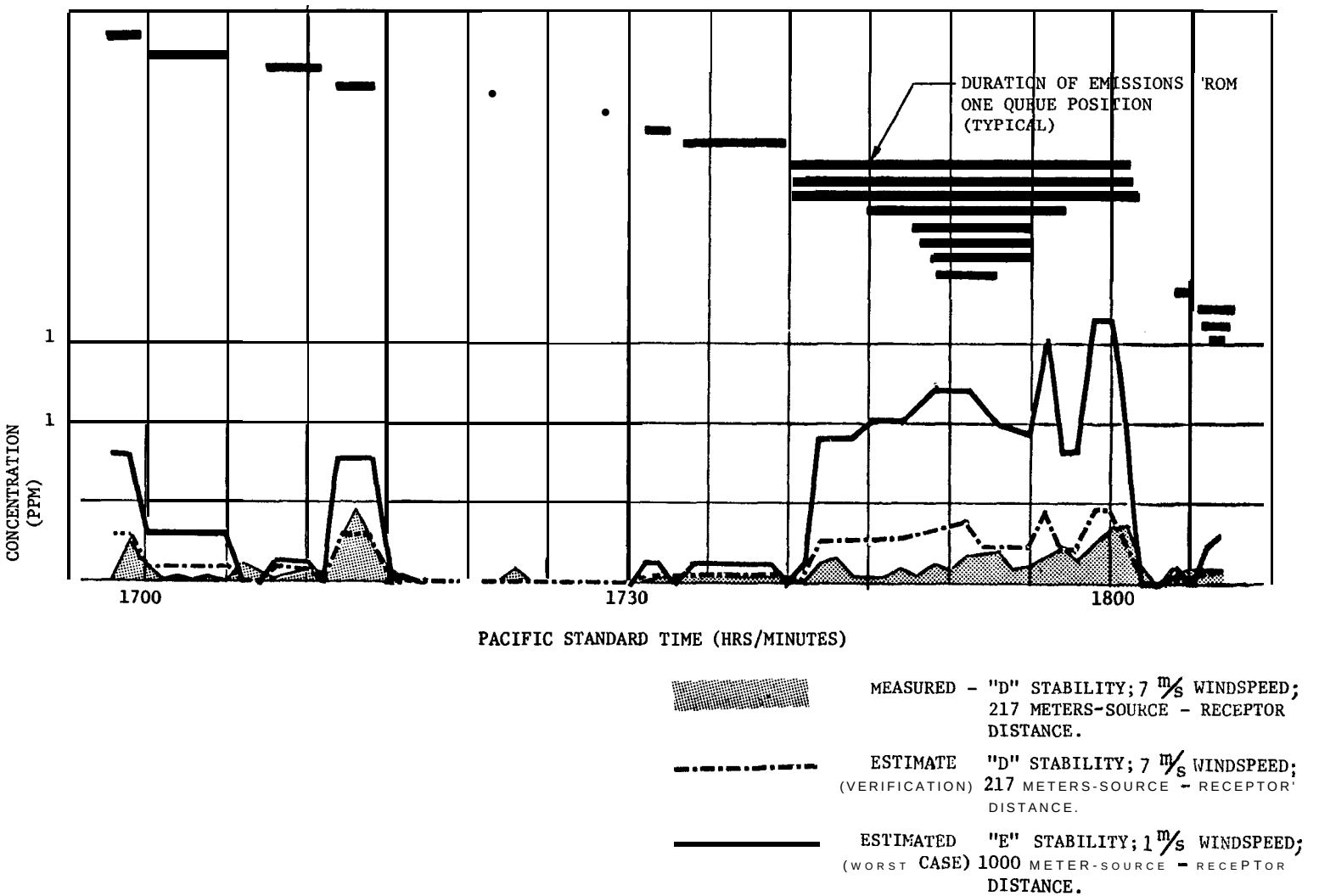

Fig. 6.5. Concentrations and Times in Queue (April 18, 1979)

tions played a significant role in the selection of Williams AFB at the site meeting these requirements for this model validation effort. Williams AFB had a high volume aircraft operations and is relatively remote from an urban area.

Thirteen months of hourly average concentrations of CO, NMHC, and NO, monitored at the five-station network, shown in Fig. 7.1, constitutes the data base used for assessing the predictive capabilities of AQAM. Parallel. data bases of hour-by-hour meteorology and aircraft activity were utilized, in conjunction with the standard emissions inventory input to AQAM, to compute pollutant concentrations at the locations of interest. To define the incremental AQAM predictive power obtained through the use of higher time resolution aircraft data, AQAM predictions were made based on both the standard AQAM input of annual total aircraft operations (referred to as AQAM I predictions) and on the hour-by-hour aircraft operations mentioned above (referred to as AQAM II predictions).

7.3 IMPACT OF AIRCRAFT ON LOCAL AIR QULAITY

As seen in Table 7.1, pollutant levels at several receptors are found to depend in a significant way on aircraft emissions though the average concentration impacts are small relative to the National Ambient Air Quality Standards (NAAQS). In all cases AQAM overpredicts the percentage role of aircraft emissions but much of this is simply due to the background levels not accounted for in AQAM. The fact that AQAM overpredicts the absolute role of aircraft at most stations is thought to be related to the model's neglect of plume rise and plume turbulence enhanced dispersion: two mechanisms which act to reduce concentrations nearby the aircraft. The largest observed average daytime impact of aircraft occurs at station 4 where, on the average, aircraft account for 36% of the CO, 28% of the NMHC and 24% of the NO,.

Both AQAM predictions and measurements agree that station 4, atypical in the sense of its close proximity to buildings, trees, and automobiles, sees the highest concentrations: a factor of 2-3 higher than station 1, 2, 3, and 5 collectively in the cumulative frequency distribution (CFD) sense. The failure of the AQAM to correctly reproduce the observed rank ordering among stations 1, 2, 3, and 5 is also thought to be due to dynamical factors such as the neglect of aircraft plume rise (which clearly leads to overprediction of

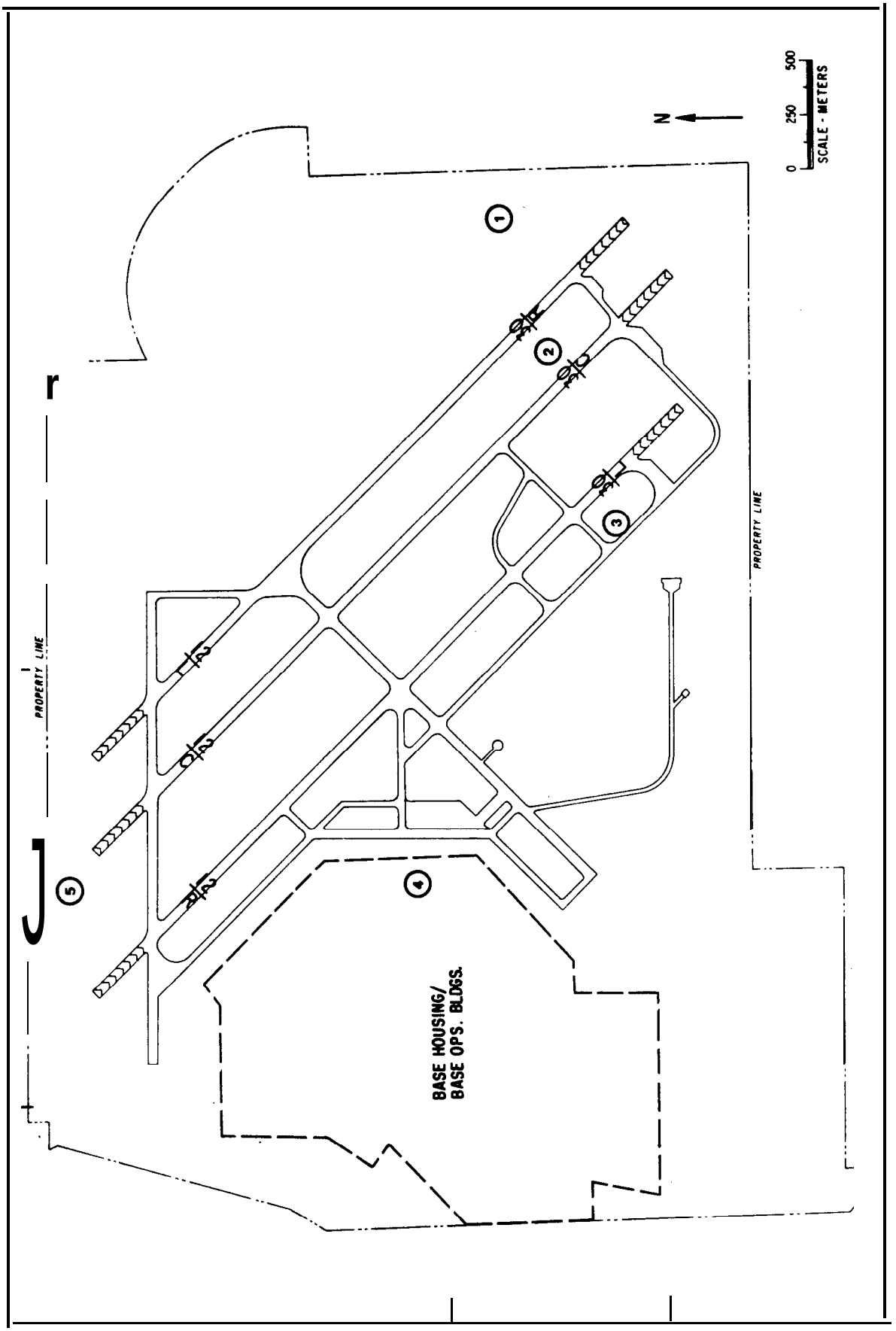

Fig. 7.1. Locations of the Five Ambient Air Quality Monitoring Trailers

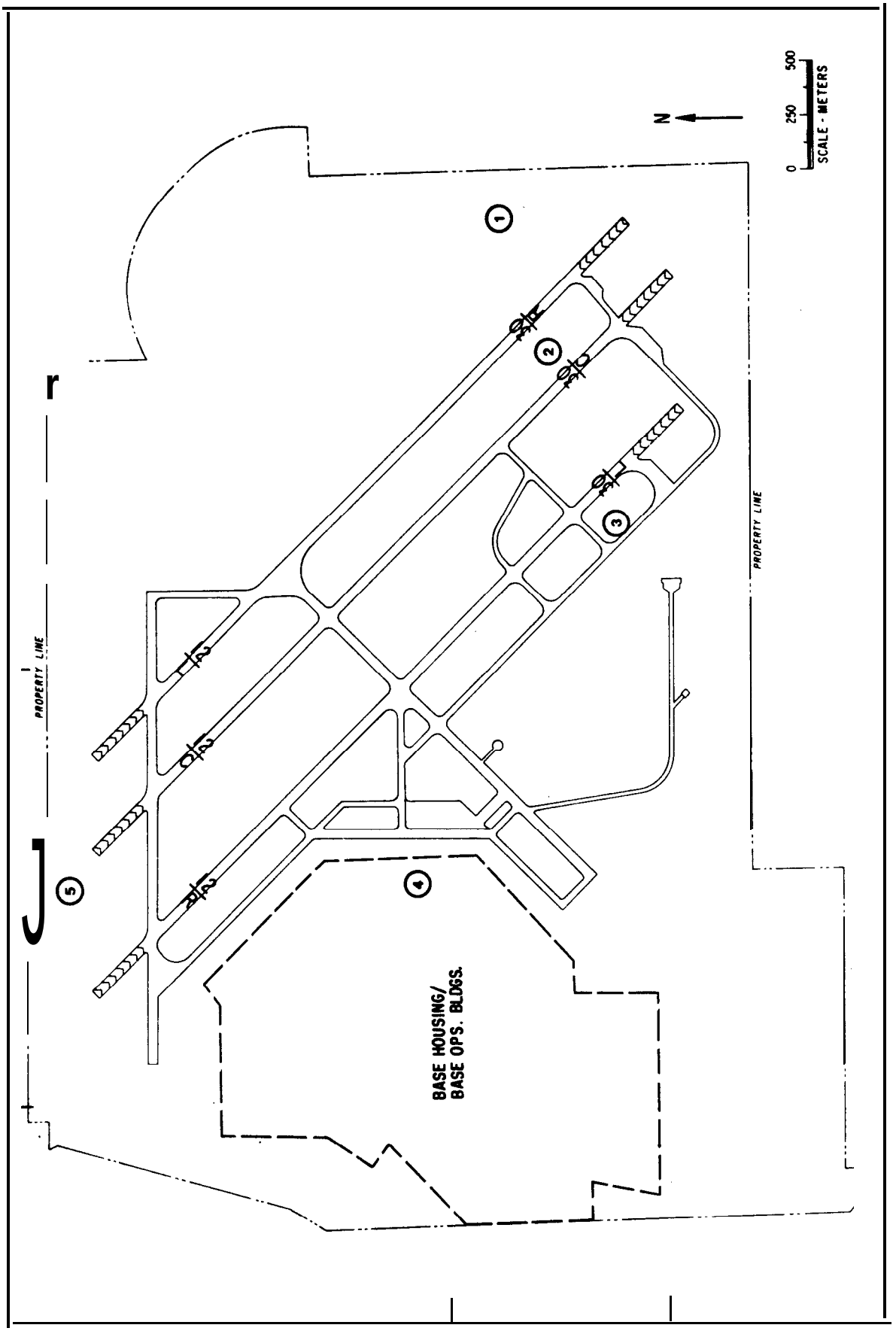

Fig. 7.1. Locations of the Five Ambient Air Quality Monitoring Trailers

CO and NMHC at station 3). Finally, using the computed CFDs for off-base populated areas and allowing for possible underprediction by a factor of 2-3, one concludes that, with the exception of the 6-9 AM National ambient guideline concentration for reactive hydrocarbons, the airbase impact is negligible relative to existing NAAQS.

No significant difference in predictive power between the AQAM I and AQAM II has been found, thus extremely detailed time histories of aircraft operations do not have a significant effect on the model's accuracy (predictive power) and the standard AQAM input of an average diurnal distribution of aircraft operations appears adequate.

7.4 PERFORMANCE OF THE MODEL

In the CFD sense, the AQAM predictions for the upper percentile concentration range agree reasonably well in magnitude and slope with the observed concentration distributions (sample case seen in Fig. 7.2), suggesting that the model simulation encompasses a range of emission and dispersion conditions comparable with reality. At the lower concentration percentile levels, the CFDs are often orders-of-magnitude different, reflecting the problem of absence of background levels in the AQAM computations. CFD estimates of the 99.99 percentile concentrations (i.e., highest hourly average concentration per year) of $\simeq 3$ ppm CO, 1-3 ppm NMHC, and 0.1-0.3 ppm NO, agree surprisingly well with observed values of 2-4 ppm CO, 1-3 ppm NMHC, and 0.08-0.15 ppm NO, if stations 1, 2, 3, and 5 are considered collectively; however, such estimates for any single station may underpredict the once per year high by as much as a factor of 1.7 for CO and NMHC and 3 for NO,. The fact that the CFDs of observed concentrations at the different stations converge at the upper percentiles while the individual station curves diverge slightly for the AQAM predictions, suggests that the most severe pollution episodes actually exist over a spatial domain much larger than the airbase and thus are probably not solely due to specific local sources such as aircraft, as suggested by the model.

In examining the performance of AQAM on an hour-by-hour basis one encounters shortcomings common to Gaussian plume models in general. If no accounting of background pollutant levels is made, hour-by-hour comparisons of AQAM with observations indicate severe underprediction for all three

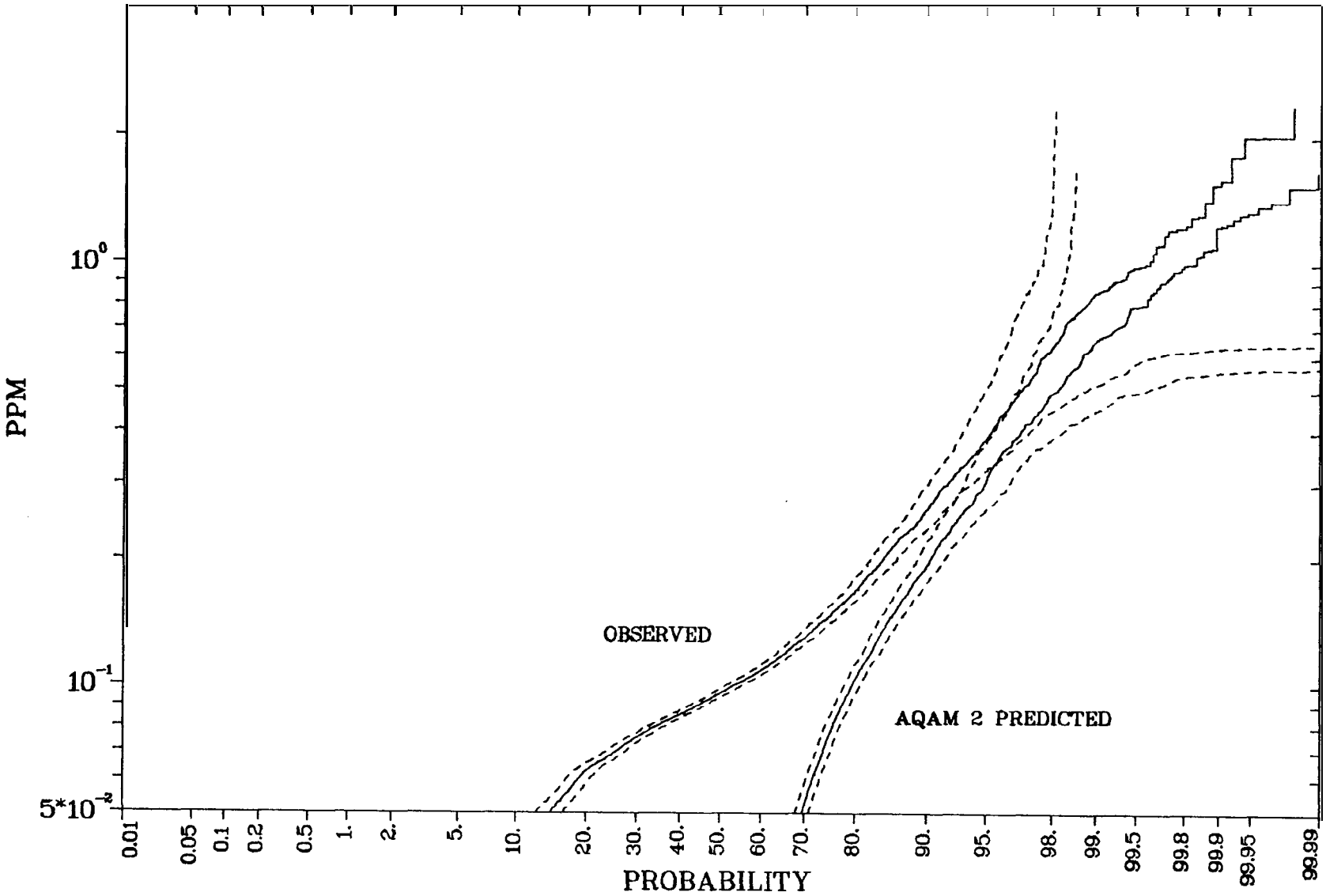

Fig. 7.2. Cumulative Frequency Distribution for Observed and AQAM II Predicted CO at Station 1 -- 95% Confidence Bounds are Indicated

pollutants (a mean factor of 3 for CO and NMHC and a factor of 5 for NO_x). In addition, the standard deviations of these distributions indicate that the unadjusted model falls short of the "50-percent within a factor-of-two'* criteria for Gaussian models. However, addition of a modest annual mean background (0.09 ppm for CO, 0.08 ppm for NMHC, and 7 ppb for NO_x) leads to a dramatic improvement in predictive power. The background adjusted model yields predictions with a factor-of-two of observation in excess of 65% of the time, while errors in excess of factor-of-ten occur at a tolerable $\simeq$1% level. The reason such order of magnitude discrepancies exist lies with the fundamental limitations of modeling a stocastic process with a deterministic model.

7.5 DIFFICULTIES WITH THE THEORY VERSUS OBSERVATION COMPARISON

At the time the experiment was being planned (circa 1975), Williams AFB had the highest level of aircraft operations of any airbase in the U.S., and, as Williams is a training base, it was expected that records of aircraft activity would be more accurately maintained than at other bases. While accurate records were available during normal training operations periods, documentation of off-hours activity (e.g. weekends) was incomplete. In addition, as most of the operations involved small twin-engine aircraft (i.e. T37, T38, and F5), selection of the airbase having the highest traffic count was not necessarily compatible with a choice based on highest aircraft pollutant emissions.

It was also thought that the remoteness of the base from other significant sources would render the resolution of airbase and aircraft generated pollution from background levels straightforward. Unfortunately, Phoenix, though some 50 km to the Northwest, contributed high background levels to the measured air quality particularly at night. These so-called background levels often exceeded the local pollutant levels, resulting in a poor signal-to-noise ratio and greatly reducing the effectiveness of the receptor network in sensing local source (i.e., airbase) created pollutant gradients. In addition, the entire Valley of the Sun appears at times to exhibit pollution reservoir characteristics which can not be predicted by a short-range Gaussian plume model such as AQAM. Even the several hour transport and dispersion of pollutant from Phoenix, though included in the AQAM inventory of environ sources, is not adequately treated due to total reliance on the

stationary state assumption. Such multihour transport could have been more realistically modeled using a backward trajectory technique, which would select the emission rate for the time period presently impacting the receptors and allow for varying dispersion rates over the trajectory of the plume, but such is not the case in the present AQAM, designed for short-range pollutant transport and dispersion calculations. Thus, it was necessary to attempt to validate the model under conditions where a major portion of the aerometric signal was related to distant, background sources not adequately treated by the model. The presence of five monitors on the base could have been useful in subtracting out these unwanted and poorly described components of the observed concentrations. However, two factors limited the effectiveness of this latter approach to investigating the local (i.e., airbase) contribution to the observed pollutant levels. First, noise in the form of spatial inhomogeneities of the background and, second, inter-instrument random and systematic errors which tended to wash out many of the more subtle effects since local signal components were often small compared to the accuracy limits of the instruments.

All of the studies of model predictive power versus meteorological parameters or time of day suggest that time of day is the most significant variable affecting AQAM performance in that AQAM reproduces the major trends in daytime observed concentrations when local sources dominate but seriously underpredicts at night when more distant sources contribute. This deficiency is probably due to an underestimate of vehicle activity between midnight and 5 a.m. and to a breakdown of the steady-state Gaussian plume assumption used in the model. Major revision of the model to incorporate backward trajectories would probably be required to rectify this latter problem; however, such a revision is perhaps of only academic interest at present since the AQAM is most successful in simulating the potential "worst case" airbase impact situations associated with morning, low wind speed, stable or low inversion height conditions coincident with the commencement of high airbase emissions.

stationary state assumption. Such multihour transport could have been more realistically modeled using a backward trajectory technique, which would select the emission rate for the time period presently impacting the receptors and allow for varying dispersion rates over the trajectory of the plume, but such is not the case in the present AQAM, designed for short-range pollutant transport and dispersion calculations. Thus, it was necessary to attempt to validate the model under conditions where a major portion of the aerometric signal was related to distant, background sources not adequately treated by the model. The presence of five monitors on the base could have been useful in subtracting out these unwanted and poorly described components of the observed concentrations. However, two factors limited the effectiveness of this latter approach to investigating the local (i.e., airbase) contribution to the observed pollutant levels. First, noise in the form of spatial inhomogeneities of the background and, second, inter-instrument random and systematic errors which tended to wash out many of the more subtle effects since local signal components were often small compared to the accuracy limits of the instruments.

All of the studies of model predictive power versus meteorological parameters or time of day suggest that time of day is the most significant variable affecting AQAM performance in that AQAM reproduces the major trends in daytime observed concentrations when local sources dominate but seriously underpredicts at night when more distant sources contribute. This deficiency is probably due to an underestimate of vehicle activity between midnight and 5 a.m. and to a breakdown of the steady-state Gaussian plume assumption used in the model. Major revision of the model to incorporate backward trajectories would probably be required to rectify this latter problem; however, such a revision is perhaps of only academic interest at present since the AQAM is most successful in simulating the potential "worst case" airbase impact situations associated with morning, low wind speed, stable or low inversion height conditions coincident with the commencement of high airbase emissions.

- The ability of the AQAM to accurately predict inter-station concentration differences is only weakly confirmed because of large measurement errors relative to these observed concentration differences and because of the unexpectedly high background concentrations.
- The AQAM could benefit from minor revisions such as the incorporation of jet plume rise and turbulence enhanced dispersion and from major revisions such as a backward trajectory calculation for more realistic assessment of the impact from distant sources.
- AQAM is ready for acceptance under EPA Guidelines on Air Quality Modeling.

8 REFERENCES

Abramovich, G.N., 1963. The Theory *of* Turbulent *Jets.* Cambridge, MA, MIT Press.

Arey, F.K., R.W. Murdoch, and F. Smith, 1979, *Audit of the Washington, D.C. National Airport Air Monitoring Sites.* Research Triangle Institute Report 43U/1487/92-01F.

Bastress, E., R. Baker, C. Robertson, R. Siegel, and G. Smith, 1971. Assessment *of Aircraft Emission Control Technology.* Northern Research and Engineering Corp. Report 1168-1.

Breuer, W., 1965. *Die Aussagekraft kontimuerlicher Immissionsmessungen.* IWL. Institut Fuer Gewerbliche Wasserwirtschaft und Luftreinhaltung E. V. Forum 65, Band 3.

Briggs, G.A., 1969. *Plume Rise.* USAEC, TID-25075, Springfield, Virginia.

Cirillo, R.R., J.F. Tschanz, and J.E. Camaioni, 1975. *An* Evaluation Of *Strategies for Airport Air Pollution* Control. Argonne National Laboratory, Argonne, IL, Report No. ANL/ES-45.

Coordinating Research Council, 1960. *Report* of *the Program* Study Group on *Aircraft Exhaust.* CRC Inc.

Daley, P. and D. Naugle, 1978. Measurement *and Analysis* of *Airport Emissions.* Proceedings, Air Quality and Aviation: An International Conference, Federal Aviation Administration Report No. FAA-EE-78-26 pp. 2-9. Also published in J. Air Pollution Control Assoc., 29, pp. 113-116, February 1979.

Duewer, W.H. and J.J. Walton, 1978. *Potential Effects* of Commercial *Aviation* on *Region-wide Air Quality* in *the* San Francisco *Bay Area.* Proceedings, Air Quality and Aviation: An International Conference, Federal Aviation Administration, Report No. FAA-EE-78-26, pp. 88-101.

Egan, B.A. et al., 1975. *The ESEERCO Model for the Prediction* of *Plume Rise* and Dispersion *from* Gas Turbine Engines. Air Pollution Control Association 68th Annual Meeting Session 49.

EPA, 1972. *Aircraft Emissions: Impact on Air Quality and Feasibility of Control.* U.S. Environmental Protection Agency, Office of Air Quality Planning and Standards, Research Triangle Park, NC.

EPA, 1980. Washington *National Airport Air Quality Study.* Source Receptor Analysis Branch, MDAD, OAQPS Report.

Federal Register, June 19, 1978, Part V, Environmental Protection Agency, 1977 Clean Air Act; Prevention of Significant Air Qualtiy Deterioration.

Federal Register, March 24, 1978, Part III, Environmental Protection Agency, Control of Air Pollution from Aircraft and Aircraft Engines, Proposed Amendments to Standards.

George, R. and R. Burlin, 1960. *Air* Pollution *from Commercial Jet Aircraft.* L.A. County Air Pollution Control District, Los Angeles, CA.

Goldberg, P., 1978. Pratt and Whitney Aircraft, E. Hartford, Connecticut, personal communication.

Greenberg, C., 1978. *Air Quality in the* Vicinity of *Airports.* Proceedings, Air Quality and Aviation: An International Conference, Federal Aviation Administration Report No. FAA-EE-78-26, pp 20-26.

Hallanger, N.L., 1974. *Meteorological Factors* in *Air Quality* Evaluation; Environmental Impact Study Los Angeles International Airport, Altedna, California: Meteorological Research, Inc.

Heywood, J.B., J. A., Fay, and L. H. Linden, 1971. *Jet Aircraft Air Pollutant* Production and Dispersion. AIAA Jour. 9 .

Hogstrom, U., 1975. *Confirming the Local Sources* of *Observed Air* Pollution in Communities. Atmospheric Environment 9, 923-929.

Hoult, D.P., J. A. Fay, and L. J. Forney, 1979. *A Theory of Plume Rise Compared with Field Observations,* J. Air Pollution Control Association 19:585-590.

Hoult, D.P., et al., 1975. Turbulent *Plume* in a Turbulent *Cross Flow; Comparison of Wind Tunnel Tests with Field Observations,* Air Pollution Control Association 68th Annual Meeting Session 49.

Jordan, B.C., 1977a. An Assessment of *the Potential Air Quality Impact* of *General* Aviation *Aircraft* Emissions. U.S. Environmental Protection Agency, Office of Air Quality Planning and Standards, Research Triangle Park, NC (June 27, 1977).

Jordan, B.C., 1977b. *Potential Impact of NO, Emissions from Commercial Aircraft* on NO_2 *Air Quality.* U.S. Environmental Protection Agency, Office of Air Quality Planning and Standards, Research Triangle Park, NC (Nov. 15, 1977).

Jordan, B.C. and A.J. Broderick, 1978. *Emissions of Oxides of Nitrogen from Aircraft.* Proceedings, Air Quality and Aviation: An International Conference, Federal Aviation Administration, Report No. FAA-EE-78-26, pp. 10-19. Also published in J. Air Pollution Control Assoc., 29, pp. 119-124 February 1979.

Junge, Christian, 1963. *Air Chemistry and Radioactivity.* Academic Press, 382 pp.

LAAPCD, 1971. *Study of Jet Aircraft* Emissions *and Air Quality* in *the* Vicinity *of Los* Angeles *International Airport.* Air Pollution Control District, County of Los Angeles, Calif. NTIS-PB-198-699.

Lawson, C.L. and R. J. Hanson, 1974. *Solving Least Squares Problems,* Englewood Cliffs, New Jersey, Prentice-Hall, Inc.

Lemke, E., N. Shaffer, and J. Verssen, 1965. *Air* Pollution *from Jet Aircraft in Los* Angeles *County.* L.A. Air Pollution Control District, Los Angeles, CA.

Lloyd, A.C., F.W. Lurmann, D.G. Godden, J.F. Hutchins, A.Q. Eschenroeder, and R.A. Nordsieck, 1979. *Development of the ELSTAR Photochemical Air Quality* Simulation *Model* and. *Its* Evaluation *Relative to the LARPP Data Base.* ERT Westlake Village, CA, Document No. P-5287.

Lorang, P., 1978. *Review of Past Studies Addressing the Potential Impact* of *CO, HC,* and NO, Emissions *from Commercial Aircraft on Air Quality.* U.S. Environmental Protection Agency, Standards Development and Support Branch, Document No. AC-78-03.

Morton, B.R., G.T. Taylor, and J. S. Turner, 1956. *Turbulent Gravitational* Convection *from* Maintained *and* Instantaneous *Sources,* Proc. Roy Soc.A., 234:1-23.

Naugle, D., B. Grems, and P. Daley, 1978. *Air Quality Impact* of *Aircraft at* Ten *U.S. Air Force Bases.* J. Air Pollution Control Assoc., 28, pp 370-373.

Norco, J.E., R.R. Cirillo, T.E. Baldwin, and J.W. Gudenas, 1973. *An Air Pollution Impact Methodology for Airports and Attendant Land Use - Phase I.* Argonne National Laboratory, Argonne, IL, Report No. APTD-1470.

Oliver, R.C., E. Bauer, H. Hidalgo, K.A. Gardner, and W. Wasylkiwskyj, 1977. *Aircraft* Emissions: *Potential Effects* on Ozone and Climate - *A Review and Progress Report.* U.S. Department of Transportation, Federal Aviation Administration, Report No. FAA-EQ-77-3.

Pace, R.G., 1977. Technical Support Report -- *Aircraft* Emissions *Factors,* U.S. EPA Report.

Patrick, M.A., 1967. *Experimental Investigation of the Mixing and Penetration* of a Round *Turbulent Jet Injected Perpendicularly* into a Traverse *Stream,* Trans. Inst. Chem. Eng. 45:16-31.

Platt, M., R. Baker, E. Bastress, K. Chng, and R. Siegel, 1971. *The* Potential *Impact* of *Aircraft Emissions on Air Quality.* Northern Research and Engineering Corp. Report 1167-1.

Pratt and Whitney, 1972. *Collection and Assessment of Aircraft Emissions* Baseline *Data* - Turbine Engines. Pratt and Whitney Aircraft Group, East Hartford, CT, Report No. P&WA 4339.

Rote, D., I. Wang, L. Wangen, R. Hecht, R. Cirillo, and J. Pratapas, 1973. *Airport* Vicinity *Air* Pollution Study. Report No. FAA-RD-73-113.

Rote, D.M. and L. E. Wangen, 1975. *A* Generalized *Air Quality Assessment Model* for Air *Force Operations,* Technical Report AFWL-TR-74-304.

Schewe, G., L. Budney, and B. Jordan, 1978. *CO Impact* of *General* Aviation *Aircraft.* Proceedings, Air Quality and Aviation: An International Conference, Federal Aviation Administration Report No. FAA-EE-78-26, pp 147-152.

Segal, H.M., 1977. Monitoring Concorde Emissions. J. of Air Pollution Control Assoc. 27(7)623.

Segal, H.M., 1980. *Emissions from Queuing Aircraft.* Air Pollution Control Association 73rd Annual Meeting, Paper 80-3.5.

Segal, H.M., 1978. *Pollution Dispersion Measurements at High Activity Fly-In of General Aviation*, Military, and Antique Aircraft. Proceedings, Air Quality Aviation: An International Conference, Federal Aviation Administration Report No. FAA-EE-78-26, pp 76-80.

Segal, H.M., 1979. Simplified *Modeling and* Measurement of *Air Quality.* Air Pollution Control Association 72nd Annual Meeting, Paper 79-37.5.

Slawson, P.R., and G.T. Csanady, 1967. *On the Mean Path* of Buoyant, Bent-Over *Chimney Plumes,* J. Fluid Mech. 23:311-322.

Smith, D.G., R.J. Yamartino, C. Benkley, R. Isaacs, J. Lee, and D. Chang, 1977. *Concorde Air Quality* Monitoring and *Analysis Program at Dulles International Airport.* U.S. DOT Report No. FAA-AEQ-77-14.

Smith, D. and D. Heinold, 1980. *Logan Airport Air Quality Study,* ERT Final Project Report A-218.

Springer, K. and T. Baines, 1977. Emissions *from Diesel Versions* of *Production Passenger Cars.* SAE Paper 770818.

Tank, W.G., and B.K. Hodder, 1978. Engine *Exhaust Plume* Growth in *the Airport Environment,* Proc. International Conference on Air Quality and Aviation, Reston, Va. FAA Report FAA-EE-78-26 pp 153-164.

Thayer, S.D., Pelton, D.J., Stadskleve, G.H., and Weaver, B.D., 1974. *Model Verification - Aircraft Emissions Impact* on Air *Quality,* Geomet, Inc. EPA-650/4-79-049.

Turner, D.B., 1964. *A* Diffusion *Model* for *an Urban Area.* J. Appl. Meteorol., 3, pp 83-91.

Turner, D.B., 1970. *Workbook* of *Atmospheric Dispersion Estimates,* U.S. Dept. of Health, Education, and Welfare, Public Health Service Publication No. 999-AP-26.

Turner, D.B., 1979. *Atmospheric Dispersion Modeling: A Critical Review.* J. Air Pollution Control Assoc., 29, pp 502-519.

U.S. Congress, 1963. *Clean Air Act.* Public Law 88-206.

U.S. Congress, 1967. *Air Quality Act.* Public Law 90-148, Section 211b.

U.S. Congress, 1970. *Clean Air Amendments of 1970.* Public Law 91-604.

U.S. DHEW, 1968. *Nature and Control* of *Aircraft* Engine *Exhaust Emissions.* HEW report to U.S. Congress, Doc. No 91-9, also NTIS-PB187-771, 388 pp.

Wang I. and D. Rote, 1975. *A Finite Line Source Dispersion Model for Mobile Source Air Pollution.* J. Air Pollution Control Assoc., 25, pp 730-733.

Wangen, L. and L. Conley, 1975. *Air Quality Assessment Model Applied to* Washington National *Airport.* U.S. AFWL Report under Contract AFWL-75-PO-071.

Segal, H.M., 1978. *Pollution Dispersion Measurements at High Activity Fly-In of General Aviation*, Military, and Antique Aircraft. Proceedings, Air Quality Aviation: An International Conference, Federal Aviation Administration Report No. FAA-EE-78-26, pp 76-80.

Segal, H.M., 1979. Simplified *Modeling and* Measurement of *Air Quality.* Air Pollution Control Association 72nd Annual Meeting, Paper 79-37.5.

Slawson, P.R., and G.T. Csanady, 1967. *On the Mean Path* of Buoyant, Bent-Over Chimney *Plumes,* J. Fluid Mech. 23:311-322.

Smith, D.G., R.J. Yamartino, C. Benkley, R. Isaacs, J. Lee, and D. Chang, 1977. *Concorde Air Quality* Monitoring and *Analysis Program at Dulles International Airport.* U.S. DOT Report No. FAA-AEQ-77-14.

Smith, D. and D. Heinold, 1980. *Logan Airport Air Quality Study,* ERT Final Project Report A-218.

Springer, K. and T. Baines, 1977. Emissions *from Diesel Versions* of *Production Passenger* Cars. SAE Paper 770818.

Tank, W.G., and B.K. Hodder, 1978. Engine *Exhaust Plume* Growth in *the Airport Environment,* Proc. International Conference on Air Quality and Aviation, Reston, Va. FAA Report FAA-EE-78-26 pp 153-164.

Thayer, S.D., Pelton, D.J., Stadskleve, G.H., and Weaver, B.D., 1974. *Model Verification - Aircraft Emissions Impact* on Air *Quality,* Geomet, Inc. EPA-650/4-79-049.

Turner, D.B., 1964. *A* Diffusion *Model* for *an Urban Area.* J. Appl. Meteorol., 3, pp 83-91.

Turner, D.B., 1970. *Workbook* of *Atmospheric Dispersion Estimates,* U.S. Dept. of Health, Education, and Welfare, Public Health Service Publication No. 999-AP-26.

Turner, D.B., 1979. *Atmospheric Dispersion Modeling: A Critical Review.* J. Air Pollution Control Assoc., 29, pp 502-519.

U.S. Congress, 1963. Clean *Air Act.* Public Law 88-206.

U.S. Congress, 1967. *Air Quality Act.* Public Law 90-148, Section 211b.

U.S. Congress, 1970. *Clean Air Amendments of 1970.* Public Law 91-604.

U.S. DHEW, 1968. *Nature and Control* of *Aircraft* Engine *Exhaust Emissions.* HEW report to U.S. Congress, Doc. No 91-9, also NTIS-PB187-771, 388 pp.

Wang I. and D. Rote, 1975. *A Finite Line Source Dispersion Model for Mobile Source Air Pollution.* J. Air Pollution Control Assoc., 25, pp 730-733.

Wangen, L. and L. Conley, 1975. *Air Quality Assessment Model Applied to* Washington National *Airport.* U.S. AFWL Report under Contract AFWL-75-PO-071.